

JPRS-UEQ-85-004

15 May 1985

# USSR Report

ENGINEERING AND EQUIPMENT

**FBIS** FOREIGN BROADCAST INFORMATION SERVICE

#### NOTE

JPRS publications contain information primarily from foreign newspapers, periodicals and books, but also from news agency transmissions and broadcasts. Materials from foreign-language sources are translated; those from English-language sources are transcribed or reprinted, with the original phrasing and other characteristics retained.

Headlines, editorial reports, and material enclosed in brackets [ ] are supplied by JPRS. Processing indicators such as [Text] or [Excerpt] in the first line of each item, or following the last line of a brief, indicate how the original information was processed. Where no processing indicator is given, the information was summarized or extracted.

Unfamiliar names rendered phonetically or transliterated are enclosed in parentheses. Words or names preceded by a question mark and enclosed in parentheses were not clear in the original but have been supplied as appropriate in context. Other unattributed parenthetical notes within the body of an item originate with the source. Times within items are as given by source.

The contents of this publication in no way represent the policies, views or attitudes of the U.S. Government.

#### PROCUREMENT OF PUBLICATIONS

JPRS publications may be ordered from the National Technical Information Service (NTIS), Springfield, Virginia 22161. In ordering, it is recommended that the JPRS number, title, date and author, if applicable, of publication be cited.

Current JPRS publications are announced in Government Reports Announcements issued semimonthly by the NTIS, and are listed in the Monthly Catalog of U.S. Government Publications issued by the Superintendent of Documents, U.S. Government Printing Office, Washington, D.C. 20402.

Correspondence pertaining to matters other than procurement may be addressed to Joint Publications Research Service, 1000 North Glebe Road, Arlington, Virginia 22201.

Soviet books and journal articles displaying a copyright notice are reproduced and sold by NTIS with permission of the copyright agency of the Soviet Union. Permission for further reproduction must be obtained from copyright owner.

15 May 1985

## USSR REPORT ENGINEERING AND EQUIPMENT

### CONTENTS

#### MARINE AND SHIPBUILDING

- Automation of Ship Control on Basis of Satellite Communications and Navigation Systems  
(A. V. Likhachev, Ye. V. Yakshevich; SUDOSTROYENIYE, No 9, Sep 84)..... 1
- Passenger Riverboat-Hovercraft 'Luch'  
(V.K. Zoroastrov, V.N. Tsipershteyn; SUDOSTROYENIYE, No 9, Sep 84)..... 2
- Electrical Propulsion Systems with Counterspining Double-Rotor Motor for Drive of Coaxial Propeller Pair  
(S.A. Alekseyev; SUDOSTROYENIYE, No 9, Sep 84)..... 2
- Comparative Evaluation of Reversing Characteristics of Turbogear and Turboelectric Propeller Drives  
(V.A. Gulyy, M.Ya. Lekakh; SUDOSTROYENIYE, No 7, Jul 84)..... 3
- Questions on the Unification of Screw Propellers  
(G.G. Martirosov, A.D. Domarev; SUDOSTROYENIYE, No 7, Jul 84)..... 4

#### NUCLEAR ENERGY

- Gas Supply System for 35-cm<sup>3</sup> Liquid Tritium Target  
(V.M. Bystritskiy, Ya. Voznyak, et al.; PRIBORY I TEKHNIKA EKSPERIMENTA, No 4, Jul-Aug 84)..... 5

# NON-NUCLEAR ENERGY

High-Altitude Testing of Selective Optical Coatings for Solar Radiators and Collectors (M.I. Umarova; IZVESTIYA AKADEMII NAUK TADZHIKSOY SSR OTDELENIYE FIZIKO-MATEMATICHESKIKH, FIZICHESKIKH I GEOLOGICHESKIKH NAUK, No 1 (91), Jan-Mar 84).....	6
Selective Coatings for Solar Heat Converters (M.I. Umarova; IZVESTIYA AKADEMII NAUK TADZHIKSOY SSR OTDELENIYE FIZIKO-MATEMATICHESKIKH, FIZICHESKIKH I GEOLOGICHESKIKH NAUK, No 2 (92), Apr-Jun 84).....	6
Cost Estimation and Cost Reduction of Solar Collector for Solar Heating System (M.I. Valov, V.A. Astashenko, et al.; GELIOTEKHNIKA, No 3, Mar 84).....	7
Choice of Optimum Surface for Intermediate Heat Exchanger in Dual-Loop Solar System (V. K. Aver'yanov, A.I. Tyutyunnikov; GELIOTEKHNIKA, No 3, Mar 84).....	8
Structural Optimization of Control System of Solar Powerplant Heliostat Field (D. Berzh, V.V. Malyshko, et al.; GELIOTEKHNIKA, No 3, Mar 84).....	8
Thermodynamic Analysis of Some Promising Chemical Reactions for Heat Storage at Solar Powerplants (R. B. Akhmedov, V.A. Pozharnov, et al.; GELIOTEKHNIKA, No 3, Mar 84).....	9
Investigation of Conical Concentrates with Axial Receiver (O.I. Kudrin, V. P. Volodin, et al.; GELIOTEKHNIKA, No 3, Mar 84).....	9
Transfer Function of Optical Sensor in Solar Radiation Flux Spatial Stabilization System (A. G. Kostyukovskiy; GELIOTEKHNIKA, No 3, Mar 84)....	10
Facet Spraying for Solar Concentrators (A. V. Kondratov, A. A. Potapenko; GELIOTEKHNIKA, No 3, Mar 84).....	10
Accumulation of Heat by Low-Temperature Melt (M. M. Poberezhnyuk, S. A. Kudrya, et al.; GELIOTEKHNIKA, No 3, Mar 84).....	11

New Switching Materials for Solar Thermal Converters Based on Bismuth and Tin Chalcogenides (K. Sh. Kakhramanov, V. A. Mazur, et al.; GELIOTEKHNIKA, No 3, Mar 84).....	11
Investigation of Solar Flat-Plate Thermal Elements (N. S. Lidorenko, O. P. Astakhov, et al.; GELIOTEKHNIKA, No 3, Mar 84).....	12
Flat Magnetohydrodynamic Induction Pump (Ya. Ya. Valdmanis, R. R. Krishberg, et al.; MAGNITNAYA GIDRODINAMIKA, No 4, Oct-Dec 84).....	12
Dependence of Characteristics of Centrifugal Magnetohydro- dynamic Conduction Pump on Electrical Conductance of End Walls, Part 1: Experiment (V. A. Gorbunov, A. A. Klyukin, et al.; MAGNITNAYA GIDRODINAMIKA, No 4, Oct-Dec 84).....	13
Error of Parametric Reliability of Magnetohydrodynamic Pump (Yu. P. Agafonov; MAGNITNAYA GIDRODINAMIKA, No 4, Oct-Dec 84).....	14
Dependence of Characteristics of Magnetohydrodynamic Induction Pump on Electrical Conductance of Channel Walls (B. N. Siplivyy, V. F. Petrov; MAGNITNAYA GIDRODINAMIKA, No 4, Oct-Dec 84).....	14
Labor Efficient Design Schemes for Foundations Under Large Turbine Sets (P. M. Sverdlov; ENERGETICHESKOYE STROITEL'STVO, No 8, Aug 84).....	15
Flexible Foundations for Thermalized 100 MW Turbines (Ye.G. Babskiy, L.V. Il'in; ENERGETICHESKOYE STROITEL'STVO, No 8, Aug 84).....	15

#### INDUSTRIAL TECHNOLOGY

Precision Optical Method for Oriented Crystal Cutting (B.A. Matveyev, N.M. Stus', et al.; OPTIKO- MEKHANICHESKAYA PROMYSHLENNOST', No 6, Jun 84).....	17
Design Method for Solid State Cryogenic Coolers (I.M. Pilat, V.S. Zinov'ev, et al.; OPTIKO- MEKHANICHESKAYA PROMYSHLENNOST', No 6, Jun 84).....	17
Interface Controller for Elektronika-DZ-28 Microcomputer and MT 1016 Numeric Printer (A.A. Abyzov, V.V. Pakhomov; PRIBORY I TEKHNIKA EKSPERIMENTA, No 4, Jul-Aug 84).....	18

Automated System for Controlling Heat Treatment of Nuclear Powerplant Articles (N. G. Afanasiadi, V.P. Demin, et al.; ENERGOMASHIN-OSTROYENIYE, No 7, Jul 84).....	18
Reliability of Automatic Control Systems for Technological Research (Yu.G. Zarenin, V.I. Kutovoy; IZMERENIYA, KONTROL', AVTOMATIZATSIYA, No 1(49), 1984).....	19
Vibrations of Rotors Connected Through Couplings with Backlash (E.L. Poznyak, G.P. Mayorov; MASHINOSTROYENIYE, No 5, Sep-Oct 84).....	19
Dynamic Characteristics of Drive with Closed-Loop Self-Braking Servomechanism (V.L. Veyts, I.A. Gidasov; MASHINOSTROYENIYE, No 5, Sep-Oct 84).....	20
Damping Systems for Random Vibratory Action (G.V. Kostin, V.I. Konychev, et al.; MASHINOVEDENIYE, No 5, Sep-Oct 84).....	20
Ultimate Capabilities and Efficiency of Resonance-Type Machines (M.Ye. Gerts; MASHINOVEDENIYE, No 5, Sep-Oct 84).....	21
Nonlinear Flexural Vibrations of Working Members in Machines with Dual Drive Mechanisms (I.I. Vul'fson; MASHINOVEDENIYE, No 5, Sep-Oct 84).....	22
Stability of Thrasher Bearings with Profile on Bushing or Shaft Surface (O.N. Tikhonenkova; MASHINOVEDENIYE, No 5, Sep-Oct 84)...	22
Heat Exchanges for Utilizing Low-Grade Heat of Fan Exhaust Air (Ye.P. Volkov; PROMYSHLENNAYA ENERGETIKA, No 9, Sep 84)...	23

#### TURBINE ENGINE DESIGN

Reliability of Vacuum Deaeration Installations in TETs (V. I. Sharapov; ELEKTRICHESKIY STANTSII, No 7, Jul 84).....	24
Adjustment and Operation of Regulating Systems for Type K-800-240-3 LMZ Turbines (V. V. Shakalo; ELEKTRICHESKIY STANTSII, No 7, Jul 84)...	24

Design of Disk Spring for Automatic Disk Safety Device (P.A. Rybin, K. B. Sarantsev, et al.; ENERGOMASHINOSTROYENIYE, No 7, Jul 84).....	25
Erosion of Working Vanes of Auxiliary Turbines (A. V. Semenyuk, A. G. Reznik; ENERGOMASHINOSTROYENIYE, No 7, Jul 84).....	25
Determination of Size and Weight Requirements of Gas Turbine Installation from Cycle Parameters (S. P. Zaritskiy, A. G. Vertepov; ENERGOMASHINOSTROY- ENIYE, No 7, Jul 84).....	26
Characteristics of Design of Turbine Stages with Tangential Inclination of Guide Vanes (A. I. Kirillov, Ya. A. Sirotkin, et al.; ENERGOMASHINOSTROYENIYE, No 7, Jul 84).....	26
Precision Die Forging of Blades for Gas Turbines (E. G. Shastin; ENERGOMASHINOSTROYENIYE, No 8, Aug 84).....	27
Stressed-Strained State of Tightening Buckles in Sectional Runners of Gas Turbines (I.K. Bakumenko, N.A. Kulakovskaya; ENERGOMASHIN- OSTROYENIYE, No 9, Sep 84).....	27
Experience with Vibration Testing and Balancing of Rotors of Large Hydraulic Units (I.R. Solov'ev; GIDROTEKHNICHESKOYE STROITEL'STVO, No 9, Sep 84).....	28
Experience with Operation and Repair of Hydraulic Turbine Impeller Chamber (M.I. Gal'perin, I.I. Shriro, et al.; GIDROTEK- HNICHESKOYE STROITEL'STVO, No 9, Sep 84).....	29
High-Temperature Fluidic Turbogenerator as Attachment to Gas Turbine (N.A. Shershnev, A.N. Sinenkoy, et al.; TEPLOFIZIKA VYSOKIKH TEMPERATUR, No 3, May-Jun 84).....	29
Experimental Study of Two-Stage Turbine Bleeder with Transition Nozzle Between Stages (I.G. Gogolev, R.V. Kuz'michev, et al.; TEPLOENERGETIKA, No 7, Jul 84).....	30
Calculation of Friction at Spherical Bearing Journals in Turbomachines (G. A. Khanin, L.G. Khanin; TEPLOTEKHNIKA, No 10, Oct 84).....	31

Erosion of Turbine Runner Blades (V.V. Pryakhin, O.A. Povarov, et al.; TEPLOENERGETIKA, No 10, Oct 84).....	31
---	----

#### HIGH-ENERGY DEVICES, OPTICS, PHOTOGRAPHY

Video Monitor Device for Electron Microscope (E.P. Bocharov, B.I. Pilenko; OPTIKO-MEKHANICHESKAYA PROMYSHLENNOST', No 6, Jun 84).....	33
---	----

Unpolarized Radiation Modulator Based on Lead Zirconate- Titanate Ceramic with Lanthanum (A. M. Sosenskiy, N.N. Kazantseva, et al.; OPTIKO- MEKHANICHESKAYA PROMYSHLENNOST', No 6, Jun 84).....	33
--	----

Technological Process for Manufacturing Multifaceted Prisms (A.I. Zhdanov; OPTIKO-MEKHANICHESKAYA PROMYSHLENNOST', No 6, Jun 84).....	34
---	----

Investigation of Influence of Polishing Conditions on Surface Roughness of Glasses of Different Composition (S.V. Kryukova, S.V. Yeremina, et al.; OPTIKO- MEKHANICHESKAYA PROMYSHLENNOST', No 6, Jun 84).....	34
---	----

Investigation of Automatic Stabilization System for Composite Mirrors of Adaptive Telescope (V.I. Kryukov, A.K. Rodionov, et al.; OPTIKO- MEKHANICHESKAYA PROMYSHLENNOST', No 6, Jun 84).....	35
--	----

Self-Scanning MDS-Integrated Photodetector Strip (Yu.Kh. Kagan, E.L. Kashcheyev, et al.; AVTOMETRIYA, No 3, May-Jun 84).....	36
--	----

Self-Scanning MDS Integrated Photosensor Strip (Yu. Kh. Kagan, E. L. Kashcheyev, et al.; AVTOMETRIYA, May-Jun 84).....	37
--	----

Holographic Intensity Correlator with Pris-type Photo- electrooptical Controllable Transparency (A.N. Oparin, O.I. Potaturkin, et al.; AVTOMETRIYA, No 3, May-Jun 84).....	48
---	----

Holographic Intensity Correlator with Pris-type Photoelectric- Optical Controlled Transparency (A.N. Oparin, O.I. Potaturkin, et al.; AVTOMETRIYA, May-Jun 84).....	49
--	----

Design Method for Telescopic System Consisting of Thin Element and Finite-Thickness Lens (V.V. Tarabukin; OPTIKO-MEKHANICHESKAYA PROMYSHLENNOST', No 6, Jun 84).....	55
---	----

Analysis of Thermo-optical Aberrations of Focusing Mirrors (G.I. Pogodin, E.V. Truneva, et al.; OPTIKO- MEKHANICHESKAYA PROMYSHLENNOST', No 6, Jun 84).....	55
Molecular Lamination of Titanium Oxygen Layers and their Influence on the Chemical Stability of Optical Glass (V.A. Tolmachev, M.A. Okatov, et al.; OPTIKO- MEKHANICHESKAYA PROMYSHLENNOST', No 6, Jun 84).....	56
High-Angular-Resolution Spectrometer with Dual Neutron Beam Monochromatization (Yu. Abov, F.G. Kulidzhanov, et al.; PRIBORY I TEKHNIKA EKSPERIMENTA, No 4, Jul-Aug 84).....	56
Diana 700-Liter Xenon Bubble Chamber (V.V. Barmin, V.N. Borisov, et al.; PRIBORY I TEKHNICA EKSPERIMENTA, No 4, Jul-Aug 84).....	57
Laser System for Holographic Recording of Information From Track Detector (Ye. Bartke, I.Ts. Ivanov, et al.; PRIBORY I TEKHNICA EKSPERIMENTA, No 4, Jul-Aug 84).....	57
Electronic Equipment Test System for Multichannel Drift Chambers (V.V. Karpukhin; PRIBORY I TEKHNICA EKSPERIMENTA, No 4, Jul-Aug 84).....	58
Spectral Properties of Variable-Focus Membrane Mirror (V.V. Motoshkin, S.M. Slobodyan; PRIBORY I TEKHNICA EKSPERIMENTA, No 4, Jul-Aug 84).....	58
Fiber-Optic Modulators (A.V. Kukhta, Ye.I. Sverchkov, et al.; PRIBORY I TEKHNIKA EKSPERIMENTA, No 4, Jul-Aug 84).....	59
Small Low-Noise Microwave-Pumped He-Ne Laser (V.M. Geller, G.I. Grif, et al.; PRIBORY I TEKHNICA EKSPERIMENTA, No 4, Jul-Aug 84).....	59
Circuit for Synchronizing Radiation from Two LTI-5 Lasers (V.I. Belousov, S.V. Chernyakov, et al.; PRIBORY I TEKHNIKA EKSPERIMENTA, No 4, Jul-Aug 84).....	60
Device for Pulse-Amplitude Modulation of Laser Radiation Power (B.A. Zverev, S.V. Pakhomov, et al.; PRIBORY I TEKHNIKA EKSPERIMENTA, No 4, Jul-Aug 84).....	60
Wide-Beam Electron Gun (Yu.V. Grigor'yev, V.I. Perevodchikov, et al.; PRIBORY I TEKHNICA EKSPERIMENTA, No 4, Jul-Aug 84).....	61

Automatic Scanning Manipulator for Mass Spectrometer Employing Laser-Plasma Ion Source (A.I. Busygin, V.V. Drozdov, et al.; PRIBORY I TEKHNICA EKSPERIMENTA, No 4, Jul-Aug 84).....	61
Light Splitter Based on Three-Dimensional Holographic Diffraction Grating (N.G. D'yachenko, V.Ye. Mandel', et al.; PRIBORY I TEKHNICA EKSPERIMENTA, No 4, Jul-Aug 84).....	62
High Speed Spectrophotometer for Measuring Spectral Characteristics of Optical Coating During Preparation in Vacuum (D.Ye. Yefremov, L.I. Zelikman, et al.; PRIBORY I TEKHNICA EKSPERIMENTA, No 4, Jul-Aug 84).....	62
High Frequency System of Jinv Proton Synchrotron for Light Nucleus Acceleration (O.I. Brovko, A.I. Mikhaylov, et al.; PRIBORY I TEKHNICA EKSPERIMENTA, No 4, Jul-Aug 84).....	63
Continuous Electron Accelerator Employing Secondary Ion- Electron Emission (M.A. Abroyan, N.A. Uspenskiy, et al.; PRIBORY I TEKHNICA EKSPERIMENTA, No 4, Jul-Aug 84).....	64
Steady-State Source of Negative Hydrogen Ions with Hollow Cathode (S.P. Antipov, L.I. Yelizarov, et al.; PRIBORY I TEKHNICA EKSPERIMENTA, No 4, Jul-Aug 84).....	64
Design and Heater Characteristics of Thermoemission Cathode for Microtron (E.A. Luk'yanenko, Yu.Ye. Tokarev, et al.; PRIBORY I TEKHNICA EKSPERIMENTA, No 4, Jul-Aug 84).....	65
Acousto-Optical Cells for Deflecting Radiation of Semiconductor Laser (Yu.N. Tishchenko, A.V. Trubetskoy; AVTOMETRIYA, No 3, May-Jun 84).....	65
Use of Semiconductor Lasers in Holographic Correlators (S.M. Borzov, O.I. Potaturkin; AVTOMETRIYA, No 3, May-Jun 84).....	66
Enhancing Accuracy of Diffraction Methods for Dimension Testing (R.M. Bychkov, B.Ye. Krivenkov, et al.; AVTOMETRIYA, No 3, May-Jun 84).....	66

Investigation of Speed of Optical Information Converter Based on MF-16 Integrated Photodetector Array (V.M. Komarov; AVTOMETRIYA, No 3, May-Jun 84).....	67
Diffraction Interferometer (V.P. Koronkevich, G.A. Lenkova; AVTOMETRIYA, No 3, May-Jun 84).....	67
Acousto-Optical Modulator with Counter Acoustic Beams on Optically Active Uniaxial Crystal (V.A. Tarkov, Yu.N. Tishchenko, et al.; AVTOMETRIYA, No 3, May-Jun 84).....	68
Automatic Device for Recording Digital Data Hologram Matrices (A.A. Blok, B.V. Vanyushev, et al.; AVTOMETRIYA, No 3, May-Jun 84).....	68
Hybrid Optoelectronic Systems for Inspection and Automatic Classification of Images (N.S. Rozin'kov; IZMERENIYA, KONTROL', AVTOMATIZATSIYA, No 1(49), 1984).....	69
Automatic Measurement of Fast Processes with Aid of Time- Scale Conversion (Yu.A. Golovastikov, S.G. Rabinovich, et al.; IZMERENIYA, KONTROL', AVTOMATIZATSIYA, No 1(49), 1984)...	70
Investigation of Possibilities of Fabricating Lightweight Thin Light-Focusing Mirrors (G. Ya. Umarov, A.K. Alimov, et al.; GELIOTEKHNIKA, No 3, Mar 84).....	71
Optimization of Cathode Lenses with 'Efir' Applied Program Package (V.P. Il'in, V.A. Kateshov, et al.; AVTOMETRIYA, No 5, Sep-Oct 84).....	71
Linear Model of MOS-Integrated Photodiode-Type Multielement Optical Signal Converters (S.I. Naymark; AVTOMETRIYA, No 5, Sep-Oct 84).....	72
Structure of Photometric Channel in High-Speed Microdensitometer and Errors of Photometric Measurement (V.P. Kosykh; AVTOMETRIYA, No 5, Sep-Oct 84).....	73
Production of Optical Fiber Bundles with Equalization of Illuminance at Exit (V.I. Shashin, V.A. Gurenko; OPTIKO-MEKHANICHESKAYA PROMYSHLENNOST', No 7, Jul 84).....	74

Use of Varnished Polyethylene Terephthalate Film as Trans-illuminated Screen (G.P. Lenisyuk, G.Ya. Solov'yev, et al.; OPTIKO-MEKHANICHESKAYA PROMYSHLENNOST', No 7, Jul 84).....	74
Protective Characteristics of Electrically Conducting Transparent Vacuum-Deposited Coatings (B.P. Krzhizhanovskiy; OPTIKO-MEKHANICHESKAYA PROMYSHLENNOST', No 7, Jul 84).....	75
Dependence of Telescope - Observer Resolving Power on Shape and Size of Front Iris (V.Ya. Vasil'yev, V.P. Dubenskov, et al.; OPTIKO-MEKHANICHESKAYA PROMYSHLENNOST', No 7, Jul 84).....	75
Matching Characteristics of Graded-Index Optical Fibers in Splice (S.N. Avakov, M.G. Zguladze, et al.; OPTIKO-MEKHANICHESKAYA PROMYSHLENNOST', No 7, Jul 84).....	76
Color Transmission by Camera Objectives with Achromatic Transparency Coatings (G.D. Pridatko, N.P. Yevteyeva, et al.; OPTIKO-MEKHANICHESKAYA PROMYSHLENNOST', No 7, Jul 84).....	76
Model ASHS-15 Automatic Machine Tool for Diamond Grinding of Optical Components (A.F. Roshak, E.T. Samuylov, et al.; OPTIKO-MEKHANICHESKAYA PROMYSHLENNOST', No 7, Jul 84).....	77
Holographic Corrector in Objective with Compound Main Mirror (Yu.D. Pimenov, Yu.Ye. Kuzilin, et al.; OPTIKO-MEKHANICHESKAYA PROMYSHLENNOST', No 7, Jul 84).....	78
Performance Evaluation of Fiber-Optic Converters (M.A. Farakhutdinova, N.T. Suleymanov; OPTIKO-MEKHANICHESKAYA PROMYSHLENNOST', No 7, Jul 84).....	78

#### FLUID MECHANICS

Planar Particle-Laden Gas Flow About Thin Bodies (R.R. Aydagulov; DOKLADY AKADEMII NAUK SSSR, No 2, Jul 84).....	80
Characteristics of Steady-State Hypersonic Flow About Blunted Bodies with Discontinuities in Generators (V.D. Sirova; VESTNIK LENINGRADSKOGO UNIVERSITETA: MATEMATIKA MEKHANIKA ASTRONOMIYA, No 3, Jun 84).....	80

Impact Starting of Plane Nozzles with Wide Divergence Angle (A.B. Britan, Ye. I. Vasil'yev; IZVESTIYA AKADEMII NAUK SSSR: MEKHANIKA ZHIDKOSTI I GAZA, No 4, Jul-Aug 84).....	81
Buildup of Oscillation of Bodies in Stratified Fluid (I.S. Dolina; IZVESTIYA AKADEMII NAUK SSSR: MEKHANIKA ZHIDKOSTI I GAZA, No 4, Sep-Oct 84).....	81
Supersonic Flow Around Blunt Wedge (S.V. Manuylovich; IZVESTIYA AKADEMII NAUK SSSR: MEKHANIKA ZHIDKOSTI I GAZA, No 4, Jul-Aug 84).....	82
Propulsion Efficiency of Vibrating Bodies in Subsonic Gas Stream (M.N. Kogan, M.V. Ustinov; IZVESTIYA AKADEMII NAUK SSSR: MEKHANIKA ZHIDKOSTI I GAZA, No 4, Jul-Aug 84).....	83
Stefan-Maxwell Relations for Plasma Diffusion Currents in Magnetic Field (A.F. Kolesnikov, G.A. Tirskiy; IZVESTIYA AKADEMII NAUK SSSR: MEKHANIKA ZHIDKOSTI I GAZA, No 4, Jul-Aug 84).....	83
Method of Calculating Separation Flow of Subsonic Gas Stream Around Wings (S.M. Belotserkovskiy, V.N. Korzhnev, et al.; IZVESTIYA AKADEMII NAUK SSSR: MEKHANIKA ZHIDKOSTI I GAZA, No 4, Jul-Aug 84).....	84
Supersonic Flow Around Weak Radiation Sources (K.V. Krasnobayev; IZVESTIYA AKADEMII NAUK SSSR: MEKHANIKA ZHIDKOSTI I GAZA, No 4, Jul-Aug 84).....	85
MECHANICS OF SOLIDS	
Elastic Equilibrium of Composite Shells with Finite Shear Rigidity (Ya. M. Grigorenko, I.S. Mukha, et al.; DOKLADY AKADEMII NAUK UKRAINSKOY SSR: SERIYA A FIZIKO- MATEMATICHESKIYE I TEKHNIЧЕСKIY NAUKI, No 7, Jul 84)....	86
Stability of Cylindrical Shells with Variable Thickness under External Pressure (V.V. Kabanov, L.P. Zheleznov; PRIKLADNAYA MEKHANIKA, No 7, Jul 84).....	86
Natural Vibrations of Reinforced Spherical Shells (V.N. Revutskiy; PRIKLADNAYA MEKHANIKA, No 7, Jul 84)....	87
Numerical Solution of One-Dimensional Nonlinear Problems of Statics for Elastic Beams and Shells under Rigid Constraints (S.A. Kabrits, V.P. Terent'yev; PRIKLADNAYA MEKHANIKA, No 7, Jul 84).....	88

Method of Solving Problems of Statics for Multilayer Shells of Revolution (B.G. Popov, E.V. Raman; PRIKLADNAYA MEKHANIKA, No 7, Jul 84).....	89
Scattering of Sounds by Piezoceramic Cylindrical Shell Near Rigid Surface (I.V. Senchenko; PRIKLADNAYA MEKHANIKA, No 7, Jul 84)....	90
Propagation of Non-Axisymmetric Elastic Waves Through Shell with Filler Under Radial Load at One End (Yu.V. Mastinovskiy, Yu.I. Nagornyy; PRIKLADNAYA MEKHANIKA, No 7, Jul 84).....	90
An Approximate Method for Solving the Heat Conductivity Problem for a Hollow Cylinder (S.Yu. Yusupov; IZVESTIYA AKADEMII NAUK TADZHIKSOY SSR OTDELENIYE FIZIKO-MATEMATICHESKIKH, FIZICHESKIKH I GEOLOGICHESKIKH NAUK, No 1(91), Jan-Mar 84).....	91
Acoustic Oscillations of Rods and Plates (A.V. Zakharov, A.R. Vazylov, et al.; IZVESTIYA AKADEMII NAUK TADZHIKSOY SSR OTDELENIYE FIZIKO-MATEMATICHESKIKH, FIZICHESKIKH I GEOLOGICHESKIKH NAUK, No 2 (92), Apr-Jun 84).....	92

#### TESTING & MATERIALS

Clamping Devices for Circular Instrumentation Transducers (B.N. Ivanov; OPTIKO-MEKHANICHESKAYA PROMYSHLENNOST', No 6, Jun 84).....	93
Practical Application of 'Grounding Effect' (M.A. Sultanov; IZVESTIYA AKADEMII NAUK TADZHIKSOY SSR OTDELENIYE FIZIKO-MATEMATICHESKIKH, FIZICHESKIKH I GEOLOGICHESKIKH NAUK, No 1 (91), Jan-Mar 84).....	93
NMR Manometer for Measuring High Pressures at Liquid-Helium Temperatures (V.D. Doroshev, N.M. Kovtun, et al.; PRIBORY I TEKHNIKA EKSPERIMENTA, No 4, Jul-Aug 84).....	94
Technology for Producing Synthetic Iron for Nuclear Power Plant Parts (N.K. Blozhko, Petrov, et al.; ENERGOMASHINOSTROYENIYE, No 7, Jul 84).....	95
Principles of Designing Digital Compensating Accelerometers (A.I. Skalon; IZMERENIYA, KONTROL', AVTOMATIZATSIYA, No 1(49), 1984).....	95

Uniaxial Angular Accelerometers (A.V. Seleznev; IZMERENIYA, KONTROL', AVTOMATIZATSIYA, No 1(49), 1984).....	96
Technological Apparatus for Laser Treatment of Materials (A.V. Kirillin, A.V. Kostanovskiy, et al.; TEPLOFIZIKA VYSOKIKH TEMPERATUR, No 6, May-Jun 84).....	97
Apparatus for Measuring Velocity of Sound in Fluids (D.L. Timrot, M.A. Serednitskaya, et al.; TOPLOFIZIKA VYSOKIKH TEMPERATUR, No 3, May-Jun 84).....	98
Liquid-Metal Transducers for Strain Measurement During In-Pile Materials Testing (V.A. Neverov, Yu.L. Revyakin; ATOMNAYA ENERGIYA, No 5, Nov 84).....	98

MARINE AND SHIPBUILDING

UDC 656.61.052.4-52:621.396.932.1

AUTOMATION OF SHIP CONTROL ON BASIS OF SATELLITE COMMUNICATIONS AND NAVIGATION SYSTEMS

Leningrad SUDOSTROYENIYE in Russian No 9, Sep 84 pp 24-26

LIKHACHEV, A. V. and YAKSHEVICH, Ye. V.

[Abstract] Automatic control of ships involves judicious use of "internal" information about equipment and facilities on board, "close range" information for navigating relative to the immediate environment and close objects, "long range" information for navigating relative to hydrological and weather forecasts, and "steering" information pertinent to the propulsion technology. The latest trend in automatic ship control is use of satellite communication and navigation systems for this purpose. These systems have generally a modular structure, with some built-in flexibility and with program software for each data processing objective (calculation of coordinates, prevention of collision, logging, etc). A characteristic feature of such an automatic control is distinct separation of primary and secondary processing, of stochastic and deterministic data respectively. The leading system now in operation is the U.S. Satellite-Aided Coastal Zone Monitoring and Vessel Traffic System. Its essential components are a PDP-11/45 computer with color display and data input/output equipment. The international COPSAT-SARSAT experiment now under way should result in a global system ready for operation by the year 1990. Recent developments indicate a trend toward maximum hardware economy and maximum compatibility with existing radio communication and navigation systems. Figures 2; references 4: 3 Russian, 1 Western.

[61-2415]

UDC 629.122.6.039

PASSENGER RIVERBOAT-HOVERCRAFT 'LUCH'

Leningrad SUDOSTROYENIYE in Russian No 9, Sep 84 pp 3-4

ZOROASTROV, V.K. and TSIPERSHTEYN, V.N.

[Abstract] Passenger riverboats of the "Zarnitsa" class are the first generation of hovercraft. After several decades of operation, they are becoming obsolete and ready for replacement. The second generation of such boats will retain all the advantages of operation on shallow-water small rivers, but with better reliability, longer service life, easier repair and overhaul, higher speed over a larger water territory, and greater passenger and crew comfort. The first new boat "Luch-1" has already been built and thoroughly tested, then in November 1983 turned over to the Astrakhan River Port Authority. The capacity of this boat is 51 passengers, with a full-load displacement of 20.1 tons. Its overall dimensions are 22.8 m length, 3.85 m width, 3.35 m height (rail height 1.2 m, skirt height 0.45 m). The base structure is built with AMg-61 aluminum-magnesium alloy, the superstructure is built with D16 aluminum alloy. The air cushion is produced in a high-pressure chamber under the bottom. A major innovation is use of a more powerful diesel engine (382 kW - 1500 rpm), a 3KD12N-520 model, which drives the waterjet motor and, through a takeoff shaft, actuates the air compressor. The propeller screws and the metal-resin thrust bearing can be removed and replaced during floating, without the boat being lifted out of water. Electric power for auxiliaries, lights and appliances is supplied by a 24 V - 1.2 kW d.c. generator on top of the diesel engine and a bank of storage batteries, with provisions for hookup to a 220 V - 50 Hz power line. Remote control and automatic fault detection-warning allow a single operator to drive the boat. The main functional divisions of the boat are prow, steering booth, guard booth, vestibule, passenger lounge, facility rooms, engine compartment, and stern. On the basis of successful acceptance tests, the design of "Luch" boats has been finalized and their construction has already begun on a commercial scale. Figures 1; tables 1.  
[61-2415]

UDC 621.313.3:629.12.03-83

ELECTRICAL PROPULSION SYSTEMS WITH COUNTERSPINNING DOUBLE-ROTOR MOTOR FOR DRIVE OF COAXIAL PROPELLER PAIR

Leningrad SUDOSTROYENIYE in Russian No 9, Sep 84 pp 27-28

ALEKSEYEV, S.A.

[Abstract] Counterspining double-rotor motors are used in variable-speed electrical propulsion systems with oppositely rotating coaxial propeller screws. Such a system consists of a prime mover, turbine or diesel engine,

driving a synchronous a.c. generator whose stator outputs voltage through a voltage regulator to the induction motor with or without brushes and slip rings. In the case of brushes and slip rings, a single-rotor generator is connected to a double-rotor motor directly or through a frequency converter, with mechanical coupling to both prime mover and propeller, or a double-rotor generator is connected to a single-rotor motor also with mechanical coupling to both prime mover and propeller. In the contactless case a single-rotor generator is connected to a double-rotor motor along with an auxiliary induction generator directly or through a frequency converter, or a double-rotor generator is connected to a single-rotor motor directly or through a frequency converter. The advantage of using an auxiliary induction generator is reduction of the shafting length to nearly one third. Prototype drives using double-rotor motors with frequency converter and single-rotor or double-rotor synchronous generator have been built and experimentally evaluated. A drive with a high-speed synchronous generator coupled to the prime mover without gear reduction, thyristor-type frequency converter, and a double-rotor induction motor was found to be most promising. A water-cooled thyristor bank can be made as small as 1-0.1 kg/kW or 2-0.25 dm<sup>3</sup>/kW for controlling 0.5-20 MW motors. Either rolling or sliding double layer bearings are required for drives larger than 300 kW and propeller speeds up to 200 rpm. Figures 3; references 8: 6 Russian, 2 Western.  
[61-2415]

UDC 629.12.03-832

#### COMPARATIVE EVALUATION OF REVERSING CHARACTERISTICS OF TURBOGEAR AND TURBO-ELECTRIC PROPELLER DRIVES

Leningrad SUDOSTROYENIYE in Russian No 7, Jul 84 pp 17-19

GULYY, V.A. and LEKAKH, M.Ya.

[Abstract] On large Soviet ships, particularly nuclear icebreakers, the main steam turbine as prime mover drives a fixed-pitch propeller screw through a reversible electric transmission. This eliminates the need for the second turbine which must be available for reverse drive in the case of a mechanical gear transmission. The advantage of a turboelectric drive over a turbogear drive can be fully realized only with an adequate torque-speed and reversing-time characteristic. These characteristics of both drives are compared here, with the braking mode included in the transition from forward to reverse motion and with a quadratic parabola closely enough approximating the pull-up range of the curve. The comparison reveals that the reversing process is slower with an electric transmission, because of larger inertia and limited means for dissipation of transient power buildup. An analysis of these characteristics indicates two ways to reduce the reversing time. One is to increase the load on the turboelectric drive running as generator during reversing. Another way is to feed the braking power from the propeller screw, which runs as turbine during reversing, to the main turbine with a specially added power dissipating

stage. Steam must be fed to the braking stage while less steam is fed to the main stages during reversing, with the speed regulators on the turbine shut down. Figures 1; references: 5 Russian.  
[62-2415]

UDC 629.12.037.1.008.03.

#### QUESTIONS ON THE UNIFICATION OF SCREW PROPELLERS

Leningrad SUDOSTROYENIYE in Russian No 7, Jul 84 pp 10-12

MARTIROSOV, G.G. and DOMAREV, A.D.

[Abstract] Arguments and proposals for the unification of screw propellers are proposed. They include stamping, the blueprints of old or outmoded designs to prevent their continuing production and use in newer ships. A unified catalog of blueprints which include an index of hydrodynamic characteristics of each design is proposed to eliminate duplication and near-duplications in designs. It would also shorten the time required for repair of defective screws and facilitate the ordering of new engines. Characteristics of some current screw propellers are tabulated. Figures 2; tables 2.  
[62-12733]

NUCLEAR ENERGY

UDC 66.086:621.384.664

GAS SUPPLY SYSTEM FOR 35-cm<sup>3</sup> LIQUID TRITIUM TARGET

Moscow PRIBORY I TEKHNIKA EKSPERIMENTA in Russian No 4, Jul-Aug 84  
(manuscript received 22 Sep 83) pp 46-49

BYSTRITSKIY, V.M., VOZNYAK, Ya., GULA, A., DZHELEPOV, V.P., KAPYSHEV, V.K.,  
MALEK, M.P., MUKHAMET-GALEYEVA, S.Sh., RIVKIS, L.A., STOLUPIN, V.A.,  
UTKIN, V.A. and SHAMSUTDINOV, Sh.G., Joint Institute of Nuclear Research,  
Dubna.

[Abstract] A gas supply and safety system for a liquid tritium target is described. The gas supply system consists of a high-vacuum evacuation system, the liquid-tritium target, a system for filling the target with tritium, a deuterium cleaning system, dosimetric monitoring equipment and a system to provide personnel protection in case of emergency. The block diagram of the system is presented and explained. The tritium source is titanium tritide heated to 800° C. The deuterium is cleaned by means of zeolite adsorbers. Hydrogen isotopes are removed from the target by absorbers filled with a titanium gas absorber. Liquid hydrogen serves as the coolant. Testing of the system revealed that the emergency protection devices are highly reliable, and satisfy safety practice requirements for experiments with liquid tritium targets. References 6: 5 Russian, 1 Western.  
[64-6900]

NON-NUCLEAR ENERGY

UDC 662.997.537.22

HIGH-ALTITUDE TESTING OF SELECTIVE OPTICAL COATINGS FOR SOLAR RADIATORS AND COLLECTORS

Dushanbe IZVESTIYA AKADEMII NAUK TADZHIKSOY SSR OTDELENIYE FIZIKO-MATEMATICHESKIKH, FIZICHESKIKH I GEOLOGICHESKIKH NAUK in Russian No 1 (91), Jan-Mar 84 (manuscript received 6 Jul 83) pp 77-80

UMAROVA, M.I., Physical-Technical Institute imeni S.U. Umarov, Tadzhik SSR Academy of Sciences.

[Abstract] This study describes the field testing of various selective coatings for solar radiators and collectors performed at elevations of 2500 m above sea level for 150 days in the mountains of Tadzhikistan. It was found that the spectral and integral optical characteristics of the solar converters are degraded far more rapidly at high altitudes than at low. The use of high-altitude exposure makes it possible to obtain more reliable data on the operating characteristics of various types of selective optical coatings. It was found that the optical properties of an absorbing coating consisting of two layers (copper oxide and tin dioxide) on an aluminum substrate remained unchanged after the testing; therefore, this coating is recommended for solar collectors for use under high altitude conditions. References 2 Russian.  
[116-6900]

UDC 662.997:537.22

SELECTIVE COATINGS FOR SOLAR HEAT CONVERTERS

Dushanbe IZVESTIYA AKADEMII NAUK TADZHIKSOY SSR OTDELENIYE FIZIKO-MATEMATICHESKIKH, FIZICHESKIKH I GEOLOGICHESKIKH NAUK in Russian No 2 (92), Apr-Jun 84 (manuscript received 6 Jul 83) pp 61-71

UMAROVA, M.I., Physical-Technical Institute imeni S.U. Umarov, Tadzhik SSR Academy of Sciences

[Abstract] The possibility of obtaining a two-layer selective coating consisting of a ferrous oxide and a transparent conducting layer by

pulverization on a foil substrate in a unified technological process is investigated. In the pulverization method, a solution containing the chemical elements needed to produce the required layer is sprayed onto a heated substrate. The characteristics of a  $\text{CuO} + \text{SnO}_2$  selective coating are investigated in field tests under high altitude conditions, and indicate that this coating is suitable for solar energy converters. The coating is easy to produce, low in cost and resistant to solar radiation.

References 4: 2 Russian, 2 Western.

[116-6900]

UDC 662.997.004.14

#### COST ESTIMATION AND COST REDUCTION OF SOLAR COLLECTOR FOR SOLAR HEATING SYSTEM

Tashkent GELIOTEKNIKA in Russian No 3, Mar 84 (manuscript received 17 May 83) pp 65-69

VALOV, M.I., ASTASHENKO, V.A. and ZIMIN, Ye. N., Moscow Order of Lenin and Order of the October Revolution Power Engineering Institute, USSR Ministry of Higher and Special Education

[Abstract] The possible unit cost of a solar collector in series production is estimated on the basis of existing technology for manufacturing analogous equipment (steel heating radiators and flat-plate heat exchangers). A collector with single glazing and mineral-wool insulation is examined. The unit cost of the solar collector varies from 14 to 43 rubles per square meter, depending upon construction and materials. Plastic collectors are least expensive, and aluminum collectors are most expensive. The use of double glazing increases the unit cost by 1-2 rubles per square meter and increases the weight of the collector by 7-8 kilograms per square meter. 40-60 percent of the cost of a collector goes for the absorbing panel, and about 10 percent for glazing, insulation and assembly. Ways of improving the characteristics of flat-plate collectors are outlined. Figures 1; references 3: 2 Russian, 1 Western.

[303-6900]

UDC 662.997:004.14

CHOICE OF OPTIMUM SURFACE FOR INTERMEDIATE HEAT EXCHANGER IN DUAL-LOOP  
SOLAR SYSTEM

Tashkent GELIOTEKHNICA in Russian No 3, Mar 84 (manuscript received  
6 Jun 83) pp 58-62

AVER'YANOV, V. K. and TYUTYUNNIKOV, A. I., Leningrad

[Abstract] The area of the intermediate heat exchanger in a dual-loop solar system is determined assuming that the heat output of the compared versions are the same. Components with constant values can be omitted by selecting the area of heat exchanger in accordance with minimization of adjusted costs. Heat exchanger efficiency is employed as the optimized variable. Derivation of the efficiency function is investigated. It is found that increasing the area of the heat exchanger increases the efficiency and effective heat release; the reverse is the case when the area is made smaller. The practical case of equal coolant consumption with antifreeze or water in the first loop is analyzed is an example. Figures 2; references 6: Russian.  
[303-6900]

UDC 62-52:552.58:662.991:519.712.3

STRUCTURAL OPTIMIZATION OF CONTROL SYSTEM OF SOLAR POWERPLANT HELIOSTAT  
FIELD

Tashkent GELIOTEKHNICA in Russian No 3, Mar 84 (manuscript received  
1 Feb 83) pp 49-52

BERZH, D., MALYSHKO, V. V. and PED'KO, V. A., Belorussian Branch, State Scientific Research Power Engineering Institute imeni G.M. Krzhizhanovskiy

[Abstract] Practical optimization problems involved in minimizing the total length of cable employed to set up an automatic control system for the heliostat field of a solar powerplant are examined. Models and methods for solving the problems are proposed on the basis of graph theory. Special heuristic optimization methods are constructed. An approximate polynomial algorithm with guaranteed error is developed which yields satisfactory relative deviation of the solution from the precise value. It is shown analytically that uniform arrangement of the heliostats within the field is essential. The algorithm is acceptably accurate and fast, permitting it to be employed in the design of high-power solar powerplants. References 5: 4 Russian, 1 Western.  
[303-6900]

UDC 662.997:537.22

THERMODYNAMIC ANALYSIS OF SOME PROMISING CHEMICAL REACTIONS FOR HEAT STORAGE AT SOLAR POWERPLANTS

Tashkent GELIOTEKHNIKA in Russian No 3, Mar 84 (manuscript received 28 Feb 83) pp 46-49

AKHMEDOV, R. B., POZHARNOV, V. A., CHAKHOVSKIY, V. M., KOLESOV, V. P. and ZHOGIN, D. Yu., State Scientific Research Power Engineering Institute imeni G. M. Krzhizhanovskiy

[Abstract] Chemical reactions are investigated which satisfy the requirements of reversibility in the case of large product yields at temperatures which are achieved in power generators and the inputs to the storage facility, and reaction speed corresponding to low activation energy or the use of a catalyst. The isobar-isotherm potential of a number of promising storage reactions is analyzed. Six candidate reactions are analyzed for which the conversion temperature falls in the 500-1000°C interval. Gas-phase reactions and decomposition of ammonium bisulfate are found to be less suitable for heat storage. Figures 1; references 4: 2 Russian, 2 Western.  
[303-6900]

UDC 662.997.537.22(088.8)

INVESTIGATION OF CONICAL CONCENTRATORS WITH AXIAL RECEIVER

Tashkent GELIOTEKHNIKA in Russian No 3, Mar 84 (manuscript received 3 Jan 83) pp 43-45

KUDRIN, O. I., VOLODIN, V. P., RABBIMOV, R. T. and AKHMEDOV, Kh., Navoysk Branch, Tashkent Order of Peoples' Friendship Polytechnical Institute imeni A. R. Beruni, Moscow Aviation Institute imeni S. Ordzhonidze, and USSR Ministry of Higher and Special Education

[Abstract] The geometry of conical concentrators required to achieve maximum mean concentration is investigated. A conical concentrator is described and analyzed. The concentration is shown to be constant along the entire receiver, which itself is conical. The area of the receiver can be increased without disturbing the uniformity of the radiation but at the expense of reduced average concentration. It is found that a conical concentrator with an axial receiver can be used to deliver radiant energy uniformly through photovoltaic cells. Figures 2.  
[303-6900]

UDC 621.3.078.001

TRANSFER FUNCTION OF OPTICAL SENSOR IN SOLAR RADIATION FLUX SPATIAL  
STABILIZATION SYSTEM

Tashkent GELIOTEKHNICA in Russian No 3, Mar 84 (manuscript received  
10 Feb 83) pp 41-43

KOSTYUKOVSKIY, A. G., Belorussian Branch, Power Engineering Institute,  
imeni G. M. Krzhizhanovskiy

[Abstract] An optical sensor developed to interface the local control system of the SES-5 heliostat as a central control computer is described and analyzed. The device is a two-coordinate optical sensor which detects altitude and azimuth stabilization errors. The collimator-type optical system employed is described, and a simplified equivalent photodiode substitution circuit is presented. It is found that a nonlinear transfer function with a low-sensitivity zone is best from the viewpoint of the power profile, the angle of insensitivity must be directly proportional to the capture angle of the central receiver and the square root of the dimensionless power of the heliostat electric drive. Figures 2; references: 2 Russian.  
[303-6900]

UDC 536.422.4

FACET SPRAYING FOR SOLAR CONCENTRATORS

Tashkent GELIOTEKHNICA in Russian No 3, Mar 84 (manuscript received  
4 Feb 83) pp 37-41

KONDRATOV, A. V. and POTAPENKO, A. A., Northwest Polytechnical Correspondence Institute, RSFSR Ministry of Higher and Special Education, Leningrad

[Abstract] The production of coatings on flat solar concentrator facets with specified widths and maximum and minimum thickness is analyzed. Formulas are derived for the distance between the evaporator and condensing surface and required to obtain the desired coating, and for the rate at which the strip carrying the facet must be moved and the feed rate of the evaporated substance. Figures 1; references 2: Russian.  
[303-6900]

UDC 697.328

#### ACCUMULATION OF HEAT BY LOW-TEMPERATURE MELT

Tashkent GELIOTEKHNIKA in Russian No 3, Mar 84 (manuscript received  
12 Feb 82) pp 22-24

POBEREZHNYYUK, M. M., KUDRYA, S. A. and MINCHENKO, T. G., "Shtorm"  
Design Bureau, Kiev Polytechnical Institute, Ukrainian SSR Ministry of  
Higher and Special Education

[Abstract] The possibility of reducing the working temperature of heat accumulators by employing low-melting nitrate-nitrite-carbamide and nitrate-nitrite-acetamide solutions as the working medium is investigated. The solutions employed have a high phase transition heat, high heat capacity and heat conductance, low cost, easy availability, chemical stability at working temperatures, convenience for recycling and non-toxicity. A low-melting nitrate-nitrite-amide melt is found with a composition of 13 percent K, Na/NO<sub>3</sub>, NaNO<sub>2</sub> and 87 percent acetamide by weight which makes it possible to drop the working temperature of the accumulator to 55°C. Figures 2; references 9: 8 Russian, 1 Western.  
[303-6900]

UDC 621.362:621.383.5

#### NEW SWITCHING MATERIALS FOR SOLAR THERMAL CONVERTERS BASED ON BISMUTH AND TIN CHALCOGENIDES

Tashkent GELIOTEKHNIKA in Russian No 3, Mar 84 (manuscript received  
3 Jan 83) pp 10-12

KAKHRAMANOV, K. Sh., MAZUR, V. A., ALIYEV, A. P. and AKHMEDLI, G. T.,  
Special Design Bureau, "Tellur" Experimental Plant, and the Institute  
of Physics of the Azerbaijan SSR Academy of Sciences

[Abstract] The possibility of employing Bi-Te, Bi-Sn, Bi-Pb and Bi-Cd eutectics as solders in low-temperature solar thermoelectric converters is investigated on the basis of a study of their mechanical compatibility with the working and switching materials employed in the device. The coefficients of linear expansion of the materials are investigated on a general-purpose vacuum dilatometer; the ultimate strength, yield strength and total plastic deformation during compression are measured on a micro-mechanical testing device. It is found that the use of these eutectics as solders makes it possible to obtain a highly elastic intermediate layer between the semiconductor and the metal which increases the service life of the thermoelectric converters. Figures 3; references 4: Russian.  
[303-6900]

UDC 621.362:621.383.5(088.8)

#### INVESTIGATION OF SOLAR FLAT-PLATE THERMAL ELEMENTS

Tashkent GELIOTEKHNICA in Russian No 3, Mar 84 (manuscript received 25 May 83) pp 7-9

LIDORENKO, N. S., ASTAKHOV, O. P. and KOLOMOYETS, N. V., All-Union Order of Labor Red Banner Scientific Research Institute for Current Sources

[Abstract] A flat-plate thermal element with a receiving area 4 cm square made of Kovar alloy is described which functions as a solar collector and a hot-junction switching bus. The thermoelectric materials employed are ternary alloys based on bismuth and tin chalcogenide alloys obtained by zone melting. Tests performed on an experimental batch of devices are described. A number of modifications are suggested to improve the efficiency of the device. Figures 3; references 4: Russian.  
[303-6900]

UDC 621.313.53

#### FLAT MAGNETOHYDRODYNAMIC INDUCTION PUMP

Riga MAGNITNAYA GIDRODINAMIKA in Russian No 4, Oct-Dec 84 (manuscript received 20 Apr 84) pp 101-104

VALDMANIS, Ya. Ya., KRISHBERG, R. R. and SHISHKO, A.Ya.

[Abstract] An experimental study of a flat MHD induction pump was made, for the purpose of evaluating the performance characteristics of such liquid-metal pumps operating at high power levels with high values of the magnetic Reynolds number and a nearly unstable average velocity profile of turbulent flow. A bilateral inductor with 20 slots and 18 turns/slot wound through the yoke, slot width 8 mm and tooth width 6 mm, was used with an 80 mm wide and 5 mm high channel for liquid sodium formed by 1.5 mm thick steel walls. The air gap was 13 mm wide. The inductor coils could be connected in three different ways to form 3, 1.5, or 1 pole pairs (pole pitch 4.2, 8.4, or 12.6 cm correspondingly). Extra coils were added at both ends of the inductor for compensation of the longitudinal end effect. Three baffle plates of stainless steel were inserted longitudinally into the channel for stabilization of the flow within the inductor zone. The tests were performed at 300°C so as to avoid impurity-related changes in the hydraulic properties of sodium at lower temperatures. The magnetic Reynolds number and the synchronous velocity varied respectively from  $3.3 \cdot 10^{-3}f$  and  $8.4 \cdot 10^{-2}f$  m/s in the 6-pole configuration to  $3.0 \cdot 10^{-2}f$  and  $25.2 \cdot 10^{-2}f$  in the 2-pole configuration, with the inductor phase current changed from 30 A to 62.5 A correspondingly and tests performed at four different frequencies  $f$  of the inductor current (50, 100, 150, 200 Hz) in each case. Tests were performed with and without shorting side rails along

the channel. The pressure-flow characteristics as well as the hydraulic drag and the electromagnetic pressure were measured. A theoretical evaluation of the results reveals that the pressure-flow characteristic and the likelihood of instability depend largely on the presence of side rails, on undercompensation of the end effect, and on hydraulic losses in the channel. At high values of the magnetic Reynolds number the electromagnetic pressure remains almost constant over a wide range of slip, without jumps associated with instability. The performance of a pump with fractional number of pole pairs (1.5) is comparable to that of pumps with integral number of pole pairs (3,1). Figures 4; tables 1; references: 2 Russian.  
[148-2415]

UDC 537.84:621.313.532

DEPENDENCE OF CHARACTERISTICS OF CENTRIFUGAL MAGNETOHYDRODYNAMIC CONDUCTION PUMP ON ELECTRICAL CONDUCTANCE OF END WALLS, PART 1: EXPERIMENT

Riga MAGNITNAYA GIDRODINAMIKA in Russian No 4, Oct-Dec 84 (manuscript received 5 Jun 84) pp 105-108

GORBUNOV, V. A., KLYUKIN, A.A., KOLESNIKOV, Yu.B. and KOLOKOLOV, V.Ye.

[Abstract] A centrifugal MHD conduction pump was studied experimentally in a special test stand for determining the dependence of its pressure-flow characteristics on the electrical conductance of its end walls. The active space of such a pump is a horizontal cylindrical cavity filled with liquid metal, flow of the latter from the axis toward the side wall being produced by application of a radial electric field and rotational flow about the axis being produced by application of a constant axial magnetic field. The combined action of both fields drives liquid metal into a pipeline tapped from an orifice in the side wall. Tests were performed with mercury and measurements were made without axial flow, to determine the dependence of the developed radial pressure and the electric field distribution on the electric current and on the magnetic induction with three different pairs of end walls. Pressure was measured with needle-indicator mercury manometers, gradients of the electric potential were measured with a pair of copper wires 0.3 mm in diameter and 2 mm apart forming a conductive probe. The voltage induced by metal flow between the two probe electrodes was measured with a microvoltmeter. The first pair of end walls were disks of a nonconducting material. The second pair of end walls were 1 mm thick disks of solid copper, their electrical conductance being much higher than that of the liquid metal. The third pair of end walls were 0.1 mm thick copper foils on textolite disks, their electrical conductance being approximately equal to that of the liquid metal - a condition similar to that in industrial liquid-lead pumps made of stainless steel. The electric field distribution was found to be qualitatively almost the same but quantitatively very different with thick and thin copper end walls respectively. Figures 6; references: 3 Russian.  
[148-2415]

UDC 621.362:537.84

ERROR OF PARAMETRIC RELIABILITY OF MAGNETOHYDRODYNAMIC PUMP

Riga MAGNITNAYA GIDRODINAMIKA in Russian No 4, Oct-Dec 84 (manuscript received 31 Jan 84) pp 130-132

AGAFONOV, Yu.P.

[Abstract] Parametric reliability is defined as the quantitative probability of operation within given performance tolerances for a given period of time. It is evaluated here relative to MHD pumps, in accordance with the theory of machine manufacturing precision. The analysis is based on the functional relation  $y_i = f_i(x_j)$  between performance parameters  $y_i$  and design parameters  $x_j$ , with allowance for relative deviations of performance parameters from nominal

$$\frac{\Delta y_i}{y_i} = \sum \frac{\partial y_i}{\partial x_j} \frac{x_j}{y_i} \frac{\Delta x_j}{x_j}$$

depending on the relative variances of design parameters  $\frac{\Delta x_j}{x_j}$ . The

error coefficients  $C_{ij} = \frac{\partial y_i}{\partial x_j} \frac{x_j}{y_i}$  are calculated for a flat MHD pump

without side rails, considering six performance parameters (efficiency, power loss, power factor, mass of active components, outlet pressure, magnetic induction in the working gap) and nine design parameters (inductor slot width and tooth width, conductor cross-sectional area, phase current density, line current frequency, flow rate, channel half-width, and coefficients characterizing the influence of the longitudinal end effect on pressure and on secondary reactive power). The parametric stability of an MHD pump can then be determined for a given standard deviation of design parameters. This analysis is never more accurate than analysis based on a mathematical model and its validity must be established for each particular application. Tables 1; references: 4 Russian.

[148-2415]

UDC 621.313.53

DEPENDENCE OF CHARACTERISTICS OF MAGNETOHYDRODYNAMIC INDUCTION PUMP ON ELECTRICAL CONDUCTANCE OF CHANNEL WALLS

Riga MAGNITNAYA GIDRODINAMIKA in Russian No 4, Oct-Dec 84 (manuscript received 24 Apr 84) pp 133-135

SIPLIVYY, B.N. and PETROV, V.F.

[Abstract] The electromagnetic force on the liquid metal in a flat MHD induction pump is calculated, for determining the dependence of its slip characteristic on the electrical conductance of the channel walls.

The analysis is based on applicable two-dimensional Maxwell equations and generalized Ohm's law, assuming a smooth inductor of finite length with equivalent "current sheets" covering the slots. The problem is reduced to an integral equation with respect to the Fourier transform of the transverse component of magnetic induction and then solved by application of the Hilbert-Schmidt theorem in the form of a series in eigenfunctions. Numerical results have been obtained for a 3-pole machine pumping liquid metal with an electric conductivity  $\sigma_m = 5$  MS/m, with the nonmagnetic gap 0.0232 m wide and the layer of liquid metal 0.0136 m high. The force-slip characteristics have been evaluated on this basis for three materials of the channel wall (non-conducting, electrical conductivity  $\sigma_w = 2.5$  MS/m and  $\sigma_w = 5$  MS/m) and for three values of the magnetic Reynolds number ( $Re_m = 3, 5, 7$ ), with and without the longitudinal end effect taken into account. Figures 3; references: 5 Russian.  
[148-2415]

UDC 621.31.002.2.621.165:621.313.322-81:62-217

LABOR EFFICIENT DESIGN SCHEMES FOR FOUNDATIONS UNDER LARGE TURBINE SETS

Moscow ENERGETICHESKOYE STROITEL'STVO in Russian No 8, Aug 84 pp 6-11

SVERDLOV, P.M. [deceased], engineer

[Abstract] Several labor efficient design schemes have been developed and have been or will be implemented for foundations under 50-1200 MW turbine sets in various state regional electric power plants (50 MW in Lenenergo GRES, 500 MW in Ekibastuz GRES, 800 MW in Surgut, Berezovo, Perm, Zaporozhye, Talimardzhan, Uglegorsk GRES), atomic electric power plants (1000 MW in Rovno, Khmel'nik, Southern Ukrainian, Crimean AES, 1200 MW in Kostroma AES), also some heat and electric power plants (100 MW in Norilsk, Northern Lenenergo TETs). The designs are based on concrete and man-hours economy, with most economical but adequate use of steel for reinforcement or in all-metal supporting structure. The necessary carrying capacity and vibration isolation are taken into account. An all-steel foundation is deemed necessary for 200-300 MW turbine sets. Figures 5.  
[72-2415]

UDC 624.15:621.165.313.322-8.621.3.012.6

FLEXIBLE FOUNDATIONS FOR THERMALIZED 100 MW TURBINES

Moscow ENERGETICHESKOYE STROITEL'STVO in Russian No 8, Aug 84 pp 12-15

BABSKIY, Ye.G., engineer, and IL'IN, L.V., engineer

[Abstract] Steel foundation for thermalized 100 MW turbine sets (type I) were built since 1965 according to the standard design by the Leningrad

Department of the Research and Planning Institute for Atomic Heat and Electric Power. Meanwhile, foundations for 50-100 MW and 100-800 MW turbine sets had to be built. While the type I design was essentially retained for foundations under larger turbines, a type II foundation with flexible frames had been designed in 1973 for smaller turbines. This design was subsequently found to be inadequate and, therefore, a study was begun in 1974 for the purpose of developing an adequate one. With the turbine set and the foundation structure treated as an integral dynamic system, this study included vibration analysis during turbine operation in various experimental modes, determining the amplitude-frequency characteristics of shaft bearings and their supports, determining their dynamic compliance as well as that of the foundation structure, and acceptance tests under dynamic conditions with balanced turbine runners. Measurements were made in the Chelyabinsk TETs (type I foundation), Kuybyshev and Saratov TETs's (type II foundation), and Northern Lenenergo TETs (type III foundation). The results indicate an average vibration level even lower than allowed by Soviet and foreign norms in type III foundation, all three foundations having roughly the same dynamic compliance. They also indicate that turbine vibrations are smallest on flexible foundations and that balancing runners in an accelerate-and-run (at nominal speed) machine after balancing in a low-speed machine has a beneficial effect on the dynamic characteristics of turbine and foundation with flexible frames. Figures 5; references: 4 Russian.  
[72-2415]

INDUSTRIAL TECHNOLOGY

UDC 621.382.3.019.3

PRECISION OPTICAL METHOD FOR ORIENTED CRYSTAL CUTTING

Leningrad OPTIKO-MEKHANICHESKAYA PROMYSHLENNOST' in Russian No 6 Jun 84,  
(manuscript received 8 Jul 83) pp 34-36

MATVEYEV, B.A., STUS', N.M. and TALALAKIN, G.N.

[Abstract] A simple method is proposed for oriented cutting of  $A^{35}B$ -type semiconductor crystals, in which a thin trial plate is cut from the blank and studied to determine necessary cutting corrections as indicated by the deviations of reflected laser beams in the xz and yz planes. This information is then used to reorient the blank for subsequent cutting. The accuracy of the method is close to that provided by X-ray methods, but is simpler and requires no expensive equipment. The method can be used to orient various crystal materials, inasmuch as its success depends only on the ability of obtaining mirror chips. References: 7 Russian.  
[46-6900]

UDC 621.362(088.8)

DESIGN METHOD FOR SOLID STATE CRYOGENIC COOLERS

Leningrad OPTIKO-MEKHANICHESKAYA PROMYSHLENNOST' in Russian No 6, Jun 84  
(manuscript received 15 Sep 83) pp 43-45

PILAT, I.M., ZINOV'EV, V.S., ARAKELOV, G.A., KRUGLOVA, N.V.,  
PIROZHENKO, S.I. and CHAYKA, S. V.

[Abstract] A method is presented for designing an optimized solid state cryogenic cooler which takes the temperature and field behavior of the kinetic coefficients of the thermoelectric materials into account; the selection of materials with best efficiency in each temperature range is discussed. Allowing for the temperature behavior of the kinetic coefficients leads to the conclusion that there is an extremal relationship between the cooling factor and the magnetic field. It is shown analytically that the value of the optimum magnetic field is determined by the amount of cooling and the maximum acceptable number of stages. References 4: 3 Russian, 1 Western.  
[46-6900]

UDC 681.327

INTERFACE CONTROLLER FOR ELEKTRONIKA-DZ-28 MICROCOMPUTER AND MT 1016 NUMERIC PRINTER

Moscow PRIBORY I TEKHNIKA EKSPERIMENTA in Russian No 4, Jul-Aug 84 (manuscript received 15 Sep 83) pp 78-80

ABYZOV, A.A. and PAKHOMOV, V.V., Radio Physics Scientific Research Institute, Gorkiy.

[Abstract] A controller is described that is designed to synchronize an Elektronika DZ-28 microcomputer and an MT 1016 numeric printer, and to convert the serial-parallel output to 16 four-bit groups which are input to the numeric printer in parallel. Schematic and block diagrams of the controller are presented and explained; the two subprograms employed are described. Timing diagrams of the data output from the DZ-28 microcomputer and the data input to the MT 1016 printer are compared. The controller is based on 155-series microcircuits, and is housed in a separate chassis. Output information can be printed at up to 24 lines per second.  
[64-6900]

UDC 658.52:621,78

AUTOMATED SYSTEM FOR CONTROLLING HEAT TREATMENT OF NUCLEAR POWERPLANT ARTICLES

Moscow ENERGO MASHINOSTROYENIYE in Russian No 7, Jul 84 pp 28-30

AFANASIADI, N. G., DEMIN, V. P. and LAUNIN, B.N., engineers

[Abstract] An automated heat-treatment process control system has been developed and implemented at the "Atommash" plant for controlling processes in the thermal furnace section of the hardening complex of the heat pressing shop. The system controls the technological equipment in the furnace section by following programs entered from the console of local devices; it acquires and processes technological and engineering cost information; it displays information for on-line monitoring, and outputs technological certificates for the articles being processed, as well as reporting documents for the technological process. The functional diagram of the two-level control system is traced and analyzed. Annual savings of 260,000 rubles have been calculated, with a payback of 1.5 years.  
[317-6900]

UDC 658.012.011.56-192

# RELIABILITY OF AUTOMATIC CONTROL SYSTEMS FOR TECHNOLOGICAL PROCESSES

Moscow IZMERENIYA, KONTROL', AVTOMATIZATSIYA in Russian No 1(49), 1984  
pp 72-80

ZARENIN, Yu.G., doctor of technical sciences, and KUTOVOY, V.I., candidate of technical sciences

[Abstract] Various factors affecting the reliability problem as it applies to automatic process control systems are identified and analyzed, with cost-benefit of preeminent concern. An approach to a solution is outlined in general terms. Extensive use of the decomposition method for reduction of the dimensionality and for simplification without sacrifice of integrability, is recommended, as are methods such as heuristic sifting for a priori reliability and standardized testing of reliability, followed by prediction and improvement of reliability. Technical and methodological documentation is necessary for all stages of automatic reliability-oriented design of automatic process control systems. An approach to improving reliability in such systems is recommended, which utilizes "internal" or existing capabilities of certain Ministry of Instrumentation departments rather than some special measures on a ministry-wide or All-Union scale. Figures 2; references: 12 Russian.  
[311-2415]

# VIBRATIONS OF ROTORS CONNECTED THROUGH COUPLINGS WITH BACKLASH

Moscow MASHINOSTROYENIYE in Russian No 5, Sep-Oct 84 (manuscript received 23 Dec 81, after completion 23 Jan 84) pp 36-42

POZNYAK, E.L. and MAYOROV, G.P., Moscow

[Abstract] Couplings with backlash for turbine sets, while suitable for compensation of manufacturing and assembly imprecision, cause vibration of the rotors they connect - especially when the shifts of those rotors are not perfectly aligned. Such couplings are either of the fixed type without friction or of the flexible type with very significant friction, flange couplings and end sleeves belonging in the first group while those in the second group have a sleeve and claw, a sleeve with slit, or a sleeve with teeth. A qualitative performance and vibration analysis for the various types of couplings is based on corresponding force and motion diagrams. A computer-aided quantitative analysis for coupled rotors in an SKV 150 MW - 3000 rpm turbine set (total length 12 m, total mass 30 tons, pitch circle of toothed sleeve coupling 14 cm in diameter) confirms the theoretical prediction that the force distribution becomes more uniform with a decreasing relative magnitude of unbalance force as the load is increased. Experimental data indicate, however, that the mechanism of vibration buildup is much more complex, being not only different for vertical and horizontal vibrations but also leading to instability,

especially under conditions of thermal asymmetry combined with excessive and nonuniform wear, which can result in seizure and conversion of such a flexible coupling into a fixed one. Figures 6; references 14: 13 Russian, 1 Western.  
[48-2415]

UDC 621.531.3

#### DYNAMIC CHARACTERISTICS OF DRIVE WITH CLOSED-LOOP SELF-BRAKING SERVO-MECHANISM

Moscow MASHINOSTROYENIYE in Russian No 5, Sep-Oct 84 (manuscript received 19 Sep 83) pp 30-35

VEYTS, V.L. and GIDASPOV, I.A., Leningrad

[Abstract] A servomechanism is considered which consists of a compound self-braking gear transmission in a closed kinematic loop with pretightening. Such a mechanism is used in the automation of metal-cutting machine tools and welding machines as well as for homing radio telescopes and radar antennas. The driving shaft and the driven shaft, at right angles to each other, are coupled through a miter pair of bevel gears and each carries a worm. The worm on the driving shaft is mounted with tight fit, the worm on the driven shaft is mounted with loose fit for some radial play and with a spring which loads it axially from the opposite shaft end. Both worms engage a common wheel so that this double worm gearing and the miter pair close a kinematic loop. The spring, through the worm on the driven shaft, imparts a pretightening torque to the wheel. Two modes of motion are considered:  $M_0 \omega_2 < 0$  and  $M_0 \omega_2 > 0$  ( $M_0$  - pretightening torque on wheel,  $\omega_2$  - angular velocity of driven shaft); and two loading variants:  $M_2 \omega_2 < 0$  or  $M_2 \omega_2 > 0$  ( $M_2$  - restraining moment on driven shaft). After taking into account the linearized dynamic characteristics of the motor, the characteristic equation yields the trajectory for each running mode and loading variant. The resulting transient processes in the drive and stability conditions are examined as well as the constraints they impose on the design parameters. Figures 5; references: 4 Russian.  
[48-2415]

UDC 629.7.051:534.29

#### DAMPING SYSTEMS FOR RANDOM VIBRATORY ACTION

Moscow MASHINOVEDENIYE in Russian No 5, Sep-Oct 84 (manuscript received 23 Jun 83, after completion 12 Jan 84) pp 23-29

KOSTIN, G.V., KONYCHEV, V.I. and YAGODKIN, V.N., Novosibirsk and Moscow

[Abstract] A vibration isolating system with six degrees of freedom is considered, assuming that geometrical symmetry and the configuration of

constraints permit breakup of such a system into an array of dynamically independent subsystems with negligible interaction between them. From this array is extracted a multidimensional system with Voigt damping. Its response to coupled random vibrations along two axes during translational motion along one of them and rotation about the third axis in a Cartesian system of coordinates is calculated, after Fourier transformation of the corresponding equations of motion. The algorithm of their solution, which yields the frequency spectrum and the energy characteristics of such a multiresonance damper structure as a perfectly rigid body, has been programmed for a digital computer. An evaluation of the vibration damping characteristics of a real compound protective structure in a laboratory experiment has confirmed the correctness of this theoretical approach to the problem and has yielded results in close agreement with calculations. Figures 4; references 3 Russian. [48-2415]

UDC 534.14

#### ULTIMATE CAPABILITIES AND EFFICIENCY OF RESONANCE-TYPE MACHINES

Moscow MASHINOVEDENIYE in Russian No 5, Sep-Oct 84 (manuscript received 14 Apr 83, after completion 2 Jan 84) pp 15-22

GERTS, M.Ye., Moscow

[Abstract] Various methods of tuning resonance-type machines with two degrees of freedom and cubic nonlinearity are evaluated comparatively, a vibration test stand with electrodynamic exciter serving as a typical representative of such machines. The analysis is based on the four-pole network model of A.A. Kharkevich which adequately describes interaction of a mechanical vibratory system and its drive. Its dynamic characteristics are determined first for the case of harmonic input action and then for three kinds of input limiting: 1) excitation signal (amplitude) limiting; 2) drive force limiting; 3) power (maximum or average) limiting. A cubically nonlinear mechanical system with only one degree of freedom is considered for comparison. The amplitude and frequency are calculated for each case, and these determine the optimum tuning and ultimate capability of the machines as well as its efficiency at that optimum tuning. The approximate relations derived for each kind of limitation become exact when the operating process is linear, with a one-to-one correspondence between vibration amplitude and excitation frequency and thus with no Sommerfeld discontinuity. It is demonstrated on a vibration stand with a 20JE 20B electrodynamic exciter, as an example, that halving the dissipation losses and doubling the electromechanical coupling coefficient will increase the vibration amplitude in the limited-excitation mode 3 to 20 times above the level attained by conventional resonance tuning. Figures 5; references: 15 Russian. [48-2415]

UDC 531.3:534.01

NONLINEAR FLEXURAL VIBRATIONS OF WORKING MEMBERS IN MACHINES WITH DUAL  
DRIVE MECHANISMS

Moscow MASHINOVEDENIYE in Russian No 5, Sep-Oct 84 (manuscript received  
10 Oct 83) pp 8-14

VUL'FSON, I.I., Leningrad

[Abstract] Textile and polygraph machines are typical examples of machines with long bars in reciprocating motion, driven by several identical rotating mechanisms through appropriate linkages. The inevitable and appreciable flexural vibrations of such a bar are analyzed here on the basis of the simplest dynamic model: a long beam of uniform cross section resting on two identical mass-spring supports with equally long free overhangs at both ends. The corresponding fundamental fourth-order differential equation of motion under quasi-harmonic perturbation producing both torsional and flexural vibrations is solved for nonlinear springs with increasing stiffness. The resulting algebraic frequency equation yields harmonic and quasi-harmonic as well as nonlinear modes of the natural spectrum. The results of calculations agree closely with experimental data and, therefore, the model is suitable for analysis of forced vibrations following kinematic perturbations of various norms most common in such machines. Figures 3; references: 5 Russian.  
[48-2415]

UDC 621.822.5

STABILITY OF THRASHER BEARINGS WITH PROFILE ON BUSHING OR SHAFT SURFACE

Moscow MASHINOVEDENIYE in Russian No 5, Sep-Oct 84 (manuscript received  
28 May 83) pp 99-104

TIKHONENKOVA, O.N., Leningrad

[Abstract] The stability problem of vertical high-speed gas thrasher bearings is analyzed for a bearing with at least three symmetrically spaced deep axial slots on either bushing or shaft surface, holding gas under atmospheric pressure, and with identical circumferential profiling of the surface of all teeth to form a micropocket in each. After such bearing has been conformally mapped from the Cartesian x-y plane into the Cartesian z-v plane, with the z-coordinate normalized to the shaft radius and the v-coordinate representing the angle, the corresponding Reynolds equation of hydrodynamics in dimensionless form is solved for the lubricant pressure squared as function of both space coordinates and time. The parameters of the problem are the relative depth and width of micropockets, the corresponding two different thicknesses of the lubricant layer in the coaxial configuration, and the bearing eccentricity. The results of an analytical

solution, made possible by assuming an infinitely high Stokes compressibility number, indicates that profiling of the shaft raises the stability of a vertical thrasher bearing appreciably. The added stability margin will depend on the characteristic dimensions of micropockets as well as on the real compressibility number and the bearing length. Figures 5; references: 4 Russian.  
[48-2415]

UDC 628.83.004.86.004.1

# HEAT EXCHANGERS FOR UTILIZING LOW-GRADE HEAT OF FAN EXHAUST AIR

Moscow PROMYSHLENNAYA ENERGETIKA in Russian No 9, Sep 84 pp 14-16

VOLKOV, Ye.P., engineer, Ministry of the Electronic Industry

[Abstract] A rotating regenerative heat exchanger has been developed and is being produced by the electronic industry which utilizes the heat of exhaust air for heating cold air in a room air-conditioning system. It consists of heat-storing vanes on a low-speed (10-12 rpm) rotor inside a box. As the vanes rotate they pass through the air stream (typically 24°C) pulled out of the room by the exhaust fan and transfer heat to the air stream (typically 16°C) pulled into the room by the blower fan. Vanes made of aluminum foil or chips were used in the experimental development study, those made of aluminum chips having somewhat worse aerodynamic characteristics but being less costly. This VRT-2 heat exchanger has a 0.35 m wide and 2x2 m<sup>2</sup> square box and weighs 800 kg, its air capacity being 20,000 m<sup>3</sup>/h at an aerodynamic drag equivalent to a pressure head of 20 mmH<sub>2</sub>O. It has operated for four years already, saving annually an average 500 Gcal of thermal and thus 80 tons of standard fuel by utilizing 60 to 80 percent of wasted heat. Other heat exchangers based on this principle are those with up to 60 heat transferring 0.1-0.3 mm thick aluminum sheets (air capacity 4300 m<sup>3</sup>/h, heat economy 60 Gcal/yr, weight 200 kg) and those with heat transferring 0.45 mm thick vinyl plastic film (air capacity 5000 m<sup>3</sup>/h or 2100 m<sup>3</sup>/h in single flow, fuel economy 7.5 t/yr, weight 58 kg). Figures 2.  
[75-2415]

TURBINE ENGINE DESIGN

UDC 621.311.22:621.187.124

RELIABILITY OF VACUUM DEAEREATION INSTALLATIONS IN TETs

Moscow ELEKTRICHESKIY STANTSII in Russian No 7, Jul 84 pp 34-36

SHARAPOV, V. I., candidate of technical sciences, TETs-1, Ul'yanovsk

[Abstract] The vacuum deaereation installations now employed in heat and electric powerplants are analyzed and found to be unreliable. Failures of installation components and degraded water deaereation performance reduce the effectiveness of safeguards against internal corrosion of equipment and pipelines, and make it impossible to realize fully the advantages which should be provided by vacuum deaerators. Basic steps are recommended as technically and economically feasible for improving the reliability of the deaereating installations. Figures 1; references: 2 Russian.  
[318-6900]

UDC 621.165:681.5.004

ADJUSTMENT AND OPERATION OF REGULATING SYSTEMS FOR TYPE K-800-240-3 LMZ  
TURBINES

Moscow ELEKTRICHESKIY STANTSII in Russian No 7, Jul 84 pp 30-33

SHAKALO, V. V., engineer, Dontekhenenergo

[Abstract] The results of implementation of an electrohydraulic automatic regulation system for K-800-240-3 turbines at the Uglegorskaya state regional electric powerplant are presented. It was found through experience that insensitivity of the automatic turbine regulation system is determined by two basic factors: impurities in the non-flammable liquid, and the occurrence and amount of play in the feedback components of the servo motors. An array of adjustments to the system is described which facilitated achieving the original design indicators. Extensive operating experience with 800-MW power units has indicated that the assemblies of the turbine regulating system are sufficiently reliable. Figures 1, references: 1 Russian.  
[318-6900]

UDC 621.438.001.24-621.165.001.24

DESIGN OF DISK SPRING FOR AUTOMATIC DISK SAFETY DEVICE

Moscow ENERGOMASHINOSTROYENIYE in Russian No 7, Jul 84 pp 14-16

RYBIN, P.A., candidate of technical sciences, SARANTSEV, K. B. and  
FATYKHOV, V. G., engineers

[Abstract] The basic restrictions on the geometric dimensions of disk springs are obtained. The parameters of the loads placed on a particular spot of a disk spring which provide the required adjustment of the safety device are found. A formula is derived for estimating the maximum stress level in the spring. The method provides satisfactory agreement between analytical and experimental data. Figures 3; references 7: 5 Russian, 2 Western.

[317-6900]

UDC 621.165:534

EROSION OF WORKING VANES OF AUXILIARY TURBINES

Moscow ENERGOMASHINOSTROYENIYE in Russian No 7, Jul 84 pp 12-13

SEMENYUK, A. V., candidate of technical sciences and REZNIK, A. G.,  
candidate of technical sciences

[Abstract] An analysis is made of the condition of the duct area of several auxiliary turbines subjected to finely dispersed moisture. These turbines operate for lengthy periods with low initial vapor temperatures throughout the entire operating period (approximately 80,000 hours). Practically all of the stages operated in the wet vapor zone during these periods. Erosion of the working vanes of a regulating stage with dual rims subjected to finely dispersed moisture is investigated. Severe loss of metal is observed in the first working rim and on the outlet edges. This is apparently due to separation of droplets from the surface of the liquid film by the strong eddies which form in the detachment zones followed by inertial ejection of the droplets at a high rate. References: 6 Russian, figures 5.

[317-6900]

UDC 621.438(088.8)

DETERMINATION OF SIZE AND WEIGHT REQUIREMENTS OF GAS TURBINE INSTALLATION  
FROM CYCLE PARAMETERS

Moscow ENERGOMASHINOSTROYENIYE in Russian No 7, Jul 84 pp 5-8

ZARITSKIY, S. P., candidate of technical sciences and VERTEPOV, A. G.,  
engineer

[Abstract] A method is developed for estimating the relative influence of the basic parameters of gas turbine installations on the size and weight requirements during the development stage as well as in working out the optimum placement of the system at the compressor plant; the method makes it possible to normalize the size and weight of any installation with respect to a corresponding standard value, and to estimate the size and weight of installations with known thermodynamic parameters. The method is intended for open-cycle gas-turbine installations employing axial compressors.

Figures 2; references: 2 Russian.

[317-6900]

UDC [621.165+621.438.]001.2

CHARACTERISTICS OF DESIGN OF TURBINE STAGES WITH TANGENTIAL INCLINATION OF  
GUIDE VANES

Moscow ENERGOMASHINOSTROYENIYE in Russian No 7, Jul 84 pp 2-5

KIRILLOV, A. I., doctor of technical sciences, SIROTKIN, Ya. A. and  
LAPSHIN, K. L., candidate of technical sciences

[Abstract] The variation and the degree of reactance of a turbine stage along the radius is investigated. The use of tangential placement of the guide vanes is recommended for improving the efficiency of turbine stages and for improving the characteristics of stages subjected to high aerodynamic loading. Stages of this type can be designed confidently by using existing methods for designing turbine stages with tangential placement of the guide vanes. Approximate methods with experimental adjustments, true dimensional axisymmetrical method of curvature of the current line, and the variation-distance method are evaluated. The latter two provide good agreement with experimental results regardless of the twist of the guide vanes. Methods are identified under which the theory of a viscous liquid, or approximate methods employing experimental adjustments, should be used. References:

13 Russian.

[317-6900]

UDC 621.73.043

# PRECISION DIE FORGING OF BLADES FOR GAS TURBINES

Moscow ENERCOMASHINOSTROYENIYE in Russian No 8, Aug 84 pp 20-22

SHASTIN, E.G., engineer

[Abstract] Precision die forging of blades for "supersonic" gas turbines and compressors is continuously competing with precision die casting, such blades being made of either heat-resistant alloy steels or titanium alloys. One problem in die forging is preheating the blanks and heat treatment without building up a weak surface layer thicker than the allowance for subsequent machining, this layer being either depleted of carbon and alloying elements (steels) or saturated with oxygen and hydrogen (titanium alloys). This problem has been solved by forging in a protective atmosphere or under vacuum. Two other problems are ensuring the necessary deformation of materials with low plasticity within a narrow temperature range and ensuring adequate mechanical strength and stability of the dies. These two problems, solved earlier by sequential forging and by hardening the platen, are now solved by utilizing the "superplasticity" effect in alloys with certain structural characteristics during deformation along certain temperature - strain-rate curves. The technological process of producing blades for GT-100 gas turbines and GTK-10 gas turbine-compressors from EI893 alloy steel includes preparation of regular-shape blanks, buildup of thickness at the "tail" end by upset forging in four passes with a force of 8000 kN and subsequent press forging the blanks in two passes with a force of 63 MN during heating to 1160°C, then calibration of the blanks in a coining press. Heat treatment that follows in a turret furnace consists of soaking 2 1/2 hours at 1020°C, air cooling, heating to 1160°C for austenitization and soaking 3 hours, and final air cooling. This process has yielded an annual cost saving of 90,000 rubles in one factory. Its one disadvantage is instability of actual allowances, which precludes "Metabo" machine finish grinding and requires manual finish grinding. Another disadvantage is the danger of a defective surface layer forming without availability of an oxidation-free heating furnace. Both problems should be resolved during the 1984-85 period. Figures 3; tables 1; references 5: 3 Russian, 2 Western.  
[63-2415]

UDC 621.438.251.539.4

# STRESSED-STRAINED STATE OF TIGHTENING BUCKLES IN SECTIONAL RUNNERS OF GAS TURBINES

Moscow ENERCOMASHINOSTROYENIYE in Russian No 9, Sep 84 pp 7-10

BAKUMENKO, I.K., engineer, and KULAKOVSKAYA, N. A., engineer

[Abstract] The mechanical state of the 10 tightening buckles in sectional runners of GTN-16 gas turbine-generator sets at high operating temperatures

and speeds, after balancing, is analyzed on the basis of the total force and moment balance. The Poisson effect for rotating disks and a 2.5 to 4-times nominal safety margin under variable load are taken into account. Rotational and thermal stresses as well as contact stresses are included, in addition to plain flexural and torsional stresses. A safety factor for tightness is defined for the joints, which can be higher or lower depending on the balance of forces on a joint. The calculations have been programmed in FORTRAN-4 for an M-222 computer. Calculations have been checked by experiments, the object being to design tightening buckles with more stable joints so as to reduce vibrations. Figures 1; references 11: 10 Russian, 1 Western (in Russian translation).  
[63-2415]

UDC 621.311.12.001.4

EXPERIENCE WITH VIBRATION TESTING AND BALANCING OF ROTORS OF LARGE  
HYDRAULIC UNITS

Moscow GIDROTEKHNIЧЕСКОYE STROITEL'STVO in Russian No 9, Sep 84  
pp 17-19

SOLOV'EV, I.R., engineer

[Abstract] Vibration testing and balancing of the rotors at a hydroelectric plant equipped with R0400-960a-11-V-450 turbines and SV712/227-24U4 generators turning at 250 rpm and producing 260 MW are described. The heavy point on the generator rotor was found by placing a shaft wobble sensor beneath the rotor and employing a shaft speed indicator which indicated the location of the first pole of the rotor at every moment of time. The findings indicated that, in general, mechanical rotor imbalance is a common defect in hydroelectric equipment, generally caused by improper installation, which eventually results in distortion of the rotor shape. Increased equipment vibration is usually caused by rotor imbalance in conjunction with other defects; a change in any of these defects can have an effect on shaft wobble, which means that all of the bearing assemblies along the entire shaft drive must be checked carefully for vibration and wobble. References 3 Russian.  
[47-6900]

UDC 621.244-253

EXPERIENCE WITH OPERATION AND REPAIR OF HYDRAULIC TURBINE IMPELLER CHAMBER

Moscow GIDROTEKHNIЧЕСКОYE STROITEL'STVO in Russian No 9, Sep 84 pp 23-26

GAL'PERIN, M.I., SHRIRO, I.I. and YABLONSKIY, G. A., engineers

[Abstract] This article describes different designs for hydraulic turbine impeller chambers (the facing of the duct portion of the turbine in which the impeller turns), and experience gained in operating and repairing different types of chambers at various installations. Cast-iron chambers were replaced with cast carbon-steel or stainless steel forged parts; the chambers for axial hydraulic turbines are now made of rolled two-layer or stainless steel with the sectors welded together during installation. Because correct shape and dimensions of the working chamber are critical, extreme care must be taken during installation and repair to ensure that the cement poured around the chamber does not deform it. References 3 Russian. [47-6900]

UDC 629.7.064.58

HIGH-TEMPERATURE FLUIDIC TURBOGENERATOR AS ATTACHMENT TO GAS TURBINE

Moscow TEPLOFIZIKA VYSOKIKH TEMPERATUR in Russian Vol 22, No 3, May-Jun 84 (manuscript received 18 Jan 82) pp 581-587

SHERSHNEV, N.A., SINENKOV, A.N. and GORIN, A.I., Moscow

[Abstract] A fluidic turbogenerator of electric energy is proposed in the form of attachment to a gas turbine driven by the combustion by-products of natural gas. The working gas mixture is fed into a cylindrical eddy chamber through tangential injection orifices in the lateral wall uniformly spaced around the circumference. The end walls of the chamber can be flat or conical, with a nozzle orifice at the center of one for exhaust of the gas. The gas flow in this chamber is vortical along spiral trajectories from the periphery toward the axis. A mass of liquid metal, much heavier than the gas, is injected into the chamber and rotated about the axis where inertia will contain it within a cylindrical layer around the periphery and the inlet orifices. Rotation of the liquid metal layer is maintained by momentum imparted to it by the incoming gas which passes through it like through a porous wall. A thermohydrodynamic performance analysis and evaluation of various liquid metals, especially their oxidation characteristics in an atmosphere of flue gas containing principally  $O_2$  and  $OH^-$  but also  $NO$ ,  $CO$ ,  $CO_2$ ,  $SO_2$ ,  $H_2O$  under typical operating pressures of 5-15 MPa indicates that liquid copper is most stable and thus most suitable at operating temperatures within the 1350-2400 K range. Liquid nickel becomes most stable at higher operating temperatures, cobalt is less stable at all temperatures, and bismuth is stable only within the 540-1800 K temperature

range. Model experiments with water simulating liquid copper in an air working gas at room temperature have yielded efficiencies as high as 49 percent. The main three problems of making such a turbogenerator feasible with a low rate of copper consumption (of the order of a few percent) are reducing the leakage of liquid copper, reducing the evaporation of liquid copper, which increases exponentially with rising temperature, and separating copper vapor from the liquid copper. Figures 5; tables 1; references: 6 Russian.  
[149-2415]

UDC 621.438

EXPERIMENTAL STUDY OF TWO-STAGE TURBINE BLEEDER WITH TRANSITION NOZZLE  
BETWEEN STAGES

Moscow TEPLOENERGETIKA in Russian No 7, Jul 84 pp 62-64

GOGOLEV, I.G., candidate of technical sciences, KUZ'MICHEV, R. V., candidate of technical sciences, DROKONOV, A. M., candidate of technical sciences, and KOCHEGAROV, A.A., engineer, Bryansk Institute of Transportation Machinery Design

[Abstract] A bleeder for gas turbines with split shaft consists of two stages connected through a transition nozzle, usually an annular diffuser with reinforcing stubs inside and a low expansion ratio. Such a nozzle with and without control of the boundary layer by diversion of stagnant liquid from the surfaces of stubs was tested in an experimental two-stage bleeder. Its inlet stage was modeled after the last stage of a high-pressure turbine and its outlet stage modeled after the first stage of a low-pressure turbine. Measurements of flow pattern and aerodynamic characteristics reveal that the entrance conditions are unaffected by the stubs, that control of the boundary layer reduces the flow nonuniformity and the energy losses while restoring more of the static pressure. The advantage of controlling the boundary layer becomes more significant as the operation of the turbine stage on the inlet side deviates more appreciably from the optimum mode. The overall effect of such control is economy and a higher vibration resistance of a split-shaft gas turbine. The transition nozzle had been designed and constructed at the Tula Metal Works upon recommendations made by the Bryansk Institute of Transportation Machinery Design. Figures 3; tables 2; references: 2 Russian.  
[307-2415]

UDC 621.165-822

# CALCULATION OF FRICTION AT SPHERICAL BEARING JOURNALS IN TURBOMACHINES

Moscow TEPLOTEKHNIKA in Russian No 10, Oct 84 pp 61-63

KHANIN, G. A., candidate of technical sciences, and KHANIN, L. G., engineer, Turbine Production Department, Leningrad Metal Works

[Abstract] Formulas are derived for calculating the friction at spherical thrust bearing journals in turbomachines, under either axial or axial and radial load. They are based on the equation of force balance in a spherical system of coordinates, assuming a symmetric cosinusoidal pressure distribution over the contact surface. The friction force is expressed as a surface integral of the pressure, the friction torque is expressed as a surface integral of pressure times radius. Both expressions are then replaced with equivalent simple algebraic ones containing an appropriate conversion coefficient each. These coefficients ( $\sigma$  in the formula for force,  $\beta$  in the formula for torque) are represented in the form of triple factorial-trigonometric sums not too unwieldy for computer-aided evaluation, with the two angular coordinates replaced expediently by half their sum and half their difference. In design calculations it is necessary to observe the constraint that the force acting at the mean shoe radius must not exceed the maximum allowable load. Figures 4; tables 2; references: 3 Russian. [65-2415]

UDC 621.165.620.193.1

# EROSION OF TURBINE RUNNER BLADES

Moscow TEPLONERGETIKA in Russian No 10, Oct 84 pp 25-30

PRYAKHIN, V.V., candidate of technical sciences, POVAROV, O.A., doctor of technical sciences, and RYZHENKOV, engineer

[Abstract] While the problem of erosion resistance in steam turbines is practically all solved for trailing edges of runner blades, it has not yet been solved for their leading edges and especially those running with peripheral velocities up to 800 m/s. Experimental studies were made at the Kaluga Turbine Manufacturing Plant with assistance from the Moscow Institute of Power Engineering regarding four major aspects of this problem. First are the fundamental relations governing erosive wear of metals (steels, stellite, titanium alloys) of which blades are made during a process in which the crucial incubation period is followed by a period of maximum wear rate and then a period of slower wear before it stabilizes to and continues at a constant rate. Second is the erosion resistance of various blade metals and coating materials, in relation to surface hardness, heat treatment, aggressive agents as well as moisture carried by steam, and the mass-time factor. Third is the dependence of erosive condensate formation

and impact on the operating conditions, an important indicator of this dependence being the inverse relation between size of liquid droplets and minimum impact velocity - a relation quantitatively different for different blade materials. Fourth is the method of data evaluation for the purpose of reliable design and prediction of erosion resistance. Neither on the basis of this study nor on the basis of the many other previous ones made in the USSR and abroad can any reliable definitive formulas be recommended for erosion resistance of the entire runner blade. There are needed, above all, more data on the gas dynamics of wet steam under variable load. Figures 9; references 27: 9 Russian, 18 Western.  
[65-2415]

HIGH-ENERGY DEVICES, OPTICS, PHOTOGRAPHY

UDC 621.385.833

VIDEO MONITOR DEVICE FOR ELECTRON MICROSCOPE

Leningrad OPTIKO-MEKHANICHESKAYA PROMYSHLENNOST' in Russian No 6, Jun 84  
(manuscript received 14 Sep 83) pp 26-27

BOCHAROV, E.P. and PILENKO, B.I.

[Abstract] A device is examined which provides a double magnification mode by alternate scanning of the field in its entirety and of a fragment of the object, and generating their images on a field CRT and a fragment CRT. The proposed method makes it unnecessary to move the electron probe of the column and the beam of the CRT vertically at the line frequency, and overcomes the shortcomings in existing devices. A block diagram of the monitor is traced and explained. By reducing the scanning area, the frame frequency can be increased by a factor of sixteen with the same video signal bandwidth. An experiment with a monitor on an EVM-100 lm electron microscope indicated that the device is reliable and convenient to operate. References 4: 2 Russian, 2 Western.  
[46-6900]

UDC 535.241.13

UNPOLARIZED RADIATION MODULATOR BASED ON LEAD ZIRCONATE-TITANATE CERAMIC WITH LANTHANUM

Leningrad OPTIKO-MEKHANICHESKAYA PROMYSHLENNOST' in Russian No 6, Jun 84  
(manuscript received 9 Jun 83) pp 28-29

SOSENSKIY, A. M., KAZANTSEVA, N.N., KOSHKIN, G.V., FEYGIN, D. M. and PERSHIN, M.P.

[Abstract] This study investigates the characteristics of a modulator based on 9/65/35 lead zirconate-titanate ceramic with lanthanum, which has high contrast and good radiation conversion efficiency. The optical arrangement of the modulator, which consists of a polarizing beam splitter, lenses, ceramic plates and electrodes, is presented. The spectral behavior of the transmission of the p- and s- components of the polarization beam

splitter, and of the overall transmission of the ceramic mirror, is calculated. The modulator is found to be capable of controlling unpolarized radiation in the near infrared region of the spectrum with good efficiency, and to provide a high degree of suppression. References: 6 Russian.  
[46-6900]

UDC 681.7.02:681.7.069

#### TECHNOLOGICAL PROCESS FOR MANUFACTURING MULTIFACETED PRISMS

Leningrad OPTIKO-MEKHANICHESKAYA PROMYSHLENNOST' in Russian No 6, Jun 84 (manuscript received 20 Sep 83) pp 36-39

ZHDANOV, A.I.

[Abstract] A technological process designed for manufacturing and testing multifaceted optical prisms is described. In the first stage the blank is cut and center holes are drilled. The blank is rounded and ground, and the parallel sides are polished. In the second stage the blanks are assembled into a column held together by adhesive, after which preliminary diamond grinding of the facets is performed, followed by a fine grinding and polishing of the facets of the prism block. The assembly of the blanks into columns is described. The procedure by which the facets are diamond-ground is explained. An attachment is described for securing the column of blanks prior to fine grinding and polishing. The process, which can be used to produce 24-faceted polyhedrons, reduces the manufacturing labor from twenty to six standard hours. Mechanized fine grinding and polishing processes on 3806L machines in conjunction with objective testing means make it possible to produce polyhedrons with guaranteed angular errors of less than two angular seconds. References 3: 2 Russian, 1 Western.  
[46-6900]

UDC 666.11.01:620.178.12

#### INVESTIGATION OF INFLUENCE OF POLISHING CONDITIONS ON SURFACE ROUGHNESS OF GLASSES OF DIFFERENT COMPOSITION

Leningrad OPTIKO-MEKHANICHESKAYA PROMYSHLENNOST' in Russian No 6, Jun 84 (manuscript received 14 Oct 83) pp 16-18

KRYUKOVA, S.V., YEREMINA, S.V. and BONDAR', V.V.

[Abstract] Variations in the surface roughness of glasses of different composition as the abrasive and material of the grinder are changed is investigated; the relationship between the quality of a surface polished under fixed dispersion conditions and the composition of optical silicate glasses produced commercially is studied. It is found that, for the abrasives examined, the surface roughness of the glasses increases little

as the tool hardness increases. The change in hardness of the tool has practically no effect on the relative roughness for the entire series of glass selected. As the hardness of the abrasive increases, the surface roughness of glasses with different hardness increases irregularly: the influence of the abrasive on the roughness of glasses with relative hardness less than unity is practically constant; and the effectiveness increases for hardness exceeding unity as the  $\text{SiO}_2$  content in the glasses increases. A linear relationship is established between the coefficient of relative roughness and the total content of glass-forming oxides participating in the tetrahedral framework. References: 10 Russian.  
[46-6900]

UDC 681.51:522.2

INVESTIGATION OF AUTOMATIC STABILIZATION SYSTEM FOR COMPOSITE MIRRORS OF ADAPTIVE TELESCOPE

Leningrad OPTIKO-MEKHANICHESKAYA PROMYSHLENNOST' in Russian No 6, Jun 84 (manuscript received 27 Jun 83) pp 1-4

KRYUKOV, V.I., RODIONOV, A.K., SERGEYEV, P.V. and SYCHEV, V. V.

[Abstract] An automatic stabilization system designed to ensure the required form of the composite main mirror of a telescope by stabilizing each elementary mirror with respect to the required position is investigated. The influence of crosstalk between the channels controlling each elementary mirror is analyzed. It is found that the stability margins in a system with crosstalk becomes smaller as the angles  $\gamma$  and  $\psi$  become larger ( $\gamma$  is the angle of rotation between the abscissas of the coordinate system of the sensor in the elementary reflector, and  $\psi$  the angle between the axes of the coordinate system of the elementary reflector measured over the shortest distance). The regulation performance is also degraded (overregulation increases, as does the amount of oscillation and transient time); and the accuracy with which the input is processed becomes lower. It is found that acceptable accuracy and satisfactory adjustment performance can be achieved in systems with crosstalk by introducing correcting devices and selecting their parameters. References: 3 Russian.  
[46-6900]

UDC 681.383.181.48:681.327.68.778.38

SELF-SCANNING MDS-INTEGRATED PHOTODETECTOR STRIP

Novosibirsk AVTOMETRIYA in Russian No 3, May-Jun 84 (manuscript received 10 Jun 83 after revision) pp 50-56

KAGAN, Yu.Kh., KASHCHEYEV, E.L., KRUGLIKOV, S.V., MAYORCHUK, M.A.,  
MANUKHIN, Yu.A. and NAYMARK, S.I., Novosibirsk

[Abstract] Findings from the development and experimental investigation of an MDS-photodiode strip of 128 photocells are presented. The erase and read circuits of each cell in these strips are controlled by two identical shift registers, with the register which controls the read circuits operating with a delay with respect to the register which controls the erase circuits. The parameters of the strips are measured, as well as the speed, photo-sensitivity and output signal spread in terms of amplitude and charge storage time. The characteristics of the devices investigated permit them to be used in television systems, pattern recognition systems, optical data input-output, storage and processing systems, inter alia. References 7: 4 Western. 3 Russian.  
[1-6900]

UDC 681.383.181.48:681.327.68.778.38

#### SELF-SCANNING MDS-INTEGRATED PHOTSENSOR STRIP

Novosibirsk AVTOMETRIYA in Russian Vol 3, May-Jun 84 (manuscript received 10 Jun 83) pp 50-56

[Article by Yu. Kh. Kagan, E. L. Kashcheyev, S. V. Kruglikov, M. A. Mayorchuk, Yu. A. Manukhin and S. I. Naymark, Novosibirsk]

[Text] Multielement MDS [metal-dielectric-semiconductor]-integrated photo-sensor strips are one of the new advances of semiconductor MDS technology. The most widespread types of these devices are photosensors based on CCD [charge-coupled devices] [1, 2], MDS-photodiode sensors [3, 4] and also structures of the "photodiode-CCD-register" type [5].

If charge-coupled devices and photodiode sensors are compared, the advantages of MDS-photodiode sensors should include higher sensitivity, especially in the blue region of the spectrum, and higher homogeneity of sensitivity [6]; the more significant disadvantages should include the dependence of video output capacitance on the number of elements connected to the output bus and, as a result, a reduction of the output signal voltage and an increase of noise. The effect of output bus capacitance can be reduced by introducing a preamplifier based on an MDS transistor into each photocell, which is connected by a source repeater scheme. The presence of a preamplifier uncouples the low signal current of the photodiode and the high capacitance of the output bus.

The results of development and experimental investigations of an MDS-photodiode sensor strip consisting of 128 photocells are presented in this paper. The diagrams, structure, manufacturing technique and the functioning of the device are considered and the experimental results are discussed.

Diagram and functioning of the photocell. Let us consider the schematic diagram of the photocell, shown in Figure 1, a, which includes a photodiode D, a milking key  $T_0$ , MDS preamplifier  $T_1$  and readout key  $T_2$ , which gates the output current of the preamplifier. It is obvious from the figure that there are separate milking (erasure) circuits of the photodiode on transistor  $T_0$  and signal current readout on transistor  $T_2$  in the cell. The radiation flux impinging on the photodetecting surface of the photodiode with key  $T_0$  open, causes a variation of voltage  $\Delta U$  on the capacitance of the photodiode  $C_D$ , which modulates the working current of the MDS preamplifier. When key  $T_2$  is closed, we have with regard to the signal pattern in Figure 1, b

$$I_1 = I_{01} + (S_\lambda \Phi (\theta + \tau_D) / C_D) g_m. \quad (1)$$

where  $\tau_D$  is the time constant of the photodiode,  $I_1$  is the discharge current of transistor  $T_1$ ,  $S_\lambda$  is the current sensitivity of the photodiode,  $\theta$  is the interval between closings of keys  $T_0$  and  $T_2$  (see Figure 1, a),  $g_m$  is the steepness of control through the gate of transistor  $T_1$ , determined by the expression

$$g_m = \beta(E - V_0).$$

Here  $\beta$  is the specific steepness of the integrated transistor  $T_1$ ,  $V_0$  is its threshold voltage and  $I_{01}$  is the constant component of the current of transistor  $T_1$ , equal to  $I_{01} = \beta(E - V_0)^2/2$ .

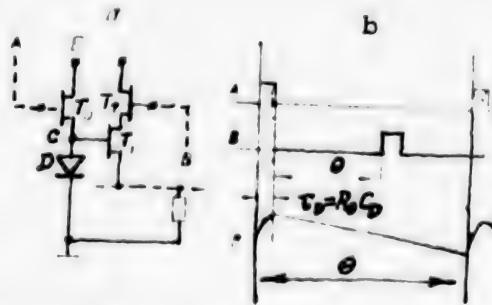


Figure 1. Diagram of Cell of MDS Photodiode Sensor (a) and Time Diagram of Its Operation (b)

The current sensitivity of the photocell is determined from expression (1) provided that  $\theta \gg \tau_D$ :

$$\frac{\tau_D}{C_D} S_\lambda g_m < \hat{S} = \frac{\partial I_1}{\partial \Phi} \cong \frac{S_\lambda \theta}{C_D} g_m \leq \frac{S_\lambda \theta}{C_D} g_m, \quad (2)$$

where  $\tau_D = R_0 C_D$  is the time constant of the MDS photodiode,  $\theta$  is the length of the frame and  $R_0$  is the channel resistance of transistor  $T_0$ .

It follows from (2) that separation of the erasure and readout circuits provides the capability of regulating the sensitivity  $\hat{S}$  by using parameter  $\theta$ .

The minimum value of the optical signal on the photodiode, determined by the noise level presented to the amplifier input, is

$$\Phi_{\min} = C_D U_N / \theta S_\lambda \geq C_D U_N / \theta S_\lambda. \quad (3)$$

According to (2) and (3), the ratio of the maximum optical output to the minimum output  $D = \Phi_{\max} / \Phi_{\min}$  satisfies the condition

$$D \leq \hat{D} \leq D(\theta / \tau_D), \quad (4)$$

where  $D = E/U_N$  is the natural dynamic range of the photocell at fixed storage time, while voltage  $U_N$  is stipulated by the noise source.

It is easy to establish from expressions (3) and (4) that an increase of the storage time leads to a decrease of level  $\Phi_{\min}$  of the minimum detectable optical signal, while a decrease leads to an increase of the saturation signal  $\Phi_{\max}$ ; accordingly, the effective dynamic range  $\hat{D}$  of the cell is  $\Theta/\tau_D$ -fold greater than  $D$  in the limiting case. This multiplier can essentially be very large, since the storage time  $\Theta$  from the direction of the photocell is limited only by the charge storage time on capacitor  $C_D$  (or by the leakage currents of the photodiode), which comprises 0.001-0.1 s in standard models, while the typical values of the time constant are  $\tau_D \approx 2 \cdot 10^{-8}$  s.

The block diagram and structure of the sensor. Sensor strips of 128 light-sensitive cells were investigated. The erasure and readout circuits of each cell are controlled in these sensors from two identical shift registers (SR), which generate a "traveling one" code; moreover, the shift register used to control the readout circuits operates by the ratio of the erasure circuit control with time delay to the shift register, which determines the charge storage time on the photodiodes (parameter  $\Theta$ ).

Let us consider two connection diagrams of the photosensor strip. The first of them, shown in Figure 2, a, contains two 128-bit shift registers, the outputs of which are connected to 128 photocells. The output buses of all the photocells are connected to a common output of the video signal. The second diagram is presented in Figure 3. The photosensor is divided into four fragments of 32 cells each, controlled from two 32-bit shift registers having independent output. The block diagram of each of the fragments is similar to that in Figure 2, a. Thus, the photosensor, manufactured by the second diagram, includes eight shift registers and four video outputs; it has no filters and all 128 photodiodes are arranged with spacing of 0.075 mm. The effective speed of data access in this circuit is fourfold faster than in the first circuit.

The shift registers in both types of photosensors, generate a "traveling one" code. Pulse control voltages must be shaped according to the time diagram presented in Figure 2, b to control them. "Ones" are entered in the shift register by feeding a starting pulse  $\phi_{zap}$  to its input, while it is moved along the register by feeding shift pulses  $\phi_1$  and  $\phi_2$ . When the "one" reaches the end of the register, the reset pulse  $\phi_{sbr}$  sets its last bit to zero.

To increase the level of voltage fed from the shift register to the gates of the keys that control the operation of the photodiodes, an MOS-varactor (or a "bootstrap") [4], which significantly increases the speed of the register and reduces its consumed power, is used in each bit of the register.

We investigated sensors with two sizes of photodiode surfaces ( $0.04 \times 0.04 \text{ mm}^2$  and  $0.85 \times 0.04 \text{ mm}^2$ ) and with spacing of 0.075  $\mu\text{m}$  between them. The integrated circuit of the sensor was manufactured by p-channel MDS technology with polysilicon gate. Source domains of transistors  $T_0$  (see Figure 1, a), above which a thick oxide was etched, were used as the photodiodes. An overall view of the device, mounted in a housing with 64 leads, is presented in Figure 4.

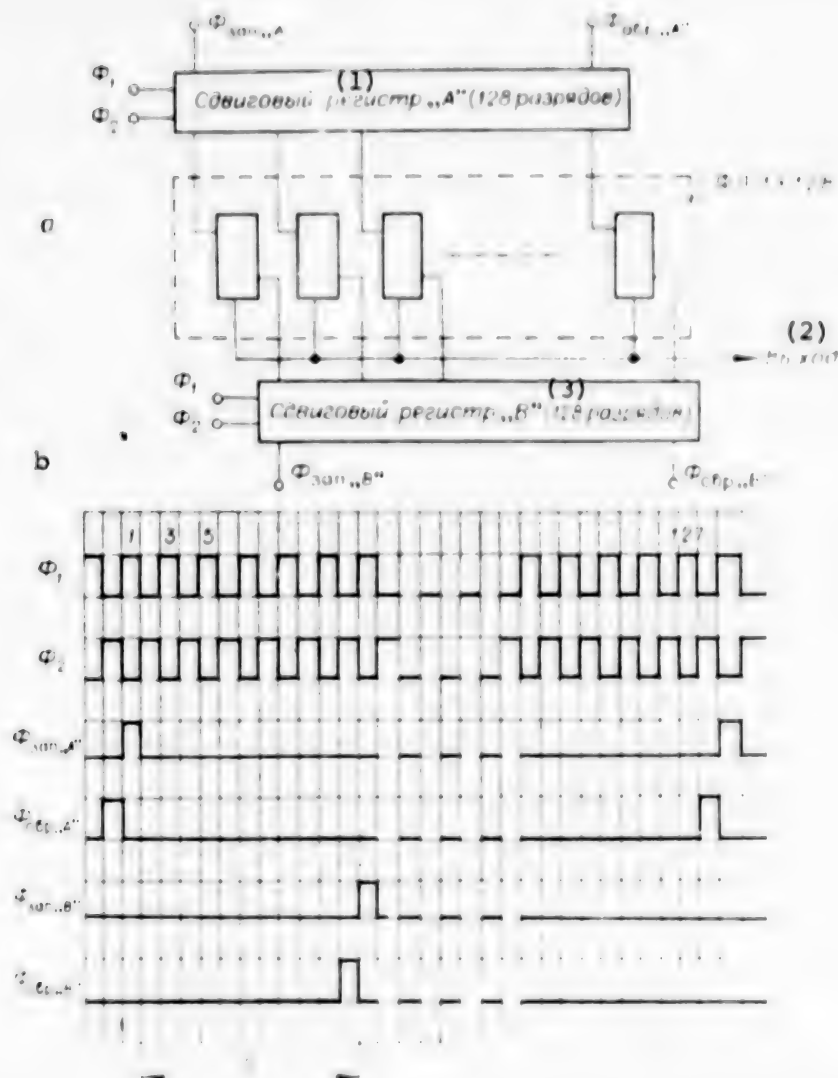


Figure 2. Photosensor (FL) of 128 Light-Sensitive Cells With Two 128-Bit Shift Registers (SR): a--block diagram; b--time diagram required to control shift registers

KEY:

- |                                  |                                  |
|----------------------------------|----------------------------------|
| 1. Shift register "A" (128 bits) | 2. Output                        |
|                                  | 3. Shift register "B" (128 bits) |

Experimental results. Such parameters of photosensors as speed, photosensitivity, variation of output signals in amplitude and charge storage time were measured.

The equipment used contained a time pulse generator, which controls the scanning frequency of photodetector cells, a 128-bit shift register and pulse shapers  $\Phi_1$  and  $\Phi_2$ . All the control pulse voltages  $\Phi_1$ ,  $\Phi_2$ ,  $\Phi_{zap}$  and  $\Phi_{sbr}$  were amplified to 10-18 V and there was the capability of regulating the amplitude. Generators, which play the role of regulated delay lines, were introduced into the

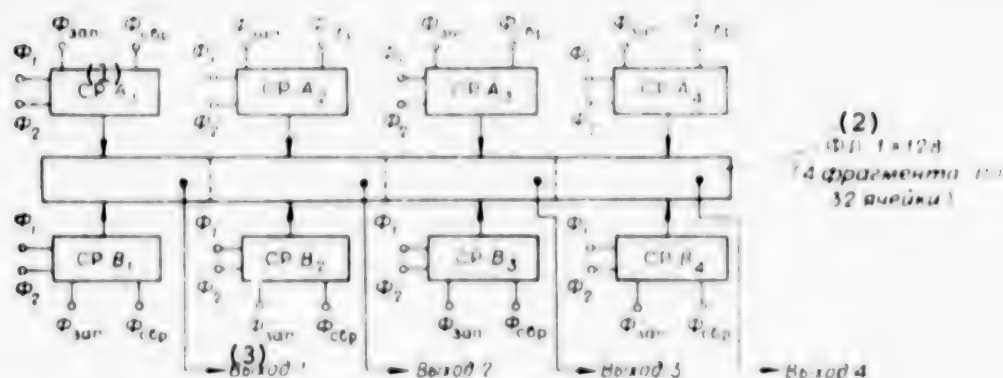


Figure 3. Block Diagram of Photosensor Measuring  $1 \times 128$ , Containing Four Fragments, Each Consisting of 32 Light-Sensitive Cells

KEY:

- |                                   |           |
|-----------------------------------|-----------|
| 1. Shift register                 | 3. Output |
| 2. Photosensor $1 \times 128$     |           |
| (four fragments of 32 cells each) |           |

corresponding channels to select the optimal time ratios between  $\Phi_1$  and  $\Phi_2$  and also  $\Phi_{zap}$  and  $\Phi_{sbr}$ .

Speed. The operating speed of the photosensor may not exceed the speed of the control shift registers and is limited by the speed of the light-sensitive cells. When investigating the sensors, the operating frequency of the timing oscillator varied in the range of 0.1-10 MHz. It is obvious from Figure 5 that the maximum operating frequency of the register increases as the amplitude of the control pulse increases and reaches 9.6 MHz at amplitude of 17 V.

The speed of the photocell is mainly dependent on the time constants of the MDS photodiode ( $\tau_D$ ) and of the output circuit. The minimum time of reading data from the cell with load resistor of  $R = 1.2 \text{ k}\Omega$  and control pulse amplitude of 17 V was 60 ns. The photocell operated in two cycles when measuring the minimum erasure time. A light pulse with fixed emission energy was fed to the photodiode in the first, preliminary cycle after preadjustment of the cell (an erasure pulse was fed to it). The photodiode was not illuminated during the second, measuring cycle and was discharged only by dark currents. Therefore, if the capacitance of the photodiode is milked completely upon erasure (regardless of the energy level of the preceding illumination), the signal taken from the photocell during readout should correspond to the dark current. If the photodiode cannot be fully charged during erasure, a drop of the output voltage compared to dark-current voltage is observed.

The dependence of the output voltage (with incomplete milking of the photodiode after preliminary illumination of it) on the erasing pulses is shown in Figure 6. The graphs in Figure 6, a were obtained at erasing pulse amplitude of 10 V and those in Figure 6, b were obtained at amplitude of 17 V. The parameter of the reduced graphs is the pulse energy of the preceding illumination and this energy



Figure 4. Self-Scanning Integrated Sensor on 128 Light-Sensitive Cells. Overall view of device in housing

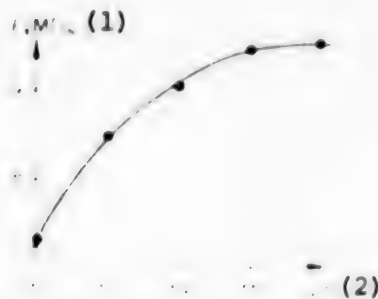


Figure 5. Graph of Dependence of Maximum Operating Frequency of Shift Register on Amplitude of Control Pulses  $\phi_1$ ,  $\phi_2$ ,  $\phi_{zap}$  and  $\phi_{sbr}$

KEY:

1. MHz

2. V

is equal to saturation energy of  $3 \cdot 10^{-11}$  J for graphs 1. The measurements were made at block frequency of shift register operation of 1 MHz and reading pulse length of  $\tau_{sch} = 1 \mu s$ .

As can be seen from the given data, the minimum required length of the erasing pulses decreases significantly as the erasing pulse amplitude increases. This is related to the fact that the time constant of photodiode milking  $\tau_D$  decreases as the voltage on the gate of transistor  $T_0$  increases (see Figure 1, a). The measurements showed that essentially complete erasure of data is achieved at erasing pulse length of 130 ns.

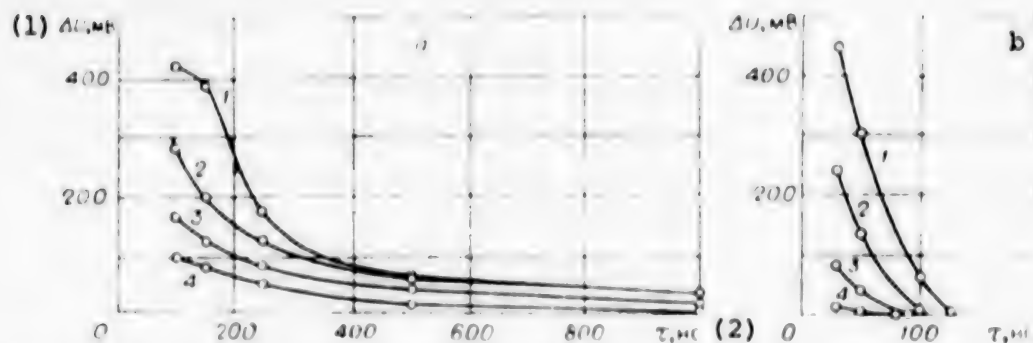


Figure 6. Dependence of Output Signal of Photocell (With Regard to Preceding Illumination of It) on Length of Erasing Pulses: a--at erasing pulse amplitude of 10 V; b--at amplitude of 17 V; the graphs were obtained at different pulse energy of preceding illumination (1--at saturation energy of  $3 \cdot 10^{-11}$  J; 2-- $1.2 \cdot 10^{-11}$  J; 3-- $2.2 \cdot 10^{-12}$  J; 4-- $5 \cdot 10^{-13}$  J)

KEY:

1. mV

2. ns

Photosensitivity. The dependence of the variation of output signal amplitude on the light energy fed to the photosensors during the exposure time is presented in Figure 7. Curve 1 corresponds to photodiodes measuring  $40 \times 40 \mu\text{m}^2$  and curve 2 corresponds to those measuring  $40 \times 850 \mu\text{m}^2$ . It follows from the given functions that the voltage sensitivity of square photosensors is equal to  $2.8 \cdot 10^{11}$  V/J and that of rectangular sensors is  $3 \cdot 10^{10}$  V/J, i.e., almost as many times worse as the area of the photodiodes is larger. The complete agreement is related to the fact that spurious capacitances, caused by other elements and buses of the photosensor, have a significant effect on the output signal from the interrogating component, as well as the natural capacitance of the photodiode, proportional to its area.

It is obvious from Figure 7 that the saturation signal for the first type of photosensors is equal to  $(2.5-3) \cdot 10^{-12}$  J and that for the second type is  $(2.5-3) \cdot 10^{-11}$  J.

Variation of output voltage amplitude. The variation of output voltage amplitude was measured on fragments of photosensors consisting of 32 light-sensitive cells in the absence of light and at luminous pulse energy equal to  $10^{-11}$  J.

Histograms of the output signals are shown in Figure 8; the distribution of the output signals of two fragments, located on a single crystal and having identical cell configuration, are shown in Figure 8, a and b and the signals of the same two fragments, but located on a different crystal, are shown in Figure 8, c and d. Hence, it follows that the maximum variation of the output signals of the cells within a single crystal does not exceed  $\pm 10$  mV.

Storage time. The storage time of the data written in the form of a charge on the photodiode capacitor is determined by the dark leakage currents that discharge

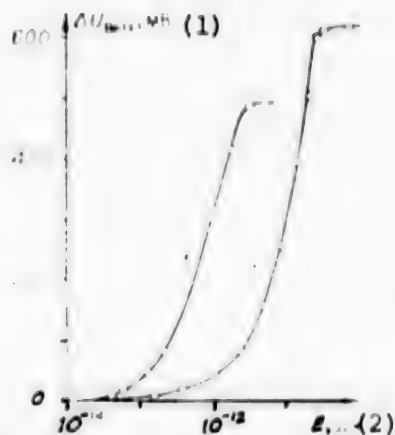


Figure 7. Dependence of Variation of Amplitude of Output Signal From Photosensor on Illumination Energy: 1--in photodiodes measuring  $40 \times 40 \mu\text{m}$ ; 2--in photodiodes measuring  $40 \times 850 \mu\text{m}$

KEY:

1. mV

2. J

the barrier capacitor  $C_D$ . The output signal amplitude is reduced due to discharge of the capacitor; therefore, the storage time can be determined as the maximum time interval in which the output voltage varies in the absence of illumination, for example, by 10 percent of the initially measured voltage. With this criterion, the data storage time in experimental models of photosensors reached 510 ms.

Discussion of the results. The main parameters of photosensors are presented in the table. The dynamic range  $D$  of the photosensitive cells was determined with regard to "fixed-distribution noise" [7], which can be suppressed by using an external filter. Parameter  $D$  is then limited by fluctuating noise and reaches values of  $\sim 10^3$ - $10^4$ .

The switching noise present in the signal decreases the dynamic range. However, the switching noise for low frequencies (1-3 MHz) has a spectrum, considerably different from the reading frequency and, accordingly, can also be filtered. The requirements on the filter increase as the scanning frequency increases.

The shift register of the photosensor operate reliably at comparatively low scanning frequencies (up to 1-2 MHz) at control voltages of  $\phi_1$ ,  $\phi_2$ ,  $\phi_{zap}$  and  $\phi_{sbr}$  not greater than 10 V. Therefore, there is no need to increase the control voltages to higher levels in devices that do not require high scanning frequencies of the photocells. The control voltages should be increased to 17-18 V in devices where the photocells should be scanned at higher frequencies (up to 9-9.6 MHz).

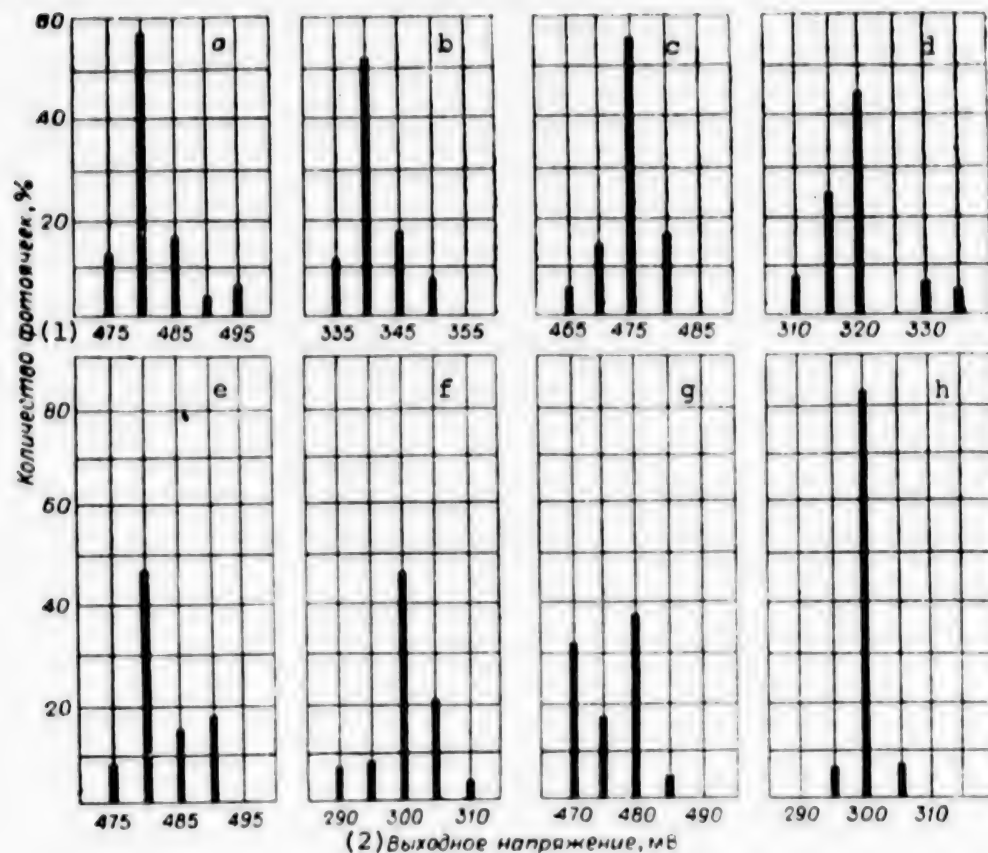


Figure 8. Histograms of Output Signals From Fragments Measuring  $1 \times 32$  Photosensors: a, c, e and g--in absence of light; b, d, f and h--at luminous pulse energy of  $10^{-11}$  J; the histograms in figures a, b, c and d correspond to two fragments of the photosensor located on the same crystal; the histograms in figures e, f, g and h correspond to two fragments on a different crystal

KEY:

- |                                  |                       |
|----------------------------------|-----------------------|
| 1. Number of photocells, percent | 2. Output voltage, mV |
|----------------------------------|-----------------------|

The characteristics of developed self-scanning photosensors and those that we investigated permit their successful use in television systems, in pattern identification systems, input-output systems, optical data storage and processing systems and so on.

(1) Условное обозначение параметра	(2) Наименование параметра	(3) Размеры фото- чувствительных ячеек, мм	(4) Эксперимен- тальное значение	(5) Единица изме- рения
$I_D$	Амплитуда темнового тока (6)	$0,04 \times 0,04$ $0,04 \times 0,85$	415 530	мкА (7)
$\delta I_D$	Разброс амплитуды темного сигнала (8)	Оба типа (9)	$\pm 8$	мкА
$W_H$	Энергия насыщения (10)	$0,04 \times 0,04$ $0,04 \times 0,85$	2,5-3 25-30	пДж (11)
$S_{IW}$	Токовая чувствительность по энергии (12)	$0,04 \times 0,04$ $0,04 \times 0,85$	230 25	$\frac{\text{мкА}}{\text{пДж}}$ (13)
$D$	Динамический диапазон по энергии (14)	Оба типа	22,5	Относительные единицы (15)
$f_{\max}$	Максимальная частота сканирования (16)	Оба типа	9,6	МГц (17)

KEY:

- |   |                                |
|---|--------------------------------|
| 1. Notation of parameter                  | 10. Saturation energy          |
| 2. Name of parameter                      | 11. pJ                         |
| 3. Dimensions of photosensitive cells, mm | 12. Energy current sensitivity |
| 4. Experimental value                     | 13. $\mu\text{A/pJ}$           |
| 5. Unit of measurement                    | 14. Dynamic energy range       |
| 6. Dark current amplitude                 | 15. Relative units             |
| 7. $\mu\text{A}$                          | 16. Maximum scanning frequency |
| 8. Variation of dark signal amplitude     | 17. MHz                        |
| 9. Both types                             |                                |

BIBLIOGRAPHY

1. Press, F. P., "Formirovateli videosignala na priborakh s zaryadovoy svyaz'yu" [Video Signal Shapers Based on Charge-Coupled Devices], Moscow, Izdatel'stvo "Radio i svyaz'", 1981.
2. Barton, D. B. et al., "Pribory s zaryadovoy svyaz'yu" [Charge-Coupled Devices], translated from English, Moscow, Izdatel'stvo "Mir", 1981.
3. Kruglikov, S. V. and S. I. Naymark, "Integral'nyye MDP-fotodiodnyye ustroystva i ikh primeneniye. Ch. 1. Integral'nyye MDP-fotodiodnyye elementy, lineyki i matritsy" [Integrated MDS Photodiode Devices and Their Application. Part 1. Integrated MDS Photodiode Elements, Photosensors and Photomatrices], Moscow, TsNIIelektronika, 1980.
4. White. M. H., "Photodiode Matrices," in "Poluprovodnikovyye formirovateli signalov izobrazheniya" [Semiconductor Image Signal Shapers], translated from English, Moscow, Izdatel'stvo "Mir", 1979.

5. Ohba, S. et al., "A 1,024-Element Linear CCD Photosensor With Unique Photodiode Structure," IEEE Transactions on Electron Devices, Vol. ED-27, No. 9, 1980.
6. Ohba, S. et al., "MOS Area Sensor. Part 1. Low-Noise MOS Area Sensor With Antiblooming," IEEE Transactions on Electron Devices, Vol. ED-27, No. 8, 1980.
7. Fry, P. W. et al., "Fixed Pattern Noise in Photomatrix," IEEE Transactions on Solid-State Circuits, Vol. SC-5, No. 5, 1970.

COPYRIGHT: Izdatel'stvo "Nauka", "Avtometriya", 1984

6521

CSO: 8144/1917

UDC 535.317.2:681.332

HOLOGRAPHIC INTENSITY CORRELATOR WITH PRIS-TYPE PHOTOELECTRO-OPTICAL  
CONTROLLABLE TRANSPARENCY

Novosibirsk AVTOMETRIYA in Russian No 3, May-Jun 84 (manuscript received  
22 Sep 83) pp 57-61

OPARIN, A.N., POTATURKIN, O.I., FEL'DBUSH, V.I. and SHIPOV, P.M.,  
Novosibirsk

[Abstract] A holographic intensity correlator which averages the resultant light distribution, employing a Pris-type transverse-electro-optical controllable transparency, is developed and investigated. The transparency is based on a single crystal of bismuth germanate 1mm thick with (111) orientation. The device permits recognition of real half-tone terrain images. Coincidence functions of the contoured recognized images and reference images acts as a correlation function. References 8: 7 Russian, 1 Western.  
[1-6900]

UDC 535.317.2:681.332

# HOLOGRAPHIC INTENSITY CORRELATOR WITH PRIS-TYPE PHOTOELECTRO-OPTICAL CONTROLLED TRANSPARENCY

Novosibirsk AVTOMETRIYA in Russian Vol 3, May-Jun 84 (manuscript received 22 Sep 83) pp 57-61

[Article by A. N. Oparin, O. I. Potaturkin, V. I. Fel'dbush and P. M. Shipov, Novosibirsk]

[Text] An opto-electronic image recognition system (IRS), in which online entry and preliminary processing were carried out by using a Fototitus-type photoelectrooptical controlled transparency (CT) [2], was considered in [1]. The process of processing contour identified images was realized successfully in this system. However, when processing silhouette and half-tone images that comprise most real identified images (industrial features, images of terrain and so on), the dynamic range of the values of the correlation functions decreased significantly due to the low contrast of the produced contours which, in turn, led to a decrease of the reliability of identifying these images. Therefore, we were faced with the problem of enhancing the contrast of identified image contours, which was solved by using a controlled transparency on the transverse electro-optical effect. As is known, online input and preliminary processing of identified images are carried out in these controlled transparencies within one "write-erase" cycle of the modulator (instead of two), which provides an additional advantage.

The purpose of this article is to outline the results of development and investigation (on test and real identified images) of a holographic intensity correlator (HIC) with averaged resulting light distribution [3, 4], in which a controlled transparency was used on a PRIS-type transverse electro-optical effect [5, 6].

Let us assume that the amplitude transmission of the identified image is proportional to  $f(r)$ . This image is illuminated in the holographic intensity correlator by a collimated light beam with time-variable angle of inclination  $\alpha(t)$ ; because of this, the light distribution, proportional to the Fourier spatial spectrum, describes trajectory  $S(\omega)$  in the plane of the holographic filter. The pulse amplitude response of the system  $h(r)$ , which is the reference image, is modulated by a random phase mask and is recorded in the form of a Fourier hologram with envelope  $\mathcal{F}[h(r)]$ , where  $\mathcal{F}$  is the symbol of a Fourier transform. As a result of squaring and averaging the resulting amplitude distribution at the correlator output in time, we find [4]

$$g(r) = \int \int g(r, r_1) g^*(r, r_1) \gamma(r_1 - r_1) dr_1 dr_1.$$

(1)

where  $\tilde{g}(r, r_0) = f(r_0)\tilde{h}(r - r_0)$ ,  $\gamma(\cdot) = \mathcal{F}[S(\omega)]$ . Function  $\gamma(\cdot)$  characterizes the spatial dependence of radiation in the image plane and has the meaning of the degree of partial spatial coherence, although it is actually the Fourier spectrum of trajectory  $S(\omega)$ .

It follows from (1) that linearity of processing the identified image in amplitude is provided in the holographic intensity correlator at  $\gamma(\cdot) = \text{const}$ , while the linearity of processing in intensity is provided at  $\gamma(\cdot) = \delta(\cdot)$ . In the second case of interest to us, it is more optimum from the viewpoint of the isotropicity of processing and simplicity of realization to deflect the collimated input light beam along a circle of radius  $\omega_0 = (2\pi/\lambda)\text{tg } \alpha$ . Then  $\gamma(\cdot)$  will have smaller width of the central peak  $\delta_0 \sim 1/\omega_0$ , the greater the angle of deflection of the deflector  $\alpha$ . However the value of angle  $\alpha$  is limited by the upper bound of the aperture of the holographic filter, which in turn is determined by the dimension of the resolution element of the random phase mask  $\delta_1$ . Therefore,  $\omega_0$  can be selected approximately equal to one-fourth the size of the hologram and  $\delta_1$  can be selected considerably smaller than the size of the element of resolution of the identified image. Function  $\gamma(\cdot)$  will then approach a delta-function and we find from (1) that

$$g_{hc}(r) = |f(r)|^2 \cdot |h(r)|^2.$$

The additional error, arising due to the finite dimension of  $\delta_0$ , will comprise a value on the order of  $\delta_0/l_0$ , where  $l_0$  is the linear aperture of the correlator in the plane of the identified image [7].

The characteristic feature of PRIS-type light modulators is the capability of outlining the images to be recorded. The fact is that the images are recorded in single crystal bismuth silicate and germanate plates with orientation [110] and [111] due to the occurrence of a spatially distributed positive charge in them due to the effect of the recorded emission and homogeneous external longitudinal electrical field [8]. As a result, a transverse electrical field, which is visualized due to the presence of the internal transverse electro-optical effect in the indicated crystals, proportional to the charge gradient, occurs.

The derived charge distribution is transient and deteriorates within  $10^{-1}$  to  $10^{-2}$  s as a function of the crystal specimen. Accordingly, there is the possibility of selecting a controlled transparency with regulated image storage time (over a wide range), which is determined by the charge deterioration time. If need be, the recorded images are erased by illuminating the controlled transparency with a homogeneous light beam.

A controlled transparency, created on the basis of a single crystal of bismuth germanate 1 mm thick and with orientation [111] with transparent electrodes applied to the surface, was used in the investigation. High-frequency spraying of the conductor in a vacuum with simultaneous control of transmission made it possible to increase the transparency of the controlled transparency from initial

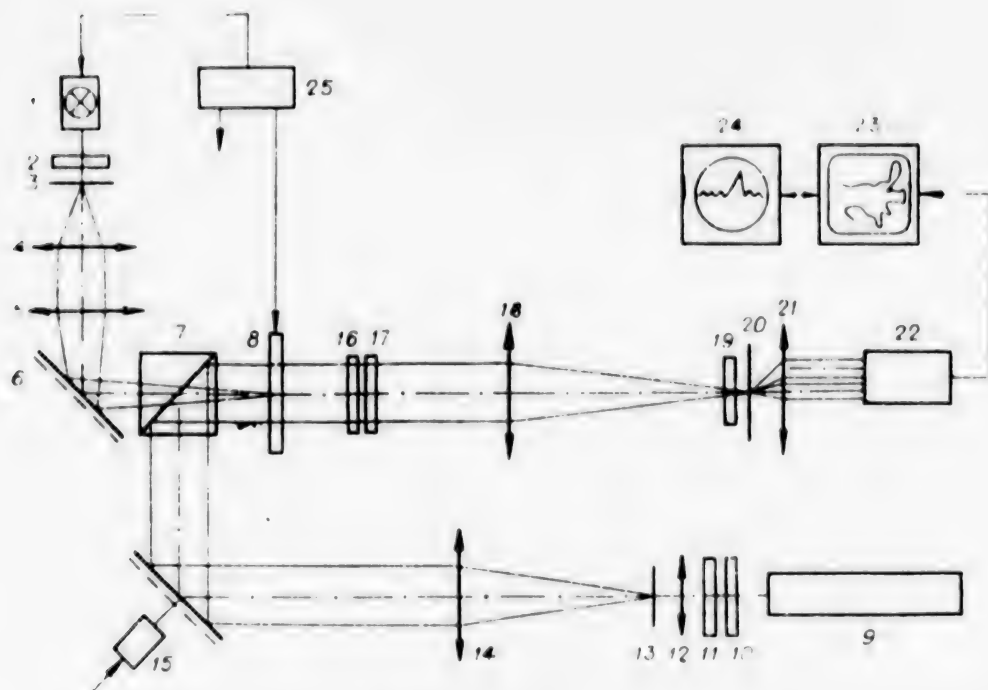


Figure 1

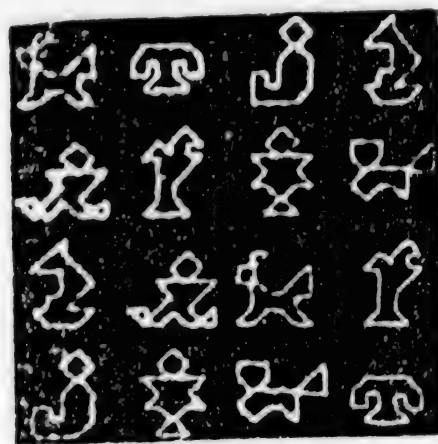


Figure 2

values of 70 to 85 percent in the red region of the spectrum. The diameter of the controlled transparency was 30 mm, power supply voltage was 3 kV, storage time was 10-15 s and the thickness of the contour of the recorded two-gradation silhouette image was 50  $\mu\text{m}$ . To illuminate the anisotropy of the transverse electrooptical effect, readout was accomplished by circular-polarized light with subsequent compensation and separation of the perpendicular (with respect to the initial) component of the polarization vector. This made it possible to accomplish isotropic outlining by averaging in all directions.

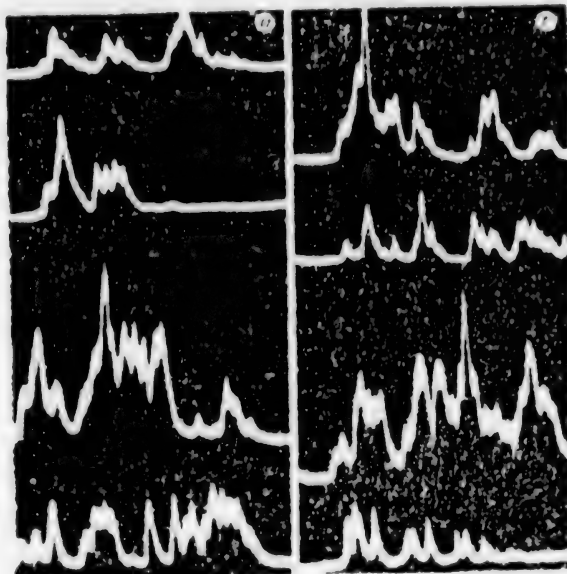


Figure 3



Figure 4

A diagram of the developed holographic intensity correlator is presented in Figure 1, where 1 is the light source, 2 is a blue light filter, 3 is the plane of the identified image, 4 and 5 are the objectives of a telescope system, 6 is a rotary mirror, 7 is a light-splitting tube, 8 is a photoelectro-optical controlled transparency, 9 is a laser, 10 is a polarizer, 11 and 16 are quarter-wave plates, 12 is a micro-objective; 13 is a diaphragm, 14 is a collimating objective, 15 is a rotary mirror, 17 is an analyzer, 18 and 21 are Fourier objectives, 19 is a red light filter, 20 is a unit with replaceable holographic filters, 22 is a photoreader, 23 is a monitor, 24 is an oscillograph with dedicated television line and 25 is the electronic unit for system control.

The telescope system, which includes objectives 4 and 5, projects from the plane of the identified image to the plane of the controlled transparency. A time-variable sloping light beam is shaped by a rotary mirror, as a result of which the spatial spectrum of the identified image describes the trajectory in plane 20 in the form of a circle with diameter equal to half the linear aperture of the holographic filter. The quarter-wave plate 11 is designed to transform linear polarization to circular polarization, while plate 16 is a compensating plate. Objective 18 accomplishes direct Fourier transformation of the recorded identified image and that processed in the controlled transparency, while objective 21 carries out inverse Fourier transformation. Light filter 19 is used to absorb the recorded emission passing through the controlled transparency.

The elements of the holographic intensity correlator are Yupiter-36B objectives 4 and 5 ( $f = 250$  mm and the aperture ratio is 1:3.5), an LG-79-1 laser (emissive power of 10 mW), micro-objective with magnification of 20, Yupiter-6-2 objective 14 ( $f = 180$  mm, 1:2.8), O-2 objective 18 ( $f = 750$  mm, 1:10) and Kaleynar-3B objective 21 ( $f = 150$  mm, 1:2.8), quarter-wave mica plates and standard light filters, polarizers, light source and vidicon.



Figure 5



Figure 6

The patterns presented in [1] in Figures 4 and 5, a, were used as the test silhouette identified patterns and contour reference patterns in the investigation. Identified patterns, recorded and outlined on a controlled transparency, are presented in Figure 2 and the scanning patterns of correlation functions for both reference images, respectively (scanning was carried out along four lines through the conditional centers of the identified patterns), were used in Figure 3, a and b.

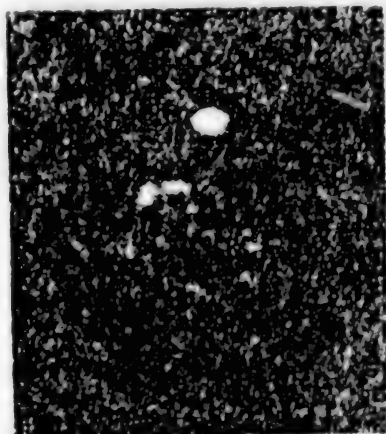


Figure 7

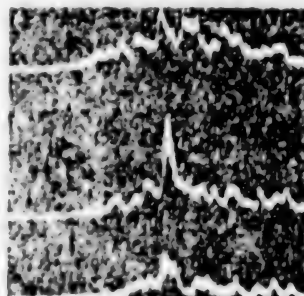


Figure 8

The real identified pattern was a terrain image shown in Figure 4. The reference image, regenerated from the holographic filter, is presented in Figure 5, while the identified pattern, recorded and outlined in the controlled transparency, is presented in Figure 6. The light distribution of the correlation function is presented in Figure 7, while its scanning patterns along three lines, one of which passes through the autocorrelation maximum, which exceeds more than two-fold the values of the cross-correlation functions, are presented in Figure 8. Hence, it follows that the desired fragment is located within the pattern, while the coordinates of its center are determined by the position of the maximum.

Thus, the developed holographic intensity correlator with simultaneous online input and preliminary processing of the identified pattern on a PRIS-type controlled transparency permits one to realize the process of identification of real half-tone terrain images. The similarity function in this case is the correlation function of the outlined identified pattern and reference image.

The authors are grateful to Ye. S. Nezhevenko for constant discussions and assistance in the investigation and to L. A. Gibina for participation in the experimental investigations.

#### BIBLIOGRAPHY

1. Gibina, L. A. et al., "Optoelectronic System With Online Input and Preliminary Processing of Identified Patterns," AVTOMETRIYA, No. 2, 1984.
2. Dun, A. Z. et al., "Photoelectro-optical Converter Based on Cooled  $KD_2PO_4$  Crystal and Selenium Photographic Emulsion," ELEKTRONNAYA TEKHNKA, SERIYA 4, ELEKTROVAKUUMNYE I GAZORAZRYADNYE PRIBORY, Vol. 71, No. 7, 1978.
3. Chavel, P and Lowenthal, "A Method of Incoherent Optical-Image Processing Using Synthetic Holograms," JOURNAL OF THE OPTICAL SOCIETY OF AMERICA, Vol. 66, 1976.
4. Potaturkin, O. I., Ye. S. Nezhevenko and V. I. Khotzkin, "Coherent Intensity Correlator," JOURNAL OF OPTICS, Vol. 11, 1980.
5. Petrov, M. P. et al., "Transient Phenomena in Space-Time Light Modulator," PIS'MA V ZHURNAL TEKHNIЧЕСКОY FIZIKI, Vol. 6, No. 7, 1980.
6. Fel'dbush, V. I., "A Controlled Transparency for Pattern Outlining," AVTOMETRIYA, No. 6, 1980.
7. Potaturkin, O. I., "Diffraction Intensity Correlators," in "Primeneniye metodov opticheskoy obrabotki informatsii i golografii" [The Use of Optical Data Processing and Holographic Methods], Leningrad, Leningrad Nuclear Physics Institute, 1980.
8. Petrov, M. P., S. I. Stepanov and A. V. Khomenko, "Fotochuvstvitel'nyye elektroopticheskiye sredy v golografii i opticheskoy obrabotke informatsii" [Photosensitive Electrooptical Media in Holography and Optical Data Processing], Leningrad, Izdatel'stvo "Nauka", 1983.

COPYRIGHT: Izdatel'stvo "Nauka", "Avtometriya", 1984

6521

CSO: 8144/1918

UDC 535.317

DESIGN METHOD FOR TELESCOPIC SYSTEM CONSISTING OF THIN ELEMENT AND FINITE-THICKNESS LENS

Leningrad OPTIKO-MEKHANICHESKAYA PROMYSHLENNOST' in Russian No 6 Jun 84  
(manuscript received 18 May 83) pp 19-20

TARABUKIN, V.V.

[Abstract] Telescopic systems consisting of a thin element plus a finite-thickness lens are part of a number of Gauss objective lens systems. An analytical method is developed which can be used to calculate the composite parts of such an objective in the region of third-order aberrations and then to synthesize the objective as a whole. The optical system is analyzed by the 'plate' reduction method. Formulas are derived which can be used directly to find the basic parameters  $P$  and  $W$  of the thin compensating component in the system; these are then used to determine the construction members. The method simplifies the analytical task, since there is no need to get exact values of the Seidel coefficients  $S_I$ ,  $S_{II}$  and  $S_{III}$ . The aberrations of both parts of the objective are cross-corrected, which makes it possible to adjust the values of the aberration coefficients of each part over a wide range. References: 3 Russian.  
[46-6900]

UDC 621.373.536

ANALYSIS OF THERMOOPTICAL ABBERRATIONS OF FOCUSING MIRRORS

Leningrad OPTIKO-MEKHANICHESKAYA PROMYSHLENNOST' in Russian No 6, Jun 84  
(manuscript received 13 Jul 83) pp 20-24

POGODIN, G.I., TRUNEVA, E.V. and KHANKOV, S.I.

[Abstract] Analytical relationships are proposed which describe the steady-state thermooptical aberrations of parabolic and spherical mirrors caused by absorption of part of the incident radiation by the working surface. The relationships derived are valid for long-focus disk mirrors which

expand freely upon being heated. Absorption by the working surface of part of the incident radiation results in a temperature distribution which is approximately uniform in the axial direction, parabolic in the radial direction, and which drops off toward the edge of the mirror. This distribution distorts the profile of the mirror; the temperature shift of the paraxial focus differs from the shift during uniform heating. The longitudinal spherical thermooptical aberration of a parabolic mirror is negative when the temperature on the axis of the mirror is maximum. References: 13 Russian. [46-6900]

UDC 539.23

#### MOLECULAR LAMINATION OF TITANIUM OXYGEN LAYERS AND THEIR INFLUENCE ON THE CHEMICAL STABILITY OF OPTICAL GLASS

Leningrad OPTIKO-MEKHANICHESKAYA PROMYSHLENNOST' in Russian No 6, Jun 84  
(manuscript received 19 Oct 83) pp 57-59

TOLMACHEV, V.A., OKATOV, M.A. and PAL'CHEVSKIY, V.V.

[Abstract] This study describes the use of molecular lamination to apply protective molecular films on polished optical glass. Titanium oxygen layers were synthesized in a vacuum reactor by treating the specimens in  $TiCl_4$  and  $H_2O$  vapors in alternation with vacuum treatment at various temperatures. The chemical stability was estimated by the yield of dissolved glass components ( $BaO$  and  $ZnO$ ) in the etching solution at various temperatures. The surface had to be cleaned with a 0.05 N  $HNO_3$  solution, because the application of titanium oxygen layers on the surface of ground glass produced no useful effect when various chemical compounds were formed as the surface contacted moisture, including silicic acid salts that break down the adhesion. The chemical stability of TK8 glass etched in a solution of  $CH_3COOH$  at various temperatures is analyzed for different etching temperatures and numbers of etching cycles. It is found that the chemical stability increases as the heating temperature of the titanium oxide. Specimens obtained at  $20^\circ C$  were found to be especially stable. References: 6 Russian. [46-6900]

UDC 539.1.078

#### HIGH-ANGULAR-RESOLUTION SPECTROMETER WITH DUAL NEUTRON BEAM MONOCHROMATIZATION

Moscow PRIBORY I TEKHNIKA EKSPERIMENTA in Russian No 4, Jul-Aug 84  
(manuscript received 23 May 83) pp 52-57

ABOV, Yu., KULIDZHANOV, F.G., YELYUTIN, N.O., NIZOVOY, S.N., Moscow Engineering-Physics Institute.

[Abstract] A neutron spectrometer with high angular resolution ( $10^{-5}$  rad) is described which incorporates a dual monochromator. The high angular

resolution is achieved by using near-perfect germanium crystals in the parallel (n, -n)-position. A diagram of the spectrometer is presented, showing the dual monochromator module and a pair of goniometer devices secured to the optical bench. The performance of the system is described, and stable long-term operation is demonstrated. The spectrometer can be used to investigate the neutron optics of perfect crystals and the scattering of neutrons at small angles on objects as large as  $1 \text{ mm}^2$ . The instrument can easily be adjusted for traditional neutron-diffraction problems. References 12: 8 Russian, 4 Western.  
[64-6900]

UDC 539.1.073.3

#### DIANA 700-LITER XENON BUBBLE CHAMBER

Moscow PRIBORY I TEKHNIKA EKSPERIMENTA in Russian No 4, Jul-Aug 84  
(manuscript received 24 Oct 83) pp 63-65

BARMIN, V.V., BORISOV, V.N., GOLUBCHIKOV, V.M., GOROKHOV, A.I., DEMEKHIN, V.I., DEMIDOV, V.S., DOLGOLENKO, A.G., KOLPASHCHIKOV, G.A., KONOPLEV, N.S., KUTEPOV, M.M., MESHKOVSKIY, A.G., NIKITIN, A.A., SOLOV'EV, A.P., KHROPOV, M.S., CHUVILO, I.V. and SHEBANOV, V.S., Institute of Theoretical and Experimental Physics, Moscow

[Abstract] The DIANA (neutral hadron detector and analyzer) xenon bubble chamber, which has a  $150 \times 70 \times 70 \text{ cm}^3$  working chamber, is described. The short radiation length of xenon makes the DIANA as effective as the Gargamelle and SKAT freon chambers as a  $\gamma$ -quantum detector. The chamber is designed to record radiation processes involving high-energy processes with near-100% efficiency under 4 -geometry conditions. The structural diagram of the device and operating specifications are presented. A photograph is reproduced which illustrates fast-particle trails detected in working with a relativistic particle beam. References 5: 4 Russian, 1 Western.  
[64-6900]

UDC 535.317.1

#### LASER SYSTEM FOR HOLOGRAPHIC RECORDING OF INFORMATION FROM TRACK DETECTOR

Moscow PRIBORY I TEKHNIKA EKSPERIMENTA in Russian No 4, Jul-Aug 84  
(manuscript received 14 May 83) pp 76-77

BARTKE, Ye., IVANOV, I.Ts. and EKSNEROVA, Ya., Joint Institute of Nuclear Research, Dubna.

[Abstract] A laser system consisting of a 6y rhodamine-dye laser pumped by a nitrogen laser is described for recording Gabor holograms. The system

is shown capable of providing high quality holograms of thin glass fibers simulating tracks in a bubble chamber model. The recording scheme employed in the experiment incorporates the nitrogen laser, a quartz lens, the dye laser, a collimator, the object being recorded and a camera. The capabilities of the method are compared by recording holograms of the same objects in the light from an He-Ne laser with good spatial and temporal coherence. The quality of the holograms obtained is comparable, which confirms the suitability of the LKR6y rhodamine-dye laser for holographic recording of information from track detectors. References 2: 1 Russian, 1 Western.  
[64-6900]

UDC 621.382.04

#### ELECTRONIC EQUIPMENT TEST SYSTEM FOR MULTICHANNEL DRIFT CHAMBERS

Moscow PRIBORY I TEKHNIKA EKSPERIMENTA in Russian No 4, Jul-Aug 84  
(manuscript received 2 Jun 83) pp 80-83

KARPUKHIN, V.V., Joint Institute of Nuclear Research, Dubna.

[Abstract] A drift-chamber electronic equipment test system is described which automatically tests and adjusts the drift chamber data readout system. The test system is connected to the inputs of the data readout system via signal wires, which makes it possible to find broken wires in the drift chamber. The test system outputs test pulses to the signal wires and compares the number of the selected channel with the number received from the data readout system; if these numbers are the same, the channel is working properly. Block diagrams of the test system and controller are presented, along with schematic diagrams of the pulse switcher and splitter; the timing diagram of the test system is explained. The basic specifications of the test system are listed, and operation of the system on line with a computer is described. References 6: 4 Russian, 2 Western.  
[64-6900]

UDC 681.7.062.47:681.514

#### SPECTRAL PROPERTIES OF VARIABLE-FOCUS MEMBRANE MIRROR

Moscow PRIBORY I TEKHNIKA EKSPERIMENTA in Russian No 4, Jul-Aug 84  
(manuscript received 25 Apr 83) pp 156-158

MOTOSHKIN, V.V. and SLOBODYAN, S.M., Automated Control Systems and Radio Electronics Institute, Tomsk.

[Abstract] A variable-focus membrane mirror is described which is designed to correct the focusing of the input beam by using the measured distortions of sounding radiation. The spectral properties of the

metallized coating of the mirror are investigated. The membrane mirror is based on polymer films from 5 to 50  $\mu\text{m}$  thick with a multilayered dielectric - metal - dielectric reflecting surface. The optimum selected reflecting coating structure is found to be a composition with a copper layer 10 nm thick. The reflecting properties of this structure in the medium-wave part of the optical band are plotted as a function of wavelength. References 12: 8 Russian, 4 Western.  
[64-6900]

UDC: 681.7.068

#### FIBER-OPTIC MODULATORS

Moscow PRIBORY I TEKHNIKA EKSPERIMENTA in Russian No 4, Jul-Aug 84  
(manuscript received 25 May 83) pp 165-168

KUKHTA, A.V., SVERCHKOV, Ye.I., TELEGIN, G.I., Radio Engineering and Electronics Institute, USSR Academy of Sciences.

[Abstract] The arrangement and parameters of phase and polarization fiber-optic modulators employed by the authors for fiber-optic interferometry are described. A series of modulator versions based on a TsTS-19 piezo-ceramic and fiber-optic light guides are investigated. The parameters of the phase and polarization modulators investigated are tabulated. Fiber-optic phase modulators are described in which efficient modulation is achieved with low mechanical stresses in the light guides and with low supply of voltage. These devices consist of duralumin disks 50 - 70 mm in diameter and 3 - 5 mm thick. The disks contain openings in which the piezo-ceramic is inserted. References 5 Russian.  
[64-6900]

UDC 621.373.826.038

#### SMALL LOW-NOISE MICROWAVE-PUMPED He-Ne LASER

Moscow PRIBORY I TEKHNIKA EKSPERIMENTA in Russian No 4, Jul-Aug 84  
(manuscript received 21 Feb 83 after revision) pp 176-179

GELLER, V.M., GRIF, G.I. and KHRUSTALEV, V.A., Electrical Engineering Institute, Novosibirsk.

[Abstract] A microwave-pumped He-Ne laser with a low intrinsic noise level that provides single-mode operation at  $\lambda = 632.8 \text{ nm}$  is described. The laser incorporates a radiator, a microwave power source and a microwave cable segment. The laser radiator employs a coaxial design; the gas-discharge tube containing the microwave device and the optical cavity are contained in a common housing. Tests show that the output power is a monotonic function of the microwave pumping power, which makes it

possible to adjust the power continuously and modulate the radiation. The advantages of the device include the fact that there are no reactive oscillations, and the intrinsic noise level is low. References 4 Russian. [64-6900]

UDC 621.311.6:621.375.826

#### CIRCUIT FOR SYNCHRONIZING RADIATION FROM TWO LTI-5 LASERS

Moscow PRIBORY I TEKHNIKA EKSPERIMENTA in Russian No 4, Jul-Aug 84  
(manuscript received 28 Aug 83 after revision) pp 180-182

BELOUSOV, V.I., CHERNYAKOV, S.V. and DERZHIYEV, V.I., Physics Institute,  
USSR Academy of Sciences

[Abstract] This study describes a circuit for synchronizing the radiation produced by two LTI-5 lasers in order to obtain pairs of giant pulses separated by variable intervals (up to 800  $\mu$ sec). The synchronization circuit incorporates a charge module, a discharge module, a univibrator, a flip-flop, a pulse generator, a comparison device, a commutator and charge/discharge blocking circuits. Schematic diagrams of the univibrator and blocking circuits are presented, along with a timing diagram describing operation at 50 Hz. Synchronization is based on tying the charging of each laser to the phase of the power supply circuit. In tests, the circuit has provided stable generation of pairs of 1.06  $\mu$ m giant pulses at 12.5, 25 and 50 Hz. Reference 1 Russian. [64-6900]

UDC 621.376.5

#### DEVICE FOR PULSE-AMPLITUDE MODULATION OF LASER RADIATION POWER

Moscow PRIBORY I TEKHNIKA EKSPERIMENTA in Russian No 4, Jul-Aug 84  
(manuscript received 14 Apr 83) pp 183-185

ZVEREV, B.A., PAKHOMOV, S.V. and SAVOSTIN, P.I., Moscow Physical Technical Institute.

[Abstract] A linear device is described for controlling the power of laser radiation. The device employs commercially produced electronic and optical components, and provides good precision and speed; it is designed for use in high precision optical-mechanical devices for reproducing half-tone images. The control element is an ML 201 acousto-optical modulator that is arranged so that the incident light flux creates a Bragg angle with the front of the acoustic wave induced in the modulator. The schematic diagram of the electronic section of the device, which incorporates seven microcircuits, is presented. The amplitude of the high frequency signal is

controlled by means of combined collector modulation. The amplitude-frequency and phase-frequency characteristics of the device are plotted, and show that the device operates stably up to 250 KHz. The adjustment characteristics of the device are plotted with and without radiation power feedback. The nonlinearity of modulation is less than 1 percent over the range of input signals from 0 to 10 V, with contrasts up to 4500:1, and efficiency approaching 0.81. References 4 Russian.  
[64-6900]

UDC 621.385.832

#### WIDE-BEAM ELECTRON GUN

Moscow PRIBORY I TEKHNIKA EKSPERIMENTA in Russian No 4, Jul-Aug 84  
(manuscript received 3 Oct 83) pp 237-238

GRIGOR'YEV, Yu.V., PEREVODCHIKOV, V.I. and STEPANOV, A.V., All-Union Electrical Engineering Institute, Moscow.

[Abstract] A gun is described that produces a beam of accelerated electrons by means of a four-electrode electro-optical system with flat electrodes and filament thermocathodes. The device is contained in a cylindrical housing, and is produced in two versions: one with an open high voltage input employing metal ceramic insulators, and one with cable inputs. Accelerating voltages of 130 -180 kV are employed, and the average energy of the electrons ejected is 75 - 145 keV. The maximum density of ejected current in the pulse mode is 10 mA/cm<sup>2</sup>.  
[64-6900]

UDC 621.384.8

#### AUTOMATIC SCANNING MANIPULATOR FOR MASS SPECTROMETER EMPLOYING LASER-PLASMA ION SOURCE

Moscow PRIBORY I TEKHNIKA EKSPERIMENTA in Russian No 4, Jul-Aug 84  
(manuscript received 9 Aug 83) p 240

BUSYGIN, A.I., DROZDOV, V.V., SMIRNOV, V.P., UL'MASBAYEV, B.Sh., and SHCHERBAKOV, A.Yu., Current Sources Scientific Research Institute (All-Union), Moscow.

[Abstract] An automatic scanning manipulator is described which moves a specimen uniformly in sync with laser pulses over rectangular areas. The manipulator control system provides the capability of changing the dimensions of the areas, the number of total scanning cycles and the amount of overlap of the laser pulse etching craters. Scanning can be controlled automatically and manually. Digital readouts indicate the current coordinates of the laser etching point with respect to the starting point, as

well as the current scanning cycle. For convenient operation, the control module employs a remote hand-held control box which duplicates the basic control operations - start, stop and step-by-step manual control of the tables. The scanning areas are 15 x 15 millimeters square; the counter capacity along both axes is  $9 \cdot 10^3$  pulses. In the manual mode, the specimen can be moved rapidly, slowly or in steps along one or two coordinates simultaneously.

[64-6900]

UDC 662.99:088.8

#### LIGHT SPLITTER BASED ON THREE-DIMENSIONAL HOLOGRAPHIC DIFFRACTION GRATING

Moscow PRIBORY I TEKHNIKA EKSPERIMENTA in Russian No 4, Jul-Aug 84  
(manuscript received 18 Jul 83) pp 241-242

D'YACHENKO, N.G., MANDEL', V.Ye., NECHAYEVA, T.A. and TYURIN, A.V.,  
Odessa State Scientific Research Institute of Physics

[Abstract] A light splitter is described that consists of a three-dimensional diffraction grating in an additively colored single-crystal plane-parallel KCl or NaCl plate. The device is designed to operate in the visible and near-infrared regions, and allows the intensity ratio of two streams of radiation to be adjusted continuously over a wide range while maintaining a fixed angle between them. The splitter can be used in optical devices employing dual beams and in data input/output devices, inter alia. The intensity ratios of the light beams can be varied over the range 0 - 1, with a spectral region of 0.4 - 1.4  $\mu\text{m}$  and corresponding Bragg angles of 2.5 - 60°. Reference 1 Russian.

[64-6900]

UDC 681.7.064.45

#### HIGH SPEED SPECTROPHOTOMETER FOR MEASURING SPECTRAL CHARACTERISTICS OF OPTICAL COATING DURING PREPARATION IN VACUUM

Moscow PRIBORY I TEKHNIKA EKSPERIMENTA in Russian No 4, Jul-Aug 84  
(manuscript received 15 May 83) p 242

YEFREMOV, D.Ye., ZELIKMAN, L.I., LEKHTSIYEV, Ye. N., STEPANOV, B.M.,  
TALALAYEV, N.G. and YURKOV, A.A.

[Abstract] A high speed spectrophotometer is described for measuring the spectral characteristics of thin optical coatings after the application of each separate layer. The device measures the spectral coefficient of transmission of the substrate without any coating; it then measures the substrate with the coating applied and computes the ratio of the two

figures. The device incorporates an illumination source with a fiber optic collector, and a controller and data processor. Scanning is controlled by the scanning system drive. The operator can program any scanning range from the static mode at any wavelength and extending to the full spectral range. Information about the wavelength and coefficient of spectral transmission at a given wavelength is displayed digitally. The spectral transmission curve can be observed in real time on a CRT display. The device provides a spectral range of 50 - 1100 nm, with spectral range resolution better than 3nm. Measurement time is 10 - 60 s, with a dynamic range of 0.01 - 1.  
[64-6900]

UDC 621.384.634.142.5

HIGH FREQUENCY SYSTEM OF JINR PROTON SYNCHROTRON FOR LIGHT NUCLEUS  
ACCELERATION

Moscow PRIBORY I TEKHNIKA EKSPERIMENTA in Russian No 4, Jul-Aug 84  
pp 32-36

BROVKO, O.I., MIKHAYLOV, A.I. and CHEKHLOV, K.V., Joint Institute of  
Nuclear Research, Dubna

[Abstract] Redesign of the HF accelerating system of the proton synchrotron developed by the Joint Institute of Nuclear Research (Dubna) in order to increase the amplitude of the accelerating voltage for accelerating light nuclei is described. The optimum acceleration version is determined analytically to be that employing a multiplicity of two and a 17-kV HF voltage amplitude on the accelerating electrode at 0.3 - 2.88 MHz. The structural diagram of the accelerating system is analyzed, and the schematic diagram of the output stage is presented. Testing in various nucleus and proton acceleration modes indicate that varying the magnetization current from 0 to 300 A tunes the resonant frequency of the loop through the range 0.3 - 3.0 MHz. The redesign of the accelerating system has doubled the intensity of the beams of accelerated nuclei as compared with the single-stage acceleration mode. References 5 Russian.  
[64-6900]

UDC 621.384.649

CONTINUOUS ELECTRON ACCELERATOR EMPLOYING SECONDARY ION-ELECTRON EMISSION

Moscow PRIBORY I TEKHNIKA EKSPERIMENTA in Russian No 4, Jul-Aug 84  
(manuscript received 4 Jul 83) pp 24-26

ABROYAN, M.A., USPENSKIY, N.A. and FEDYAKOV, V. P., Electrophysical  
Apparatus Scientific Research Institute, Leningrad.

[Abstract] An electron accelerator is described in which the plasma in the ion source is formed by auxilliary beams of electrons. The accelerator produces a  $180 \times 600 \text{ mm}^2$  beam; the geometry of the accelerating space is optimized. A high voltage secondary-emission cathode and an anode are used to produce 2,549 slightly diverging electron beams. The arrangement, geometry and operation of the device are described. Steady-state operation with a gas (helium or air) flow rate of  $300 \text{ cm}^2/\text{hr}$  is described. Currents up to 50mA are achieved for 0.15mV accelerating potentials. The accelerator is found promising for use in technological radiation processes because of its efficiency and the simplicity of the design of the accelerator and its power supply and vacuum system. References 7: 6 Russian, 1 Western.  
[64-6900]

UDC 537.533

STEADY-STATE SOURCE OF NEGATIVE HYDROGEN IONS WITH HOLLOW CATHODE

Moscow PRIBORY I TEKHNIKA EKSPERIMENTA in Russian No 4, Jul-Aug 84  
(manuscript received 21 Feb 83) pp 42-44

ANTIPOV, S.P., YELIZAROV, L.I., MARTYNOV, M.I. and CHESNOKOV, V.M.

[Abstract] An axisymmetrical hollow-cathode plasma source of negative hydrogen ions employing a radial magnetic field is described. The source consists of a magnetic system which produces a radial magnetic field, a cesium hollow cathode, an auxilliary anode which ignites the discharge, a main anode that serves simultaneously as an emission electrode, and an accelerating electrode. Ion current as high as 0.7 A is produced in the steady state mode. It is found experimentally that an optimum magnetic field of approximately  $2 \cdot 10^{-3} \text{ T}$  exists in the source regardless of the discharge combustion mode. The source can also operate without an external magnetic field. The optimum hydrogen consumption is determined as a function of the consumption of cesium, with a greater optimum hydrogen consumption corresponding to a high cesium consumption. The relationship between  $\text{H}^-$  ion current and the discharge current is found to be linear. Negative hydrogen ion current of up 0.1 A is obtained. References 6: 4 Russian, 2 Western.  
[64-6900]

UDC 621.384.63:621.3.032.213.12

DESIGN AND HEATER CHARACTERISTICS OF THERMOEMISSION CATHODE FOR MICROTRON

Moscow PRIBORY I TEKHNIKA EKSPERIMENTA in Russian No 4, Jul-Aug 84  
(manuscript received 4 Jul 83) pp 44-46

LUK'YANENKO, E.A., TOKAREV, Yu.Ye., KOVALEV, V.N., LYAPIN, A.A. and  
CHURSIN, M.M., Introscopy Scientific Research Institute, Moscow.

[Abstract] A lanthanum hexaboride ( $\text{LaB}_6$ ) thermoemission cathode design is described in which the heater current is 25 percent smaller than that of the usual design at a working temperature of  $1650^\circ\text{C}$ . Pyrometer measurements of the brightness temperature of the end working surface of the emitter and current conductors are described, and the brightness temperature is plotted as a function of the cathode heater current. The temperature differences of the current conductors in the immediate vicinity of the emitter and the end working surface of the emitter are also measured. It is found that emitter heating is more efficient in the cathode with parallel current conductors, apparently because of the contribution to the emitter heating of the thermal power radiated by the surface of the conductors. References 6: 5 Russian, 1 Western.  
[64-6900]

UDC 535.241.13:534:621.373.826.032.265

ACOUSTO-OPTICAL CELLS FOR DEFLECTING RADIATION OF SEMICONDUCTOR LASER

Novosibirsk AVTOMETRIYA in Russian No 3, May-Jun 84 (manuscript received 3 Jan 84) pp 103-105

TISHCHENKO, Yu.N. and TRUBETSKOY, A.V.

[Abstract] Findings from the development and investigation of deflector acousto-optical cells for deflecting optical radiation at  $\lambda = 0.89 \mu$  are presented. An acousto-optical cell is developed which incorporates an acoustic conductor made of  $\text{TeO}_2$ ,  $n\text{X-LiNbO}_3$  transducer and an epoxy-resin ultrasonic absorber. The characteristics of the cells are investigated. The diffraction efficiency of the cell, defined as the ratio of the intensity of the first-order diffracted light to the zero-order intensity after the cell, is analyzed. References: 3 Russian.  
[1-6900]

UDC 535.317.2:681.332

USE OF SEMICONDUCTOR LASERS IN HOLOGRAPHIC CORRELATORS

Novosibirsk AVTOMETRIYA in Russian No 3, May-Jun 84 (manuscript received 22 Sep 83) pp 98-101

BORZOV, S.M. and POTATURKIN, O.I., Novosibirsk

[Abstract] The possibility of using semiconductor lasers in holographic intensity correlators is investigated. The characteristics of the ILPN-2k laser are investigated, and a correlator type best suited for that light source is selected. An experimental correlator is described which provides replicable correlation results and accurate recognition of test images. The findings indicate that solid state lasers can be employed for image recognition in holographic intensity correlators which average the resultant light distribution. References 4: 2 Russian, 2 Western.  
[1-6900]

UDC 535.317.2:531.715.2

ENHANCING ACCURACY OF DIFFRACTION METHODS FOR DIMENSION TESTING

Novosibirsk AVTOMETRIYA in Russian No 3, May-Jun 84 (manuscript received 16 Jan 84) pp 75-84

BYCHKOV, R.M., KRIVENKOV, B.Ye. and CHUGUY, Yu.V., Novosibirsk

[Abstract] The effectiveness of aperture apodization and dual filtering for increasing the accuracy with which opaque objects can be measured is investigated. The influence of the aperture on distortion of the useful signal is analyzed. Apodization of the aperture makes it possible to increase the accuracy of the diffraction measurement method 10-fold. The fact that the apodizing properties of binary apertures show up only in certain directions is overcome by using dual aperture filtering. Aperture apodization is compared with spectral filtering. It is found that the overall error is strongly dependent on the relative dimensions of the object and the spectral frequency region employed in the measurements. The results of laboratory tests agree basically with the theoretical results to within 0.2 percent. References 9: 10 Russian, 1 Western.  
[1-6900]

UDC 621.382.8:681.327

INVESTIGATION OF SPEED OF OPTICAL INFORMATION CONVERTER BASED ON MF-16  
INTEGRATED PHOTODETECTOR ARRAY

Novosibirsk AVTOMETRIYA in Russian No 3, May-Jun 84 (manuscript received  
17 Jan 83 after revision) pp 68-75

KOMAROV, V.M., Rybinsk Yaroslavskoy

[Abstract] Optical information converter speed is analyzed by deriving formulas--relating the optical information accumulation time allowing the image of the object to be extracted--to the parameters defining the speed of that process. The average output voltage of a cell of the MF-16 photodetector array is found as a function of the optical radiant energy at nominal supply voltage. The formulas derived can be used to select comparison levels which will ensure that the object is extracted against the background of the scanned zone. The optimum length of the accumulation interval can be found from the assigned values of the parameters of the converter and the information sensing conditions. An example of the analysis of a converter is presented. References 11: 10 Russian, 1 Western. [1-6900]

UDC 535.4:543.46

DIFFRACTION INTERFEROMETER

Novosibirsk AVTOMETRIYA in Russian No 3, May-Jun 84 (manuscript received  
23 Jan 84) pp 61-67

KORONKEVICH, V.P. and LENKOVA, G.A., Novosibirsk

[Abstract] The interference properties of arrangements employing Fresnel zone plates are investigated in order to demonstrate the interference phenomena occurring for different positions of the entrance pupils with respect to the recording plane. By placing these zones plates one behind another and combining their negative and positive focal planes it is possible to observe bands with equal thickness if specified light beams are extracted with the help of a diaphragm and an additional optical system. The band contrast is found to be strongly influenced by the width of the source. Two different optical circuits are examined which are mirror images of one another with respect to plate placement and the position of the band localization fields. The properties of the equal thickness bands and equal-inclination rings are analyzed. The diffraction interferometer can be employed for aligning objects. References 7: 4 Russian, 3 Western. [1-6900]

UDC 535.241.13:534

ACOUSTO-OPTICAL MODULATOR WITH COUNTER ACOUSTIC BEAMS ON OPTICALLY ACTIVE UNIAXIAL CRYSTAL

Novosibirsk AVTOMETRIYA in Russian No 3, May-Jun 84 (manuscript received 3 Jan 84) pp 43-49

TARKOV, V.A., TISHCHENKO, Yu.N., TRUBETSKOY, A.V. and SHIPOV, P.M.,  
Novosibirsk

[Abstract] The use of acousto-optical modulators with counter acoustic beams for fast holographic digital recording is investigated. The proposed model of interaction of the optical and acoustic waves in a optically active uniaxial crystal and the formulas derived from it can be used to calculate the propagation angle of acoustic waves in the crystal, the characteristic acoustic diffraction frequencies and the positions of the polarization plane of the diffracted light as a function of the parameters of the crystal and the propagation angle of the incident light with respect to the optical axis of the crystal. The interaction geometry of optical and acoustic waves in a modulator using a  $\text{TeO}_2$  crystal is described, and experimental prototypes are built with a working optical wavelength of  $\lambda = 0.89 \mu$  and 60-MHz acoustic bandwidth (from 70 to 130 MHz). The diffraction efficiency for each channel is 50 percent. The modulator is designed for holographic recording of digital data arriving at up to 60 Mbps. References 8: 5 Russian, 3 Western.  
[1-6900]

UDC 681.327.68:778.38

AUTOMATIC DEVICE FOR RECORDING DIGITAL DATA HOLOGRAM MATRICES

Novosibirsk AVTOMETRIYA in Russian No 3, May-Jun 84 (manuscript received 30 Dec 83) pp 13-19

BLOK, A.A., VANYUSHEV, B.V., VOLKOV, A.V., GIBIN, I.S., KOTENKO, V.P.,  
MANTUSH, T.N., PEN, Ye.F. and POTAPOV, A.N., Novosibirsk

[Abstract] An automatic device for recording hologram matrices which is part of a holographic archive memory system is described. The automatic hologram matrix recorder consists of an optical/mechanical module and an electronic system and is controlled by an SM-4 computer. In contrast to an earlier device, the present system employs an electrically controlled liquid-crystal-based transparency for data input. Recording quality is enhanced by using subsystems which stabilize the exposure, control the angular position of the laser beam, and detect and eliminate defective areas on the recording medium. The optical and electronic control systems of the device are presented and analyzed; all of the electronic control modules are implemented in CAMAC standard and are controlled automatically

through a KK-16 crate controller. The device makes it possible to record digital data automatically in holographic memory modules (accommodating 160 x 170 holograms) with a recording density of  $0.6 \cdot 10^4$  bits/mm<sup>2</sup>. The probability of a data read error is approximately  $10^6 - 10^7$  (if no error correction is used). References: 6 Russian.  
[1-6900]

UDC 621.3.049.75:776

HYBRID OPTOELECTRONIC SYSTEMS FOR INSPECTION AND AUTOMATIC CLASSIFICATION OF IMAGES

Moscow IZMERENIYA, KONTROL', AVTOMATIZATSIYA in Russian No 1(49), 1984  
pp 62-71

ROZIN'KOV, N.S., candidate of technical sciences

[Abstract] Optical images of large-scale-integrated circuits ( $10^8-10^9$  bits) or of the earth's surface ( $10^8-10^{10}$  bits transmitted via satellite) require high-resolution high-productivity inspecting and automatic classifying equipment, hybrid optoelectronic systems being most suitable for this purpose. Such a system consists essentially of an input device, a preliminary transformer of functions characterizing the image classes, a generator of primary parameters characterizing the image structure and geometry, and a classifier with feedback to that generator through an adaptation module and a memory. Reliability and speed of image identification, in terms of classifier output signals characterizing the vector of image parameters, depend on the classification algorithm and on the set of image functionals as well as on the number of image parameters and the properties of images. Functionals decorrelated with respect to the adaptation sequence and selected so as to lower the dimensionality of the primary description vector and to ensure invariance of this vector relative to noninformative changes will yield maximum reliability and speed. Both linear and nonlinear transformation are realizable in the optical part of such a system. There are noncoherent hybrid optoelectronic systems, suitable for photomasks and for pattern or character recognition. There are coherent ones, suitable for space-time processing such as filtration and normalization. While many existing systems have a single channel for sequential processing, multi-channel systems have been developed for parallel optical processing with lens arrays and tunnels or Fresnel holograms. Figures 5; references 44: 18 Russian, 26 Western (1 in Russian translation).  
[311-2415]

UDC 621.385.832

AUTOMATIC MEASUREMENT OF FAST PROCESSES WITH AID OF TIME-SCALE CONVERSION

Moscow IZMERENIYA, KONTROL', AVTOMATIZATSIYA in Russian No 1(49), 1984  
pp 25-31

GOLOVASTIKOV, Yu.A., engineer, RABINOVICH, S.G., candidate of technical sciences, STEPANOV, B.M., doctor of physico-mathematical sciences, and FILINOV, V.N., doctor of technical sciences

[Abstract] The principle of time-scale conversion, expanding the time scale of the electric input signal without distorting its waveform, is applied in automating the measurement of fast processes such as single events of nanosecond or picosecond duration. The essential component of a time-scale converter is a cathode-ray memory tube, on the target of which the analog input signal is recorded in real time in the form of a potential relief and from which the latter is then read by a line raster. With each change in the input signal represented by a change in the time position of the readout, this in effect amounts to an analog-to-digital conversion. Each readout is, moreover, accompanied by a corresponding partial erasure of the potential relief. The low-frequency sequence of readout signals proceeds through a pulse amplifier-shaper to a data processing system with a computer. The upper frequency limit of this pulse sequence depends on the sensitivity of the cathode-ray tube and the target dimension along the amplitude axis as well as on the amplitude characteristics and the dispersion but not on the frequency characteristics of the input process. The performance of such a converter is determined principally by the speed of the recording electron beam, the maximum possible speed being the most important performance indicator, also by the speed of the sweep generator and the signal discretization step and accuracy. Errors are caused by various sources of noise in the cathode-ray tube, foremost among them being nonuniformity of the target thickness with attendant fluctuation of target-plate and target-collector capacitances, secondary electron emission, and the grid electrodes. Several time-scale converters with different matching cathode-ray tubes are now produced in the Soviet Union, the "Foton-K" with a 2TZS-8 tube being most versatile and comparable with the Tektronix R7912. Use of microchannel amplifiers in their cathode-ray tubes makes recording speeds up to  $10^5$  km/s realizable and, when used as information carrier, should make it feasible to raise that speed to  $4 \cdot 10^5$  km/s for processes of short duration corresponding to an upper frequency limit of 7-10 GHz. Figures 1; tables 2; references 26: 21 Russian, 5 Western (2 in Russian translation).  
[31i-2415]

UDC 662.997.537.22(088.8)

INVESTIGATION OF POSSIBILITIES OF FABRICATING LIGHTWEIGHT THIN LIGHT-  
FOCUSING MIRRORS

Tashkent GELIOTEKHNICA in Russian No 3, Mar 84 (manuscript received  
4 May 83) pp 35-37

UMAROV, G. Ya., ALIMOV, A.K., BOLOTOV, V. N., GUNER, Ye.A. and LAPTEV,  
V.D., Physical-Technical Institute imeni S. V. Starodubtsev, Uzbek SSR  
Academy of Sciences

[Abstract] The possibility of developing thin lightweight mirrors for  
concentrating solar rays and for focusing Cherenkov particles on the  
photo-cathode of the photomultiplier without the use of lenses is investi-  
gated. The specifications of mirror produced by sagging and by profiling  
are investigated. Profiled mirrors are found to have slightly poorer  
parameters than sagged mirrors, but better than those of devices employing  
lens focusing. Figures 1; references 7: Russian.  
[303-6900]

UDC 519.688

OPTIMIZATION OF CATHODE LENSES WITH 'EFIR' APPLIED PROGRAM PACKAGE

Novosibirsk AVTOMETRIYA in Russian No 5, Sep-Oct 84 (manuscript received  
30 Dec 83) pp 93-101

IL'IN, V.P., KATESHOV, V.A., KULIKOV, Yu.V. and MONASTYRSKIY, M.A.,  
Moscow and Novosibirsk

[Abstract] Synthesis of electronic lenses is considered as the reverse  
problem of optimum control for lens boundaries and boundary conditions.  
The problem is reduced to a finite-dimensional problem of conditional  
minimization with the target function within a bounded space of variable  
parameters characterizing the lens structure and the energization mode.  
The method of synthesis, unlike the "axial distribution of the electro-  
magnetic field" method, requires precise stipulation of the boundary  
topology and the initial approximation. The iterative algorithm of such  
a synthesis yields on each step a physically realizable lens structure  
with known electron-optical characteristics. Use of the applied program  
package EFIR for optimum synthesis of electrostatic cathode lenses is  
possible after the specific class of problems has been precisely formu-  
lated; one of these is to minimize the electron-image characteristic  
function  $I_0(x)$  under constraints  $I_k(x) = 0$  ( $k = 1, \dots, m$ ) and  $I_k(x) \leq 0$   
( $k = m+1, \dots, n$ ) with  $a \leq x \leq b$  ( $a, b$  are given vectors). This problem is  
replaced with the corresponding variational problem. The program package  
for it includes solution of integral equations for perturbations of the  
potential distribution in a straight lens layer by means of B-spline

approximations and collocation of surface charge densities, with the use of Gaussian quadratures and utilizing the asymptotics in the vicinity of singular points, and subsequent numerical solution of the corresponding dense system of algebraic equations by the method of orthogonal transformations according to the KOPLA procedure. Two typical problems which have been solved with this program package and the same initial approximation are: 1) obtaining the image plane and the crossover plane in given locations along the axis for electron-optical magnification within the  $0.06 \leq M \leq 0.07$  range; 2) obtaining a given curvature for given locations of the image plane and the crossover plane. The program package is written for a BESM-6 high-speed computer with 192 kbyte memory or a YeS-1060 computer with at least 512 kbyte memory. The machine time for solving "spherical condenser" model problems depends on the required accuracy of determining the axial distribution of the potential and its derivatives at the cathode center, and on the how many aberration orders need to be corrected for. Figures 2; tables 1; references 30: 25 Russian, 4 Western.  
[152-2415]

UDE 681.327.68:621.383

#### LINEAR MODEL OF MOS-INTEGRATED PHOTODIODE-TYPE MULTIELEMENT OPTICAL SIGNAL CONVERTERS

Novosibirsk AVTOMETRIYA in Russian No 5, Sep-Oct 84 (manuscript received 26 Dec 83) pp 79-87

NAYMARK, S.I., Novosibirsk

[Abstract] A linear mathematical model of MOS-integrated photodiode-type multielement optical signal converters is constructed in matrix form for both design synthesis and performance analysis. The operation of an MOS photodiode element is reduced to simplest terms, a measurable current flowing through its resistance after the transient period following closure of the switch, and its function is regarded as equivalent to multiplying the photocurrent by 0 or 1 when the switch is open or closed respectively. On this basis, photosensitive arrays on a semiconductor chip are examined. Orthogonal and divisible arrays are considered, with the sampling matrix in the Vilenkin-Christiansen class of functions as the principal tool for circuit design and analysis. The calculations involve essentially linear transformations of an M-dimensional system of coordinates for an array of m converter cells. They apply to a self-scanning converter, an analog of a television tube with sweeping electron beam, as well as to converters for spectral transformation or space filtration. Figures 5; references 11: 10 Russian, 1 Western (in Russian translation).  
[152-2415]

UDC 681.327.521

# STRUCTURE OF PHOTOMETRIC CHANNEL IN HIGH-SPEED MICRODENSITOMETER AND ERRORS OF PHOTOMETRIC MEASUREMENT

Novosibirsk AVTOMETRIYA in Russian No 5, Sep-Oct 84 (manuscript received 22 May 84) pp 73-79

KOSYKH, V.P., Novosibirsk

[Abstract] The structure and the performance of a photometer for scanning microdensitometers in automatic image processing systems are evaluated from the standpoint of tradeoff between high speed and high accuracy. The photometric channel consists of a light source before the object and a photomultiplier followed by an integrator behind the object. The light source emits a photon flux of intensity  $\gamma$ , the object has a transmission coefficient  $\tau$ , and the photomultiplier consisting of  $k$  identical stages with an average secondary-emission factor  $\mu$  has a quantum efficiency  $\lambda$ . The number of electrons  $n$  emitted by the photomultiplier photocathode during the measurement-integration time interval  $t$  is a random quantity with a Poisson distribution  $p(n;t,\gamma,\lambda,\tau)$ , exactly in the case of a coherent light sources and approximately in the case of a semicoherent one such as a cathode-ray tube, where any of the parameters  $\gamma,\lambda,\tau$  can also be random quantities. The probability of recording  $s$  secondary electrons produced instantaneously by a single incident one,  $s$  also being a random quantity, is characterized by mean value  $M(s)$ . Measurement of the transmission coefficient is based on the relation  $\tau = s/mt\lambda M(\cdot)$ , where  $m = \mu^k - M(e_1)$  and  $e_1$  is the photomultiplication factor. In the simplest mode of measurement, with the time interval fixed, the estimate of this transmission coefficient is unbiased and has a dispersion which is the sum of two errors. The first error, caused by noise in the recorded photon flux and by the photomultiplication process, can be minimized by appropriate selection of the measurement time interval. The second error, dependent on the light source only, must and can be reduced by addition of a reference photomultiplier-integrator channel in parallel with the measuring channel and diverting a part of the photon flux from the light source. Now the transmission coefficient becomes biased and the error due to light source instability decreases, but an error due to noise and photomultiplication in the reference channel will appear. Another mode of measurement is with the time interval varied depending on the instantaneous photon flux intensity, or with integration in the measuring channel done over the time interval necessary for the integral in the reference channel to build up to a preset value. In the latter case the error due to light source instability is completely removed, but the error due to noise and photomultiplication in the reference channel will increase proportionally to the transmission coefficient squared. The latter method is preferable, as long as its error does not exceed the acceptable limit, because it does not require ratioing two quantities. All three methods were checked experimentally in measuring the transmission coefficient of neutral filters with a cathode-ray tube as light source at three levels of intensity and with a "Zenit-M" microdensitometer, in the variable-time

mode using a single electron beam, in the fixed-time mode using two electron beams, and with a fixed integral of the reference signal using two electron beams. Figures 2; references: 4 Russian.  
[152-2415]

UDC 681.7.068.4

PRODUCTION OF OPTICAL FIBER BUNDLES WITH EQUALIZATION OF ILLUMINANCE AT EXIT

Leningrad OPTIKO-MEKHANICHESKAYA PROMYSHLENNOST' in Russian No 7, Jul 84  
pp 58-59

SHASHIN, V.I. and GURENKO, V.A.

[Abstract] Production of optical fiber bundles with uniform output illuminance at the exit is considered, such bundles consisting of single fibers 50-80  $\mu\text{m}$  in diameter and usually 150-400  $\mu\text{m}$  long. Such a bundle was produced by regular laying of fibers, this pattern being dictated by the requirement of uniform illumination coming from the other end. Accordingly, the pattern must correct any nonuniformity of input illumination at the entrance. Figures 5; references: 2 Russian.  
[111-2415]

UDC 778.24

USE OF VARNISHED POLYETHYLENE TEREPHTHALATE FILM AS TRANSILLUMINATED SCREEN

Leningrad OPTIKO-MEKHANICHESKAYA PROMYSHLENNOST' in Russian No 7, Jul 84  
(manuscript received 13 Nov 83) pp 57-58

LENISYUK, G.P., SOLOV'YEV, G.Ya. and BELOUS, V.N.

[Abstract] An evaluation was made of varnished polyethylene terephthalate film as a transilluminated screen capable of scattering light uniformly at large solid angles, in preference to not-easily-manufacturable screens of milk glass and climatically-unstable wax screens. Polyethylene terephthalate PNCh-KT-2 is strong in tension and compression, up to 1200  $\text{kgf/cm}^2$ , with high resistance to aging and oxidation, also otherwise chemically inert, at temperatures from  $-60^\circ\text{C}$  to  $+150^\circ\text{C}$ . Specimens of such films with surface varnish coating and  $\text{BaSO}_4$  filler were tested in white and monochromatic light. Their luminance and scattering indices as well as resolving power and contrast transmission were found to be excellent for the intended application. Figures 1; references: 4 Russian.  
[111-2415]

15 May 1985

UDC 535.39.666.1

## PROTECTIVE CHARACTERISTICS OF ELECTRICALLY CONDUCTING TRANSPARENT VACUUM-DEPOSITED COATINGS

Leningrad OPTIKO-MEKHANICHESKAYA PROMYSHLENNOST' in Russian No 7, Jul 84  
(manuscript received 23 Aug 83) pp 56-57

KRZHIZHANOVSKIY, B.P. (deceased)

[Abstract] Coatings of  $\text{SnO}_2$ ,  $\text{In}_2\text{O}_3$ , and  $\text{In}_2\text{O}_3+10\% \text{SnO}_2$  are vacuum-deposited on surfaces of optical-grade dielectric materials so as to make those surfaces electrically conductive to avoid condensation and static charge buildup. In an experimental study such coatings were vacuum-deposited on various glasses and crystals ( $\text{LiF}$ ,  $\text{CaF}_2$ ,  $\text{BaF}_2$ ), then air-heated to  $400^\circ\text{C}$  ( $\text{SnO}_2$ ) or  $350^\circ\text{C}$  ( $\text{In}_2\text{O}_3$ ,  $\text{In}_2\text{O}_3+10\% \text{SnO}_2$ ) and held at those temperatures for 3 h. They were subsequently exposed to atmospheric air with 98% humidity at  $40^\circ\text{C}$ . The wetting angle and the optical scattering coefficient as well as the tensile strength were measured before and after this exposure. The results indicate that  $\text{SnO}_2$  coatings are less hydrophobic and thus less protective than  $\text{In}_2\text{O}_3$  and  $\text{In}_2\text{O}_3+10\% \text{SnO}_2$  coatings, their wetting angles being  $80-82^\circ$  and  $87-91^\circ$  respectively. Heating after deposition tightens the coatings, but not sufficiently for protecting unstable glasses (OF grades) and stained glasses (SZ, SZS). The hydrophobia of  $\text{SnO}_2$  coatings can be increased to a  $90^\circ$  wetting angle by chemical deposition of a thin layer of dimethyl diethoxysilane. Tables 1; references: 6 Russian.  
[111-2415]

UDC 629.785.023.26

## DEPENDENCE OF TELESCOPE - OBSERVER RESOLVING POWER ON SHAPE AND SIZE OF FRONT IRIS

Leningrad OPTIKO-MEKHANICHESKAYA PROMYSHLENNOST' in Russian No 7, Jul 84  
(manuscript received 25 Sep 81) pp 39-41

VASIL'YEV, V.Ya., DUBENSKOV, V.P. and KAL'YANOV, Yu.A.

[Abstract] The resolving power of a "reflecting telescope - observer" system was measured in an experiment with 25x, 50x, and 80x magnification, for the purpose of determining its dependence on the shape and the size of the front iris. The latter was masked partially in three different ways: 1) a triangular shield; 2) two strip shields blocking opposite segments and leaving a symmetric zone in between; 3) a disk shield at the center leaving an annulus. Different sizes of each kind of shield were used so as to block successively 6, 12, 25, 50, 75 and 80 percent of the aperture in each case. The results indicate the limits on masking based on permissible reduction of resolving power. Typically a 20 percent

reduction of resolving power allows 25 percent sectoral or segmental masking but only 12 percent central masking. Tables 2; references: 7 Russian. [111-2415]

UDC 681.7.068.4.013

#### MATCHING CHARACTERISTICS OF GRADED-INDEX OPTICAL FIBERS IN SPLICE

Leningrad OPTIKO-MEKHANICHESKAYA PROMYSHLENNOST' in Russian No 7, Jul 84 (manuscript received 14 Nov 83) pp 43-45

AVAKOV, S.N., ZGULADZE, M.G., MESTVIRISHVILI, A.N. and SAGARADZE, V.R.

[Abstract] A splice of two optical fibers is characterized by the loss of light intensity, depending on the width of clearance between the mating ends as well as on their radial and angular misalignment. Matching of graded-index polymer fibers at the splice was studied experimentally, the equipment including a He-Ne laser and a beam widening collimator followed by a diaphragm for shaping the light beam into one with smaller cross-section but uniform intensity distribution. One fiber, rigidly positioned relative to the laser-collimator-diaphragm system, was movable relative to the other fiber with photoreceiver in fixed position for varying the clearance width up to 0.5 mm and varying the radial misalignment with the fibers remaining parallel. Four splice configurations were evaluated and all except one found to be satisfactory. The junction loss was found to be at least one order and as much as two orders of magnitude lower than in splices of a graded-index fiber with a stepped-index one. Filling the clearance with immersion fluid was found to still further reduce the optical loss. Figures 2; tables 1; references 6: 4 Russian, 2 Western. [111-2415]

UDC 681.7.064.454

#### COLOR TRANSMISSION BY CAMERA OBJECTIVES WITH ACHROMATIC TRANSPARENT COATINGS

Leningrad OPTIKO-MEKHANICHESKAYA PROMYSHLENNOST' in Russian No 7, Jul 84 (manuscript received 1 Sep 83) pp 35-39

PRIDATKO, G.D. (deceased), YEVTEYEVA, N.P., GUDKOVA, K.V., KUDRYAVTSEVA, A.G., SHCHERBAKOVA, I.L. and AVDEYEVA, L.A.

[Abstract] Design and performance of achromatic transparent coatings as correctors of color transmission by camera objectives are evaluated, coatings for this purpose being of the interference kind with multilayer thin-film structure. Their essential design parameters are the thickness

and the refractive index (material) of each layer, the number of layers, and their combination and sequence depending on the required spectral characteristics. Most importantly, they must minimize reflection of light when matching the refractive index of the substrate lens glass. The transmission wavelength band  $\Delta\lambda = \lambda_2 - \lambda_1$  corresponding to less than 0.5 percent residual reflection depends on the number of layers and on their arrangement. Ensuring any given spectral characteristics (residual reflection coefficient and ratio of upper to lower transmission edge  $\lambda_2/\lambda_1$ ) requires more layers of unequal optical thicknesses than layers of equal ones, coatings with a smaller residual reflection coefficient also having a narrower transmission band. On the basis of these properties, the corrective action of various commercial coatings on various commercial glasses is analyzed relative to three color ranges (blue:  $\lambda = 360-480$  nm, green:  $\lambda = 480-600$  nm, red:  $\lambda = 560-680$  nm) and relative to the chromaticity formula of objective lenses. Three groups of coatings are distinguished: 1) coatings whose layers have an optical thickness equal to a quarter wavelength or multiples thereof; 2) coatings whose layers have optical thicknesses not equal to or multiples of quarter wavelengths; 3) coatings whose layers are combinations of types 1 and 2. Coatings of the first group, with 2-5 layers, are technologically most feasible and can be produced by standard vacuum equipment with the minimum number of different film materials. Figures 2; tables 6; references 34: 16 Russian, 14 Western, 4 Japanese.  
[111-2415]

UDC 681.7.023.7

MODEL AShS-15 AUTOMATIC MACHINE TOOL FOR DIAMOND GRINDING OF OPTICAL COMPONENTS

Leningrad OPTIKO-MEKHANICHESKAYA PROMYSHLENNOST' in Russian No 7, Jul 84 (manuscript received 14 Nov 83) pp 32-35

ROSHAK, A.F., SAMUYLOV, E.T., YATSEVICH, O.I. and VAN'KOVICH, V.M.

[Abstract] An experimental prototype of an automatic machine tool has been developed and built for diamond grinding of optical components, with maximum economy of loading and unloading time and with maximum reliability along with minimum maintenance of the vacuum grip mechanism. It is a single-position tool with vertical spindles, electric drives and pneumatic controls. The diamond wheel rotates on a spindle at 15,000 rpm, driven by a 0.55 kW motor through a flat belt. The part rotates on a spindle at 650 rpm, driven by a 0.18 kW motor through a V-belt, and is fed to the tool manually through a worm gear at a rate of 1-20 mm/min. Emulsion for cooling and lubrication is fed separately by a 0.15 kW pump. This AShS-15 tool is designed for grinding parts 5-20 mm in diameter and 3-15 mm thick with a radius from 3 mm to infinity (flat surface). The loading disk holds up to 1000 pieces, the manipulator can load and unload in less than 4 s, a time much shorter than the grinding time, so that the productivity reaches 60-300 pcs/h. The unit weighs 700 kg, without emulsion feeder. Figures 2; references: 3 Russian.  
[111-2415]

UDC 681.7.012.681.7.067.288

#### HOLOGRAPHIC CORRECTOR IN OBJECTIVE WITH COMPOUND MAIN MIRROR

Leningrad OPTIKO-MEKHANICHESKAYA PROMYSHLENNOST' in Russian No 7, Jul 84  
(manuscript received 12 Dec 83) pp 23-26

PIMENOV, Yu.D., KUZILIN, Yu.Ye., SINTSOV, V.N. and SITNIK, N.A.

[Abstract] A holographic corrector is considered for eliminating surface aberrations of the main telescope mirror, specifically a compound mirror, on the basis of the existing relation between spectral range, wavefront distortion, and chromatic aberration. This relation is examined for typical holographic conversion of a plane wavefront into a spherical one. A hologram recorded with counter light beams yields a spectral band which widens with decreasing thickness of the light-sensitive film and makes it possible to eliminate any path-difference resulting from wavefront conversion. This requires making the curvature of the photographic plate equal to half the sum of the curvature of the original reference wavefronts. Such a correcting hologram must be placed in the plane of the exit pupil of the objective. It simulates a Mangin mirror with the radius of curvature of the first surface equal to that of the photographic plate, and the second describable by an even-power polynomial with coefficients selected for given quality and position of the image of a point on the axis. In a three-mirror system such a corrector constitutes the fourth element in the path of the light beam; replacement of the second or third mirror with a hologram has not been successful so far because of excessive chromatic aberration. An objective and a compound main mirror were experimentally evaluated in a test stand with an LG-38 laser, a point-source simulator, a collimator, a spherical mirror, then a 45°-slant plane mirror, and then an elliptical mirror lined up behind the collimator on the common axis, with the correcting hologram adjustable transversely to the beam between the plane and elliptical mirrors, also a second 45°-slant plane mirror parallel to the first one behind the objective. Decoding of interference and diffraction patterns with the aid of a DIP-1 XY-plotter and a 15VSM-5 mini-computer has confirmed the feasibility of a holographic corrector and established its basic design and performance requirements. Figures 3; tables 1; references 11: 9 Russian, 2 Western.  
[111-2415]

UDC 620.004.5:519.21:621.383

#### PERFORMANCE EVALUATION OF FIBER-OPTIC CONVERTERS

Leningrad OPTIKO-MEKHANICHESKAYA PROMYSHLENNOST' in Russian No 7, Jul 84  
(manuscript received 20 Oct 81) pp 14-16

FARAKHUTDINOVA, M.A. and SULEYMANOV, N.T.

[Abstract] Optical fibers are paired with photoelectric cells in optical receivers of measuring and data gathering systems. The two components

of each pair must be matched with respect to reliability of information about the entire field of vision, matched on an interference-free basis. For this purpose, the performance of such an optoelectric converter can be evaluated in terms of reliability, defined as the probability of error-free signal conversion - such a conversion being possible only by failure-free operation of each photoreceiver component. General relations for the reliability as function of time are derived here, considering that the reliability is a product of two associated factors, parametric and catastrophic failures. Since the four governing fiber parameters (diameter, length, internal reflection coefficient, attenuation coefficient) are subject to random variance caused by manufacturing imprecision and the dependence of the luminous flux on these parameters is intricate, an analytical performance evaluation will not be feasible. Statistical simulation is done instead, assuming a normal distribution of random quantities in accordance with the central-limit theorem. The analysis is refined by also taking into account the thickness of the opaque interlayer at its thinnest spot and including the aperture angle in terms of the refractive indexes of the fiber core, the fiber sheath, and the ambient medium. The calculations have been programmed in FORTRAN for a YeS-1022 computer. An evaluation of fiber bundles containing 300 nominally identical fibers in a hexagonal packing arrangement, one fiber for each of 300 photoreceivers, indicates after 1000 computer "tests" that such fibers are adequate for optoelectronic measuring and data gathering. References: 9 Russian. [111-2415]

FLUID MECHANICS

UDC 533.6.011

PLANAR PARTICLE-LADEN GAS FLOW ABOUT THIN BODIES

Moscow DOKLADY AKADEMII NAUK SSSR in Russian Vol 277, No 2, Jul 84  
(manuscript received 9 Nov 83) pp 319-322

AYDAGULOV, R.R., Moscow State University imeni M. V. Lomonosov

[Abstract] The flow of a gas containing particles about thin bodies in the sub-sonic mode is examined. It is found that for smooth bodies the pressure coefficient on the body, except for the nose and tail, varies continuously depending upon the Mach number, even when going from sub-sonic to super-sonic flow. A linearized system of equations describing the steady-state flow is derived. Figures 3; references: 12 Russian.  
[328-6900]

UDC 533.6.011

CHARACTERISTICS OF STEADY-STATE HYPERSONIC FLOW ABOUT BLUNTED BODIES WITH DISCONTINUITIES IN GENERATORS

Leningrad VESTNIK LENINGRADSKOGO UNIVERSITETA: MATEMATIKA MEKHANIKA ASTRONOMIYA in Russian Vol 13, No 3, Jun 84 (manuscript received 16 Sep 82) pp 80-85

SEROVA, V.D.

[Abstract] The work described in this article extends a previous study by the author on the influence of the geometry of discontinuities on the distribution of parameters in the shock wave. The present study investigates the characteristics of the flow in the shock layer on bodies with discontinuous generators (breaks), and studies the possibility of approximating the bodies employed in the previous study by using a set of smooth ones. The BVLK method is employed to calculate the multi-shock axisymmetrical problem of hypersonic flow. The processes occurring during axisymmetrical shock wave interactions are assessed qualitatively. Comparison of the pressure behavior as a function of the longitudinal coordinate

at points on the surface of smooth and discontinuous cones indicate that even a small discontinuity results in a major qualitative and quantitative difference in the threshold distribution curves. Figures 8, references: 6 Russian.  
[53-6900]

UDC 533.6

IMPACT STARTING OF PLANE NOZZLES WITH WIDE DIVERGENCE ANGLE

Moscow IZVESTIYA AKADEMII NAUK SSSR: MEKHANIKA ZHIDKOSTI I GAZA in Russian No 4, Jul-Aug 84 (manuscript received 5 Jul 83) pp 100-106

BRITAN, A.B. and VASIL'YEV, Ye. I., Moscow

[Abstract] The starting characteristics of plane or axisymmetric reflecting shock-tube nozzles are analyzed, taking into account effects of a wide divergence angle and dependence of the form of shock waves on the geometry of the transonic nozzle segment. A nozzle mounted at one end of the tube is started by a shock wave coming from the other end and passing through the supersonic nozzle segment with initially quiescent homogeneous gas, a diaphragm in the throat section producing the necessary initial pressure drop at the nozzle entrance. The corresponding integral equations of nonsteady-state gas dynamics are formulated and solved for a nonviscous nonconducting perfect gas. Numerical solution by the McCormack method on a BESM-6 high-speed computer has yielded results in satisfactory agreement with a known theoretical solution for tapered nozzles. They deviate from experimental data, however, particularly on the upstream side of the secondary shock wave. This discrepancy is attributable to the design characteristics of experimental shock tubes. Correct simulation of the starting process must include flow through the subsonic segment of a reflecting nozzle. Figures 5; references 18: 12 Russian, 6 Western.  
[50-2415]

UDC 532.59.011

BUILDUP OF OSCILLATION OF BODIES IN STRATIFIED FLUID

Moscow IZVESTIYA AKADEMII NAUK SSSR: MEKHANIKA ZHIDKOSTI I GAZA in Russian No 4, Sep-Oct 84 (manuscript received 8 Jun 83) pp 87-93

DOLINA, I.S., Gorkiy

[Abstract] Forward motion of a circular cylinder driven by an elastic spring in the lower layer of a fluid medium, perpendicularly to its generatrix and parallel to the upper boundary of the layer, is analyzed for oscillations and instability. Calculations are based on a two-dimensional model, with an equation for the scalar potential in the lower layer and an

equation for the vector potential in the upper layer of fluid. An expansion into Fourier series, with viscosity of the fluid explicitly taken into account, yields a dispersion equation whose zeros represent singularities of the Fourier integrals. It is first solved for low velocities and small oscillation amplitudes, assuming a strong damping or, for comparison, a weak damping. Next is considered buildup of the oscillation amplitude into the range of nonlinearity and up to the stability limit. The results are extended to elliptical cylinders. Figures 4; references 5: 4 Russian, 1 Western.  
[50-2415]

UDC 533.6.011.5

#### SUPERSONIC FLOW AROUND BLUNT WEDGE

Moscow IZVESTIYA AKADEMII NAUK SSSR: MEKHANIKA ZHIDKOSTI I GAZA in Russian No 4, Jul-Aug 84 (manuscript received 12 May 83) pp 137-140

MANUYLOVICH, S.V., Moscow

[Abstract] Supersonic flow of a perfect gas around a semi-infinite body in the form of a plane wedge with blunt leading edge is analyzed. The problem is assumed to be asymptotic with respect to the longitudinal coordinate and is solved by the method of asymptotic expansion. The gas is assumed to have a  $c_p/c_v$  ratio independent of the temperature and its uniform unperturbed motion is assumed to satisfy the Euler equations. The oncoming stream is assumed to flow in the direction parallel to the plane of symmetry of the wedge and to split symmetrically along the faces of the latter. There are two possible modes of streamlining as the inclination angle  $\theta$  of the attached plane shock wave changes from 0 to  $\theta_{\max}$ . In one mode the slope of the jump along each wedge face changes from  $(M_{\infty}^2 - 1)^{-1/2}$  to  $C_m$  ( $M_{\infty}$  - Mach number of unperturbed oncoming stream), with supersonic or subsonic flow behind the shock wave depending on whether  $C < C_s$  or  $C_s < C < C_m$  respectively. In the other mode the slope of the jump changes from  $\infty$  to  $C_m$  and the flow behind the shock wave is always subsonic. For a long but finite wedge the obtained solution is valid only along a very short distance from the leading edge. In the case of supersonic flow behind the shock wave the discontinuity at the end gives rise to backward propagating perturbations and in the case of subsonic flow behind the shock wave perturbations are produced not only by that discontinuity but also by bluntness of the leading edge. Figures 2; references 5: 3 Russian, 2 Western (1 in Russian translation).  
[50-2415]

UDC 533.6.011.34

PROPULSION EFFICIENCY OF VIBRATING BODIES IN SUBSONIC GAS STREAM

Moscow IZVESTIY AKADEMII NAUK SSSR: MEKHANIKA ZHIDKOSTI I GAZA in  
Russian No 4, Jul-Aug 84 (manuscript received 6 Apr 83) pp 128-132

KOGAN, M.N. and USTINOV, M.V., Moscow

[Abstract] An axisymmetric body in a subsonic gas stream, namely an airfoil periodically deforming without loss of symmetry and change of length, is examined from the standpoint of thrust-power relation. The corresponding surface-time integrals for the drag force and the propulsion power are formulated in a cylindrical system of coordinates and evaluated, assuming a potential flow of the gas with small perturbations by the body. A time-independent source distribution density term is added to this time-dependent solution to insure a positive airfoil cross-sectional area. The maximum theoretical efficiency, or minimum power for given thrust, is calculated on this basis and the shape of the body is sought for which the real efficiency will approach the maximum theoretical one as closely as possible. Making the length of the body invariable in time leads to a discretely varying drag coefficient. The resulting equation describes a body in the shape of a wave which travels along its surface at a velocity  $v = \alpha M(M+1)(M+2)$  ( $\alpha$  - acoustic velocity,  $M$  - Mach number). Figures 1; references: 2 Russian.  
[56-2415]

UDC 533.932

STEFAN-MAXWELL RELATIONS FOR PLASMA DIFFUSION CURRENTS IN MAGNETIC FIELD

Moscow IZVESTIYA AKADEMII NAUK SSSR: MEKHANIKA ZHIDKOSTI I GAZA in  
Russian No 4, Jul-Aug 84 (manuscript received 1 Jul 83) pp 148-154

KOLESNIKOV, A.F. and TIRSKIY, G.A., Moscow

[Abstract] Equations of heat and mass transfer for plasma diffusion currents in a magnetic field are derived in the approximation of elastic pairwise collisions of particles unaffected by the external electromagnetic field, assuming that the transfer coefficients do not depend on the interaction of electrons with plasma oscillations. These equations are derived from the fundamental system of equations of diffusion currents and partial thermal currents in an isothermal  $N$ -component plasma in a magnetic field, those latter equations having been obtained earlier through solution of the corresponding Boltzmann equations by the Chapman-Enskog method. Exact Stefan-Maxwell relations for diffusion currents in a magnetic field and exact relations for the transfer coefficients, including one for the thermal conductivity which extends the Muckenfuss-Curtiss relation, are obtained directly from the ratios of complex determinants of successive orders  $N(\xi - 1)$  and  $N(\xi - 1) + 1$  respectively. This method is mathematically

more economical than the known Chapman-Enskog method and takes into account higher-order approximations for a two-temperature plasma as well as for an isothermal one, also for a plasma outside a magnetic field. References 23: 15 Russian, 8 Western (2 in Russian translation). [50-2415]

UDC 533.6.013.11

METHOD OF CALCULATING SEPARATION FLOW OF SUBSONIC GAS STREAM AROUND WINGS

Moscow IZVESTIYA AKADEMII NAUK SSSR: MEKHANIKA ZHIDKOSTI I GAZA in Russian No 4, Jul-Aug 84 (manuscript received 16 Jun 83) pp 141-147

BELOTSEKOVSKIY, S.M., KORZHNEV, V.N. and SHIPILOV, S.D., Moscow

[Abstract] The nonlinear problem of steady subsonic flow of a gas around a wing is solved by the method of discrete vortices for compressible fluids, considering the case of separation flow with the separation lines assumed to be known and the Chaplygin-Joukowski condition of finite velocities satisfied at the surface of the vortex trail. The corresponding differential equation for the potential of perturbed velocities, with the boundary condition of an impermeable wing surface, is solved separately and differently for two regions. The velocity integrals for the semi-finite "corridor" around the wing and containing the vortex trail are evaluated by a numerical iteration process, after the two subregions have been subdivided into respectively finite and semi-infinitely long rectangular parallelepipeds. In the remaining space outside this region the potential of perturbed velocities is linearizable and, with the aid of a Prandtl-Glauert transformation, its differential equation is reducible to the Laplace equation in appropriate coordinates. The analytical solution for this region depends, through the boundary conditions, on the solution for the "corridor." The method has been validated on two test problems: a thin flat wing at a low angle of attack and a circular cylinder of infinitely wide span. It is applied to a delta wing with a 1.5 aspect ratio, angle of attack  $\alpha$  - 15° to 18°, Mach number  $M_\infty$  of the unperturbed stream varying over the 0.0.9 range, and the Chaplygin-Joukowski condition satisfied at all edges. The results reveal a range of angles of attack which corresponds to stabilization of nosing vortex filaments. Two estimates can and should be given for the critical angle of attack, namely a lower bound at which the iteration process ceases to converge relative to the aerodynamic load and an upper bound where the shape of the vortex sheet as well the lift coefficient and the pitching moment coefficient begin to change from one iteration to the next. The method of solution is applicable to separation flow as well as nonseparation flow and mixed flow around thin wings of arbitrary shape in the plan view. Figures 5; references: 7 Russian. [50-2415]

UDC 533.6.011.5

# SUPERSONIC FLOW AROUND WEAK RADIATION SOURCES

Moscow IZVESTIYA AKADEMII NAUK SSSR: MEKHANIKA ZHIDKOSTI I GAZA in  
Russian No 4, Jul-Aug 84 (manuscript received 27 Jun 83) pp 133-136

KRASNOBAYEV, K.V., Moscow

[Abstract] The flow of interstellar wind about an x-ray source is simulated as the steady two-dimensional supersonic flow of an ideal perfect gas around a weak radiation source (one which heats the gas by transferring to it an amount of energy  $q$  much smaller than its kinetic energy). In this case, and by permitting only small variations of density, pressure and velocity, the equations of hydrodynamics can be linearized. The latter, in a cylindrical system of coordinates  $z, r$  and with appropriate boundary conditions, are then solved for the velocity potential  $\phi_{zz} = \alpha^2(\phi_{rr} + n\phi_r/r^n) + \alpha(z, r)$  ( $\alpha^2 = 1/(M_0^2 - 1)$ ,  $\alpha = (\gamma - 1)q/\alpha_0^2(M_0^2 - 1)$ ,  $\alpha_0^2 = \partial p_0/\partial \rho_0$ ,  $n=0$  for plane flow and  $n=1$  for axisymmetric flow). Solving the hyperbolic equation for the boundary condition of zero velocity perturbation at infinity by the linearization method is sufficiently accurate for supersonic flow only. This method is applicable neither to transonic flow ( $M_0 \approx 1$ ), for which a modification of the Khokhlov method has been proposed, nor to hypersonic flow ( $M_0 \gg 1$ ). In the latter case a self-adjoint solution for steady flow far past any radiation source is most expedient and easily obtained from the theory of strong detonation for thin bodies. Figures 2; references: 12 Russian.  
[50-2415]

MECHANICS OF SOLIDS

UDC 539.3

ELASTIC EQUILIBRIUM OF COMPOSITE SHELLS WITH FINITE SHEAR RIGIDITY

Kiev DOKLADY AKADEMII NAUK UKRAINSKOY SSR: SERIYA A FIZIKO-MATEMATICHESKIYE I TEKHNICHESKIY NAUKI in Russian No 7, Jul 84 (manuscript received 9 Dec 83) pp 33-36

GRIGORENKO, Ya. M., corresponding member, Ukrainian SSR Academy of Sciences, MUKHA, I.S., SAVULA, Ya.G. and FLEYSHMAN, N. P., Institute of Mechanics, Ukrainian Academy of Sciences

[Abstract] A version of boundary conditions for composite shells with arbitrary shape is proposed. Aspects of constructing the line of intersection of their middle surfaces are considered. The problem of a cylindrical shell in contact with circular plate is calculated as an example. It is found that the stresses on the loaded surface at the point of contact of the middle surfaces obtained in accordance with the theory of shells and the theory of elasticity differ significantly, with the theory of shells yielding a higher result. Figures 3; references 8: 7 Russian, 1 Western.  
[3206-900]

UDC 621.031:539.334

STABILITY OF CYLINDRICAL SHELLS WITH VARIABLE THICKNESS UNDER EXTERNAL PRESSURE

Kiev PRIKLADNAYA MEKHANIKA in Russian Vol 20, No 7, Jul 84 (manuscript received 22 Jul 82) pp 53-59

KABANOV, V.V. and ZHELEZNOV, L.P., Novosibirsk

[Abstract] Nonlinear deformation and stability of circular cylindrical shells under external pressure is analyzed, specifically shells whose thickness varies around the circumference, considering a non-zero moment and nonlinear initial stressed-strained state. The problem is formulated in displacements and solved by the method of finite elements.

Stability is tested according to the energy criterion  $\delta(\delta^2 II) = 0$  ( $\Pi$ -potential energy of shell). The algorithms have been programmed for a BESM-6 high-speed computer. Numerical data are given for a freely supported shell with a circumferentially piecewise-variable thickness under uniform external pressure. The critical load and the ultimate load are referred to those for equivalent shells with uniform thickness equal to maximum, minimum, and mean thickness of the real shell for the purpose of accuracy analysis of the solution. For comparison, results are also given based on disregarding non-zero moments and nonlinearity in the initial stage. Figures 5; references: Russian. [59-2415]

UDC 539.3

# NATURAL VIBRATIONS OF REINFORCED SPHERICAL SHELLS

Kiev PRIKLADNAYA MEKHANIKA in Russian Vol 20, No 7, Jul 84 (manuscript received 4 Jul 83) pp 42-48

REVUTSKIY, V.N., Institute of Mechanics, UkSSR Academy of Sciences, Kiev

[Abstract] A method is proposed for analyzing the natural vibrations of a deep spherical shell clamped around its base parallel and reinforced with an array of hoops and meridional stringers. Such a shell is regarded as a compound body, a spherical segment representing the sheath and all hoops as well as stringers behaving like one-dimensional thin curvilinear elastic elements. All materials of the shell are assumed to be isotropic and to obey Hooke's law. During small vibrations all reinforcing members undergo tension-compression and flexure, the stringers flexing normal to the median surface of the sheath and the hoops flexing in their own planes. The corresponding equations for the shell are based on the Hamilton-Ostrogradskiy principle of stationary action ("least" action) and on two theories, Kirchhoff-Love theory for the sheath and Kirchhoff-Klebsch theory for the reinforcing members. The strain field of the shell is defined through the three orthogonal displacement components on the median surface and the resulting system of partial differential equations, in operator form, is solved by the Bubnov-Galerkin method. With the constraint coefficients stipulated in terms of Legendre functions of the first kind, this method reduces the problem to two infinite systems of homogeneous algebraic equations in associated Legendre polynomials. The algorithms have been programmed for a YeS-1040 computer. The method has been validated, first on smooth spherical shells and then on reinforced ones. Natural frequencies were calculated with the aid of dynamic compliance functions. Figures 4; tables 1; references: 8 Russian. [59-2415]

UDC 539.3

NUMERICAL SOLUTION OF ONE-DIMENSIONAL NONLINEAR PROBLEMS OF STATICS FOR ELASTIC BEAMS AND SHELLS UNDER RIGID CONSTRAINTS

Kiev PRIKLADNAYA MEKhanika in Russian Vol 20, No 7, Jul 84 (manuscript received 27 Jul 82) pp 96-100

KABRITS, S.A. and TARENT'YEV, V.P., Leningrad State University

[Abstract] The problem of quasi-static geometrically and physically nonlinear deformation of a one-dimensional elastic body (such as a thin beam or an axisymmetric shell) reduces mathematically to a nonlinear two-point boundary-value problem with an adjustable parameter when the characteristics of the body are smooth and its deformation is unconstrained. The problem requires a variational formulation in the case of distributed constraints on displacements. In this paper, the penalty method is proposed for solution of the problem in the latter case, with the interaction of the body and rigid perfectly smooth barriers simulated mechanically by unilateral contact with nonlinear elastic Winkler bases which follow the surface contour of those barriers in the initial state and develop a distributed normal reaction to normal penetration. The magnitude of this reaction can be stipulated in the form of a power law  $|P| = k \Delta^n$  ( $\Delta$  - displacement of elastic base by barrier,  $n \geq 1$ ,  $k$  - stiffness of base). The bases can be made sufficiently stiff to prevent excessive penetration, but the reaction of a base becomes zero once a point of the deforming body crosses into the forbidden region. The procedure for solution of the problem combines the Newton-Kantorovich method of quasi-linearization and the method of iterative continuation with respect to the numerical parameter, the latter being changed as critical points on the load-deflection curve are crossed. All linear boundary-value problems arising in this procedure are solved by the S.K. Godunov method of orthogonal elimination. The procedure is demonstrated on two examples, all algorithms having been programmed in ALGOL-60 for an M-222 computer with TA-1M translator. The first example is plane flexure for a hinge-supported vertical Kirchhoff beam under its own weight and a longitudinal loading force applied at the top, a model of problems encountered in geology and in well drilling. The beam is confined in a space between two parallel vertical plates limiting its horizontal deflection on both sides. This problem has been solved for  $n = 2$  and  $k = \text{const}$ . Most critical in the solution process is the instant at which the beam makes contact with either one of the barriers, and the iteration steps must be here decreased sufficiently to ensure convergence. The second example is a rolled-over truncated-conic elastic membrane attached around the entire periphery between two coaxial metal cylinders. This problem is solved on the basis of nonlinear zero-moment equations of statics for a membrane of revolution made of an incompressible material with potential  $\Phi = 0.5 \mu (\lambda_1^2 + \lambda_2^2 + \lambda_3^2 - 3)$ ,  $\lambda_1 \lambda_2 \lambda_3 = 1$  ( $\mu$  - linear shear modulus,  $\lambda_1, \lambda_2, \lambda_3$  - multiplicities of principal strains). Most critical in the solution process is selection of the initial approximation or point on the load-deflection curve. An expedient way to do this is by introducing a second numerical parameter which will result in a trivial solution to the thus-modified equations for a zero-pressure load. Figures 2; references: 5 Russian.

[59-2415]

UDC 539.3

METHOD OF SOLVING PROBLEMS OF STATICS FOR MULTILAYER SHELLS OF REVOLUTION

Kiev PRIKLADNAYA MEKHANIKA in Russian Vol 20, No 7, Jul 84 (manuscript received 25 Jun 82) pp 59-65

POPOV, B.G. and RAMAN, E.V., Moscow Higher Technical School imeni N.E. Bauman

[Abstract] A multilayer shell of revolution is considered whose  $N$  layers are made of orthotropic materials with different mechanical characteristics. The problem of static deformation for each layer is formulated kinematically, namely by finding the relations governing displacements along the normal. The system of orthogonal curvilinear coordinates  $\alpha_1, \alpha_2$  and rectilinear coordinate  $z$  is selected so as to make axes  $\alpha_1, \alpha_2$  coincide with the corresponding lines of principal curvatures for the undeformed coordinate surface  $z = 0$  (inside surface of shell) and the  $z$  axis coincides with the outward normal. All three displacement components of each layer are then expanded into power series in  $z$ . Retention of only the first terms for normal and both tangential displacement components results in a zero-moment model, retention of only the first term for normal displacement components and only the first two terms for both tangential displacement components results in the Timoshenko model of uniform shearing stress distribution over the shell thickness. Exclusion of transverse shearing strain corresponds to the Kirchhoff-Love hypothesis. After linear relations between displacements and strains have been established for each layer, strains are expanded into Fourier series in one of the curvilinear coordinate. Transition from individual layers with their degrees of freedom to the whole shell with its degree of freedom is effected with attendant introduction of displacement continuity conditions at interlayer boundaries. For small strains without loss of bond the problem is now formulated variationally with respect to potential energy. The resolvent system of differential equations is derived from the condition of stationary total potential energy  $V$ , with conditions of bonding added to the corresponding functional  $\delta J = \delta V - \delta A = 0$  ( $A$ -work of load), and through reduction to Euler equations by setting the Lagrange multiplier vector to zero. The problem is then solved by the method of displacements. The procedure has been applied, for illustration, to a triple-layer cylindrical shell with filler between two sheaths clamped at both ends and under internal pressure. Figures 1; references: 5 Russian.  
[59-2415]

UDC 534.1:534.232

# SCATTERING OF SOUNDS BY PIEZOCERAMIC CYLINDRICAL SHELL NEAR RIGID SURFACE

Kiev PRIKLADNAYA MEKHANIKA in Russian Vol 20, No 7, Jul 84 (manuscript received 9 Jul 82) pp 111-115

SENCHENKO, I.V., Institute of Hydromechanics, UkSSR Academy of Sciences, Kiev

[Abstract] Scattering of sound by an elastic cylindrical shell parallel to a perfectly stiff wall is analyzed, of particular interest being the effect of a reflecting surface behind the shell and of mode coupling on the diffraction field. The shell is assumed to be made of PZT-4 piezoceramic material with polarization across its thickness and with open electrodes covering it, and an ideal compressible fluid medium is assumed to fill the half-space on the shell side of the wall. The problem reduces to a boundary-value problem for a system of equations which includes the Helmholtz equation and equations of motion for a thin shell. The resultant acoustic field must have a zero potential gradient at the wall, the vibration velocity must be the same in the fluid and at the shell surface, and the dynamic condition at the shell surface is satisfied automatically. This system of equations was solved by the method of reduction, with equality of the vibration velocities in the fluid and at the shell surface as criterion of accuracy. The results reveal that dynamic excitation of modes other than the fundamental pulsating mode produces a nonuniform distribution of shell vibration velocity. The scattering pattern of the given elastic shell with that of a perfectly soft one are compared. They are identical in the far field at resonance, the slight differences in appearance being attributable to the stiffening effect of open electrodes. Excitation of higher-order harmonics has no appreciable effect on the far field as long as the shell remains near the wall, but the two patterns begin to differ appreciably as its distance from the wall measured in wavelengths increases. Figures 4; references 4: 3 Russian, 1 Western. [59-2415]

UDC 539.3:534.1

# PROPAGATION OF NON-AXISYMMETRIC ELASTIC WAVES THROUGH SHELL WITH FILLER UNDER RADIAL LOAD AT ONE END

Kiev PRIKLADNAYA MEKHANIKA in Russian Vol 20, No 7, Jul 84 (manuscript received 19 Jul 82) pp 104-107

MASTINOVSKIY, Yu.V. and NAGORNYI, Yu.I., Zaporozhye Institute of Machine Design

[Abstract] A semi-infinite shell with a filler under a non-axisymmetric radial load at the end is considered. The propagation of elastic waves

along this shell is analyzed on the basis of the linear Timoshenko theory with the filler moving only radially. The corresponding system of second-order differential equations of motion for the shell is, after introduction of dimensionless parameters and variables, reduced to matrix form representing 15 partial differential equations for unknown displacements  $f$ ,  $f'_x$ ,  $f'_t$  with three linear and two angular components each. It is solved by the method of characteristics for given initial and boundary conditions, the latter including conditions of contact between shell and filler. The dependence of wave propagation parameters on filler parameters is evaluated, assuming that the filler is a stack of frictionless disks of low-density or high-stiffness and thus effectively weightless material. The problem reduces to the Euler equation in radial displacements, solvable by the numerical method of grids. It has been solved for a shell with radial displacement  $w^* = te^{-2t}$  but zero radial velocity, axial stress, and bending moment at the end  $x = 0$  at time  $t = 0$ , with an either solid or hollow filler. Figures 3; references: 4 Russian.  
[59-2415]

UDC 536.2.01

AN APPROXIMATE METHOD FOR SOLVING THE HEAT CONDUCTIVITY PROBLEM FOR A  
HOLLOW CYLINDER

Dushanbe IZVESTIYA AKADEMII NAUK TADZHIKSOY SSR OTDEIENIYE FIZIKO-  
MATEMATICHESKIKH, FIZICHESKIKH I GEOLOGICHESKIKH NAUK in Russian No 1(91),  
Jan-Mar 84 (manuscript received 19 Jan 83) pp 73-76

YUSUPOV, S.Yu., Tadjhik Polytechnical Institute.

[Abstract] An approximate analytical method for calculating time-dependent heat conductivity based on the combined use of integral transformations and orthogonal projection is presented. The problem of the temperature field in a hollow cylinder is analyzed as an example. The approximate values are found to compare well with the exact values. The method can be used for harmonic, power-law and other variations in the temperature of the surrounding medium. References 3 Russian.  
[116-6900]

UDC 699.844

ACOUSTIC OSCILLATIONS OF RODS AND PLATES

Dushanbe IZVESTIYA AKADEMII NAUK TADZHIKSOY SSR OTDELENIYE FIZIKO-MATEMATICHESKIKH, FIZICHESKIKH I GEOLOGICHESKIKH NAUK in Russian No 2 (92), Apr-Jun 84 (manuscript received 28 Nov 83) pp 28-33

ZAKHAROV, A.V., FAZYLOV, A.R. and PIRMATOV, R.Kh., Tadzhik Polytechnical Institute.

[Abstract] An interference model of resonant and anti-resonant acoustic oscillations of rods and plates is proposed that makes allowance for energy losses to internal friction and to adjacent members. Two simple models are examined: one of a rod with free edges, in which the oscillations were determined by energy losses to internal friction, and the other of a rod with partially reflecting ends, in which oscillations were determined by the escape of energy through the ends, and to some extent by losses to internal friction. Relationships are found that make it possible to determine the oscillations of the element for both kinds of energy loss, and that are valid for resonant and antiresonant oscillations. The data obtained can be used to analyze the transmission of acoustic oscillations through vibration insulating components and building members. Reference 1 Russian.

[116-6900]

## TESTING &amp; MATERIALS

UDC 621-583.9(088.8)

## CLAMPING DEVICES FOR CIRCULAR INSTRUMENTATION TRANSDUCERS

Leningrad OPTIKO-MEKHANICHESKAYA PROMYSHLENNOST' in Russian No 6,  
Jun 84 (manuscript received 23 Aug 83) pp 49-51

IVANOV, B.N.

[Abstract] A retaining device is described that makes it easier to secure the clamping mechanism to the stationary part of the transducer (stator) while making measurements. In contrast to existing rigid, steel-band, and universal-joint retaining systems, which all produce measurement error, the proposed approach employs a pair of parallelogram mechanisms in series. The articulated design of this system eliminates angular movements with respect to the arm holding the object being measured. An alternate mechanism is described that employs a similar principle for cases in which the other device cannot be used because of space limitations. The use of these devices has made it possible to improve measurement accuracy using circular transducers. References 5: Russian.  
[46-6900]

UDC 677.11.024.324.226

## PRACTICAL APPLICATION OF 'GROUNDING EFFECT'

Dushanbe IZVESTIYA AKADEMII NAUK TADZHIXSOY SSR OTDELENIYE FIZIKO-MATEMATICHESKIKH, FIZICHESKIKH I GEOLOGICHESKIKH NAUK in Russian No 1 (91),  
Jan-Mar 84 (manuscript received 14 Jan 83) pp 28-34

SULTANOV, M.A., Institute of Chemistry imeni V.I. Nikitin, Tadzhik SSR  
Academy of Sciences.

[Abstract] This study investigates the possibility of strengthening thread guide parts and yarn bobbins in the textile industry by employing the 'grounding effect'. In the grounding effect, the degree of ablation of metallic bodies exposed to shock-compressed plasma and laser radiation depends upon whether they are neutral (electrically isolated from the

ground) or grounded (directly connected to the ground) and connected to a large metal mass that significantly exceeds the mass of the target in question. When the body is grounded or connected to a large metal mass, the parameters of the ablation of the bodies and the parameters of the shock-compressed plasma formed on the surface of the mass are much smaller than those obtained for a body isolated from the ground. Experiments are described that demonstrate the possibility of increasing surface life of the aforementioned machine parts by strengthening them by exposure to shock-compressed plasma and unfocused laser radiation with the proper parameters. It is found that the strength of a part treated with shock-compressed plasma and laser beams is far greater for a grounded part than a neutral one. The proposed methods for toughening parts are promising for use with parts and components of various sizes and configurations. References 6 Russian.  
[116-6900]

UDC 539.893+539.143.43

#### NMR MANOMETER FOR MEASURING HIGH PRESSURES AT LIQUID-HELIUM TEMPERATURES

Moscow PRIBORY I TEKHNIKA EKSPERIMENTA in Russian No 4, Jul-Aug 84  
(manuscript received 9 Aug 83) pp 195-199

DOROSHEV, V.D., KOVTUN, N.M., MOLCHANOV, A.N., POLYAKOV, P.I. and  
SYNKOV, V.G., Donetsk Physical-Technical Institute, Ukrainian SSR Academy  
of Sciences.

[Abstract] A resonance manometer is described for measuring pressures of 1 - 20 kbar at 1.5 - 4.2 K. The device operates on the basis of the pressure dependence of the NMR frequency of  $^{57}\text{Fe}$  in a weak ferromagnet - ferric borate  $\text{FeBO}_3$ . The manometer can measure the pressure directly and on line during an experiment within approximately one minute. Inasmuch as the nuclear magnetic resonance in  $\text{FeBO}_3$  is observed in superthin (internal) magnetic fields on nuclei without imposing an external magnetic field, it is possible to use any type of electric input, and the chamber can be made of magnetic materials. The NMR frequency varies linearly with pressure with a baric coefficient of 2.402 Hz/bar. The schematic diagram of the NMR spectrometer, which incorporates seven microcircuits, is presented. It is found experimentally that pressure measurement accuracy of about 1 percent can be realized at pressures between 0 and 16 Kbar. References 14: 11 Russian, 3 Western.  
[64-6900]

UDC 621.745.552

# TECHNOLOGY FOR PRODUCING SYNTHETIC IRON FOR NUCLEAR POWER PLANT PARTS

Moscow ENERGOMASHINOSTROYENIYE in Russian No 7, Jul 84 pp 27-28

BLOZHKO, N. K., PETROV, candidates of technical sciences and NARKEVICH, Ye. A., NIKITIN, L.A. and KUROCHKIN, V.S., engineers

[Abstract] It is shown possible to obtain high quality synthetic iron containing graphite for nuclear power plant castings without using expensive modifiers. The iron can be produced in existing plants equipped with industrial frequency induction furnaces. By careful melting and modification of the iron with FS75 ferrosilicon, it is possible to obtain grade 40 grey pig iron without chilling. References: 2 Russian. [317-6900]

UDC 550.34.038.8:534.647

# PRINCIPLES OF DESIGNING DIGITAL COMPENSATING ACCELEROMETERS

Moscow IZMERENIYA, KONTROL', AVTOMATIZATSIYA in Russian No 1(49), 1984 pp 43-50

SKALON, A.I., candidate of technical sciences

[Abstract] Existing digital compensating accelerometers use three types of feedback: analog feedback with voltage-to-code or current-to-code conversion, pulse-current conversion, pulse-current feedback, or mechanical feedback through mass and strings. An accelerometer with voltage-to-code conversion is the simplest, consisting of a sensor, a position transducer, and amplifier which also converts the amplified signal to feedback current, an analog-to-digital converter shunted by a precision resistor, and a compensating current-to-force or current-to-torque converter. An accelerometer with current-to-code conversion includes, instead of the analog-to-digital converter, a reversible counter, a pulse generator, a current stabilizer, and a threshold device, all in parallel between two switches feeding into the feedback loop with an integrating capacitor across. It is much more accurate, within 0.001-0.01 percent than an accelerometer with voltage-to-code conversion. In an accelerometer with a mass suspended between two orthogonal pairs of strings, the mass is the sensing element and the vibration frequency differences of the strings (compared to a quartz-tuned reference) are the basis for compensation. Accelerometers with pulse-current feedback have a modulator behind a plain signal amplifier and a low-leakage transistor switch between the modulator and the compensating converter, this switch being also connected to a current stabilizer. Usually pulse-frequency, pulse-width, or relay-pulse modulation with the appropriate equipment are used as means of converting force or torque input data to digital data for the computer and feedback. The accuracy of

these accelerometers is determined only by the error of the compensating converter, the instability and the nonlinearity of the current stabilizer, and the quality of the transistor switch or switches, but does not depend on the gain instability and nonlinearity of the position transducer and the modulator. Pulse-width modulation is simplest and can be further simplified by use of optoelectronic devices. Figures 10; references 22: 12 Russian, 10 Western.  
[311-2415]

UDC 531.768.088

#### UNIAXIAL ANGULAR ACCELEROMETERS

MOSCOW IZMERENIYA, KONTROL', AVTOMATIZATSIYA in Russian No 1(49), 1984  
pp 32-42

SELEZNEV, A.V., candidate of technical sciences, and SHVAB, I.A.,  
candidate of technical sciences

[Abstract] The basic mechanical components of an angular accelerometer are the sensor, the damper, and the transducer. The sensor determines all main accelerometer performance characteristics, namely sensitivity and response speed as well as frequency characteristics. It consists of an inertial element, usually a dynamically-balanced rotating wheel with the mass "lumped" in the rim and identical elastic elements joining the wheel to the gimbal or hub. The rim is either solid, or hollow filled with liquid, or hollow filled with gas driving it as a pneumatic motor. The damper is a correcting device which improves the amplitude-phase characteristics and reduces the dynamic error of the accelerometer by producing a drag force proportional to the angular velocity. Pneumatic dampers are simplest in construction, but the viscosity of air is very low and, therefore, dampers with special-purpose oils having a high temperature stability (synthetic silicon or organosilicon oils) are most widely used. The most common types of viscous dampers are lamellar with meshed opposed arrays of fixed and movable vanes in the dashpot, piston dampers regulated by an adjustable-length capillary tube, and dampers with paddle wheel in closed tank. Another type of damper is an impact-inertial one with large masses absorbing the rotational energy upon collision with the sensor. Conventional measuring elements are resistive (potentio-metric or tensoresistive (semiconductor) transducers), capacitive, electromagnetic, photoelectric (featuring contactless transmission of signals), and pneumatic or hydraulic. Novel types of angular accelerometers are based on such physical principles as inertia of gas jets, electron beams, and ion beams, the piezoelectric effect in p-n junctions of diodes and transistors, the electrokinetic effect in fluids, and cryogenic suspension of the sensor. Individual evaluation of each type of accelerometer and comparative evaluation of all must be based on a composite rather than single criterion, with heavier weight given to more important performance parameters, the most expedient such criterion being the product of upper frequency limit

squared and threshold sensitivity. Figures 10; references 33: 16 Russian, 17 Western (1 in Russian translation).  
[311-2415]

UDC 621.791.72:621.375.826

#### TECHNOLOGICAL APPARATUS FOR LASER TREATMENT OF MATERIALS

Moscow TEPILOFIZIKA VYSOKIKH TEMPERATUR in Russian Vol 22, No 6, May-Jun 84  
(manuscript received 15 Feb 84) pp 1200-1205

KIRILLIN, A.V., KOSTANOVSKIY, A.V. and VINOGRADOV, V.L.

[Abstract] An apparatus has been developed and its experimental prototype built for technological laser treatment of materials, specifically non-metallic nitrides now widely used as refractory ceramics. The treatment includes remelting into the liquid phase, which occurs at temperatures above 2000 K and must be done in a nitrogen atmosphere so as to avoid chemical decomposition. Development of this apparatus was accompanied by a determination of hitherto unknown melting temperature-pressure characteristics of most high-temperature nonmetallic nitrides. The apparatus is designed for heat treatment at 2000-5000 K under pressures up to 200 MPa. A set of four LGN-702 CO<sub>2</sub>- lasers serves as heat source producing beams 60 mm in diameter with a divergence not exceeding  $2.5 \cdot 10^{-4}$  rad, a radiation power of 800 W per beam being attainable by pumping the CO<sub>2</sub>:N<sub>2</sub>:He=1:1.5:15 mixture at a rate of at least 6 liters/s. There is a high-pressure chamber for treatment of solid material in buffer gas under pressures up to 200 MPa with horizontal entrance of laser beams and there is a low-pressure chamber for treatment of powdered material under pressures up to 20 MPa with **vertical** entrance of laser beams. The apparatus can be used for experimental research on chemically pure surfaces at 5000-6000 K under vacuum or in various gaseous atmospheres. It was used experimentally for study of laser treatment of aluminum nitride, with subsequent x-ray phase analysis, x-ray structural analysis, and electron-microscope examination. Figures 2; references 7: 3 Russian, 4 Western.  
[149-2415]

UDC 54.14:534.22

#### APPARATUS FOR MEASURING VELOCITY OF SOUND IN FLUIDS

Moscow TOPLOFIZIKA VYSOKIKH TEMPERATUR in Russian Vol 22, No 3, May-Jun 84  
(manuscript received 24 May 83) pp 569-573

TIMROT, D.L. and SEREDNITSKAYA, M.A., Institute of High Temperatures, USSR  
Academy of Sciences, CHKHIKVADZE, T.D., Georgian Polytechnic Institute

[Abstract] A universal apparatus has been developed for simple and accurate measurement of the velocity of sound in almost any fluid, including a chemically active one. Measurements are made by the fixed-distance pulse passage method. An ultrasonic signal travels through the test fluid between two optically treated plane-parallel windows in a hermetically closed quartz cell. The latter is dropped into a glass vessel with circulating thermostatic liquid for low-temperature measurements or into an electric furnace for high-temperature measurements. The temperature is measured with a resistance thermometer and read on a digital voltmeter, constancy of the temperature being also monitored on an oscillograph. The velocity of sound can be determined on the basis of absolute measurement of the pulse travel time, which requires precise determination of the distance between windows, or on the basis of relative measurement requiring calibration against some reference fluid. Absolute velocity measurement also requires correction for diffraction, especially in the Fresnel near-field region, which must be subtracted from the velocity reading to yield the true thermodynamic velocity of sound - if there is no dispersion or frequency dependence of that velocity. A significant systematic error of both absolute and relative measurements, in addition to the errors of distance and time measurements, is the error in referring the readings to specific state parameters. The apparatus was tested on relative measurement of the velocity of sound in water, with an error of the order of 0.03 percent. Figures 3; references 10: 5 Russian, 5 Western).

[149-2415]

UDC 531.717

#### LIQUID-METAL TRANSDUCERS FOR STRAIN MEASUREMENT DURING IN-PILE MATERIALS TESTING

Moscow ATOMNAYA ENERGIYA in Russian Vol 57, No 5, Nov 84 (manuscript received 28 Oct 83, final edition received 4 May 84) pp 349-353

NEVEROV, V.A. and REVYAKIN, Yu.L.

[Abstract] Creep and other deformation of materials caused by nuclear radiation inside a reactor can be studied by conventional methods, which involve strain measurements with various special-purpose high-precision gauges. While the destabilizing effect of gas in clearances can sometimes

be eliminated, as in the IRT-2000 research reactor, all conventional gauges become unstable at high neutron flux intensity up to  $2 \cdot 10^{19} \text{ m}^{-2} \cdot \text{s}^{-1}$  or gamma radiation intensity up to  $10^4 \text{ gr} \cdot \text{s}^{-1}$  in fast reactors at sodium coolant temperatures above  $300^\circ\text{C}$ . Acoustic transducers are also unsuitable under these conditions, because they become destabilized by gas in clearances and they distort the temperature field as well as the power source distribution in the reactor core. Liquid-metal transducers are proposed instead, requiring that the metal have a low melting point and a low vapor pressure. The liquid metal must not wet and corrode surrounding solid container surfaces and must have a small cross section for activation interaction with reactor neutrons so as to minimize transmutation into other elements with very different density. These requirements are satisfied by molten tin within the  $280\text{--}360^\circ\text{C}$  temperature range, also by gallium, indium, and at still higher temperatures by the eutectic lead-bismuth alloy. Transducers using a column of such a metal can convert small ( $0.2\text{--}0.4 \text{ um}$ ) changes in the radius of tubular material specimens to large ( $20\text{--}200 \text{ um}$ ) displacements of the liquid column, but they require not only a high degree of temperature stabilization (within  $\pm 0.25^\circ\text{C}$ ) but also appropriate calibration and correction for the effect internal gauge pressure on axial-radial strains. The transducer chamber must therefore be designed with an inside diameter matching the initial outside diameter and the gauge height of the tubular material specimen. Transducers built to these specifications and incorporated to TO-IRN instruments for radiative creep measurements have been checked, prior to reactor startup, for reproducibility of readings after temperature changes of  $\pm 25^\circ\text{C}$  and for sensitivity against that of acoustic transducers. They were subsequently used experimentally for measuring strains during deformation of  $\text{OCr18Ni15Mo3Nb}$  whose properties and characteristics are already well-known, inside a BOR-60 reactor. Creep curves for this steel, including both transient and steady stages of deformation, were obtained at  $300\text{--}340^\circ\text{C}$  under various constant loads up to  $500 \text{ MPa}$  in neutron fluxes of up to  $2 \cdot 10^{19} \text{ m}^{-2} \cdot \text{s}^{-1}$  intensity with release of up to  $6 \cdot 10^3 \text{ W/kg}$  of radiation energy. Figures 3; references 8: 6 Russian, 2 Western.

[105-2415]

2415  
CSO: 186]/105

END

**END OF**

**FICHE**

**DATE FILMED**

21 MAY 85